**Dissertations in Forestry
and Natural Sciences**

UNIVERSITY OF
EASTERN FINLAND

ANTTI VÄISÄNEN

CHEMICAL AND PARTICULATE CONTAMINANTS PRODUCED IN ADDITIVE MANUFACTURING (3D PRINTING) OF PLASTICS

CHEMICAL AND PARTICULATE CONTAMINANTS PRODUCED IN ADDITIVE MANUFACTURING (3D PRINTING) OF PLASTICS

Antti Väisänen

CHEMICAL AND PARTICULATE CONTAMINANTS PRODUCED IN ADDITIVE MANUFACTURING (3D PRINTING) OF PLASTICS

Academic dissertation
To be presented by permission of the Faculty of Science, Forestry and Technology for public examination in the auditorium SN200 in the Snellmania building at the University of Eastern Finland, Kuopio, on January 27th, 2023, at 12 o'clock

Author's address: Antti Väisänen
                     University of Eastern Finland
                     Depart. of Environmental and Biological Sciences
                     70210 KUOPIO, FINLAND
                     email: antti.vaisanen@uef.fi

Supervisors: University lecturer Marko Hyttinen, Ph.D.
                     University of Eastern Finland
                     Depart. of Environmental and Biological Sciences
                     70210 KUOPIO, FINLAND
                     email: marko.hyttinen@uef.fi

                     Research director Pertti Pasanen, Ph.D.
                     University of Eastern Finland
                     Depart. of Environmental and Biological Sciences
                     70210 KUOPIO, FINLAND
                     email: pertti.pasanen@uef.fi

Reviewers: Postdoctoral researcher Anna-Kaisa Viitanen, Ph.D.
                     Tampere University
                     Faculty of Built Environment (Civil engineering)
                     33720 TAMPERE, FINLAND
                     email: anna-kaisa.viitanen@tuni.fi

                     Industrial hygienist Aleksandr Stefaniak, Ph.D.
                     National Institute for Occupational Safety and Health
                     26505 MORGANTOWN, WEST VIRGINIA, USA
                     email: astefaniak@cdc.gov

Opponent: Senior specialist Katri Suuronen, Ph.D.
                     Finnish Institute of Occupational Health
                     P.O. Box 40
                     00032 Työterveyslaitos, HELSINKI, FINLAND
                     email: katri.suuronen@ttl.fi

ABSTRACT

Additive manufacturing (AM) technologies have become increasingly popular since the late 2000s. AM machines (or in layman's terms, 3D printers) are used especially for rapid production of small volumes of products and customized items following the quick production cycle and relatively inexpensive manufacturing costs. Many AM technologies employ plastics as their production feedstocks. Certain methods use heat to manufacture products using thermoplastics, while some methods utilize light to cure products using photocurable resins. The popularization of AM technologies has led to 3D printers being used in a wide variety of different environments. As 3D printers are brought into homes, offices, and working facilities world-wide, the hazards related to their use concern ever increasing amounts of people.

All the studied 3D printer types produced chemical or ultrafine particulate matter emissions at quite constant rates. In most cases, both were produced coincidentally. Coarse or fine particles, on the other hand, were hardly detected in the 3D printer operations. Individual volatile organic compounds (VOCs) were encountered at a maximum concentration level of 1150 μg/m^3 in this thesis, although the concentration levels were below 30 μg/m^3 in most cases. The produced VOCs were diverse and included thermal decomposition products, reactive oxygenated compounds, evaporation products with sensitizing potential, and in some cases carcinogens as well. Total VOC (TVOC) concentrations ranged from a hardly detectable concentration level in an industrial workplace up to a 1700 μg/m^3

concentration level under an office environment. Multiple carbonyl compounds, formaldehyde included, were commonly encountered in 3D printing processes as well at individual compound levels of <140 µg/m^3.

The produced ultrafine particle (UFP) concentrations were usually at the magnitude of 10^3 #/cm^3. However, the mean level of ca. 10^4 #/cm^3 was documented when industrial powder bed fusion machines were operated, while UFP levels were at the magnitude of 10^5 #/cm^3 during extrusion of an acrylonitrile butadiene styrene (ABS) filament feedstock using a desktop material extrusion 3D printer. The mean coarse and fine particle levels, on the other hand, never exceeded 30 µg/m^3 during any manufacturing process. However, high dust exposures (above 9 mg/m^3) and coarse particle levels were recorded when a powder feedstock was prepared for use and when products manufactured using the said feedstock were post-processed. The highest TVOC concentration (11,000 µg/m^3) was also recorded during a post-processing task where excess photocurable resin was washed off from a product's surface using a solvent.

The 3D printing environment, machine operation principle, and the compositions of the applied feedstocks had a significant impact on the produced contaminants and their air concentrations. Chemicals and UFPs are expected to be always produced when 3D printers are operated using plastic feedstocks, given the fact that thermal decomposition or spontaneous resin evaporation, depending on the operated AM machine, are always occurring during 3D printer operations. Long-term data on the health impacts of 3D printer operations does not exist yet, but some reports of acute health impacts have been published. Therefore, it is advisable to control exposures to 3D printer emissions whenever possible by regulating exposure time, eliminating the produced contaminants, and using manufacturing settings that reduce the amount of produced contaminants.

National Library of Medicine Classification: QV 627, WA 450, WA 754

Medical Subject Headings: Printing, Three-Dimensional; Plastics; Polymers; Powders; Air Pollutants; Air Pollution, Indoor; Environmental Exposure; Occupational Health; Workplace; Volatile Organic Compounds; Reactive Oxygen Species; Formaldehyde; Carcinogens; Particulate Matter; Dust

Yleinen suomalainen ontologia: pikavalmistus; 3D-tulostus; muovi; polymeerit; jauheet; päästöt; ilman epäpuhtaudet; ilmansaasteet; altisteet; altistuminen; työterveys; työpaikat; työperäinen altistus; haihtuvat orgaaniset yhdisteet; formaldehydi; karsinogeenit; pienhiukkaset; pöly

Acknowledgements

I'd like to direct special thanks for the reviewers, Anna-Kaisa Viitanen and Aleksandr Stefaniak, for going through this thesis for the sake of it, and their critical comments, as well as my opponent Katri Suuronen for accepting the invitation, and for the spectacle of a lifetime that is called the doctoral defence.

I'm deeply grateful for my supervisors Marko Hyttinen and Pertti Pasanen, for luring me into the IEOH research group and providing me with the necessary tools for academic growth, and for their support during the composition of this thesis. I'd also like to thank my colleagues Antti Karjalainen, Maija Leppänen, and Joonas Ruokolainen, as well as the people of the Department, for all their support and encouragement.

The Alonen brothers Lauri and Antti, and my former supervisor Esa Jääskeläinen from the Savonia University of Applied Sciences provided invaluable support and guidance especially during the early stages of this work, with Lauri and Antti providing practical support until the very end. Furthermore, Sampsa Ylönen from the Savonia University of Applied Sciences strongly supported me during my journey as a colleague and provided great practical help, while also serving as invaluable intellectual support.

I'd like to thank my family for their care during this journey, notably my parents' constant reminders of "When's your defence?", which reminded me about the fact that I'm really onto something special. I'm exceptionally grateful for my brother, who provided linguistic assistance during the composition of the research manuscripts, and who introduced me to multiple off-work activities during this journey which, temporarily, helped me forget the burden of work. A special thanks to the Kaljaliiga Association, for regularly airing me when I'd otherwise neglect it.

Emma, you were there from the very beginning, until the end, and beyond. I'm grateful for that.

Thank you, friends, close and far, for sharing our lives, for your support, bewilderment, and the good times. And finally, Jari, for asking all the questions imaginable, both foolish and wise.

Kuopio, November 2022
Antti Väisänen

LIST OF ABBREVIATIONS

3D	Three-dimensional
ABS	Acrylonitrile butadiene styrene
AM	Additive manufacturing
BC	Biocomposite
BJ	Binder jetting
CO_2	Carbon dioxide
CO	Carbon monoxide
HWP	Household waste plastic
ME	Material extrusion
MJ	Material jetting
MJF	Multi jet fusion
MM	Multi-material
MMAM	Multi-material additive manufacturing
PA	Polyamide (nylon)
PM	Particulate matter
PBF	Powder bed fusion
PLA	(Poly)lactic acid
PP	Polypropylene
UFP	Ultrafine particle
VOC	Volatile organic compound
VP	Vat photopolymerization
$\#/cm^3$	Number concentration, particles per square centimetre
$\mu g/m^3$	Mass concentration, micrograms per square metre
mg/m^3	Mass concentration, milligrams per square metre

LIST OF ORIGINAL PUBLICATIONS

This thesis is based on data presented in the following articles, referred to by the Roman Numerals I-IV.

I   Väisänen A., Hyttinen M., Ylönen S. & Alonen L. 2019. Occupational exposure to gaseous and particulate contaminants originating from additive manufacturing of liquid, powdered, and filament plastic materials and related post-processes. *Journal of Occupational and Environmental Hygiene 16(3):258–271.*

II   Väisänen A., Alonen L., Ylönen S., Lyijynen I. & Hyttinen M. 2021. The impact of thermal reprocessing of 3D printable polymers on their mechanical performance and airborne pollutant profiles. *Journal of Polymer Research 28:436.*

III   Väisänen A., Alonen L., Ylönen S. & Hyttinen M. 2022. Volatile organic compounds and particulate emissions from the production and use of thermoplastic biocomposite 3D printing filaments. *Journal of Occupational and Environmental Hygiene 19(6):381–393.*

IV   Väisänen A., Alonen L., Ylönen S. & Hyttinen M. 2022. Organic compound and particle emissions of additive manufacturing with photopolymer resins and chemical outgassing of manufactured resin products. *Journal of Toxicology and Environmental Health, Part A 85(5):198–216.*

The above publications have been included at the end of this thesis with their copyright holders' permission.

AUTHOR'S CONTRIBUTION

I)   The author formulated the research questions and designed the experiments with assistance from the supervisors P. Pasanen and M. Hyttinen. He also carried out the field experiments and analyses with the supervisors' guidance. The author acted as the main author for the publication while receiving valuable editorial support from the co-authors.

II)   The author designed the experiments and formulated the research questions with assistance from the supervisors P. Pasanen and M. Hyttinen, as well as carried out the field experiments and analyses in full, except for the material property measurements which were performed by the co-author I. Lyijynen. The author acted as the main author for the publication while receiving valuable editorial support from the co-authors, and applied for and collected the funding necessary for carrying out the research.

III) The author designed the experiments and formulated the research questions with assistance from the supervisors P. Pasanen and M. Hyttinen, as well as carried out the field experiments and analyses in full. The author acted as the main author for the publication while receiving valuable editorial support from the co-authors, and applied for and collected the funding necessary for carrying out the research.

IV)   The author designed the experiments and formulated the research questions with assistance from the supervisors P. Pasanen and M. Hyttinen, as well as carried out the field experiments in full, while receiving assistance from the supervisor M. Hyttinen during chamber emission testing. The author acted as the main author for the publication while receiving valuable editorial support from the co-authors, and applied for and collected the funding necessary for carrying out the research.

Table of contents

1 Introduction

Two terms exist for autonomous mechanical material additive production of physical objects based on a computer aided design (CAD). Professional and large-scale production is usually referred to as additive manufacturing (AM), while small-scale production is referred to as three-dimensional (3D) printing. AM and 3D printing are effectively, however, synonyms, although "3D printing" is a more universally understood layman's term. 3D printing is a process where a physical 3D-modeled object is produced autonomously by a machine by adding material in a layer-on-layer basis to a build platform, making the process vastly different from traditional material subtracting, or molding methods. The object must be 3D-modeled with a CAD software, prepared with a dedicated slicing program, and transferred to an AM machine before the manufacturing process can be initiated. Slicing refers to a process where the 3D model is divided by a software program into layers which represent each individual physical layer of the product. The process includes the formation of G-code, a series of manufacturing instructions for the AM machine. The applied AM method determines the characteristics of the manufacturing process, including the type and form of the applied feedstock material and pre- and post-processing requirements. Pre-processes include any preparations required by an AM machine to start object production, e.g., preparation and loading of the feedstock material. Post-processes are measures applied on the produced object after the manufacturing process which finish the object and whereafter the object is ready to be used. Post-processing measures include but are not limited to removal of excess material or support structures, and surface curing. Additional and voluntary post-processing, e.g., coating, infiltration, or chemical surface smoothing can be applied on the manufactured products as well. (Calignano et al. 2017, Ligon et al. 2017, Jasiuk et al. 2018, Kumbhar & Mulay 2018, Karakurt & Lin 2020, Wu et al. 2020, Pagac et al. 2021, Piedra-Cascón et al. 2021).

The popularity of AM has increased rapidly since early 2000's after the expiration of some the earliest key patents. The AM technology has, however, existed since early 1980's but major developments were hindered by the existing competition obstructions. The annual financial growth rate of the industry has been approximately 25 % since 2010, while surpassing the value of 12.5 billion dollars in

2020 (Hubs B.V. 2021, Wohlers 2021). A similar growing trend is anticipated to continue, with the focus shifting gradually from prototyping towards the large scale production of high-end and functional products. The number of sold AM machinery has also expanded greatly, especially as ever superior feedstocks are developed and the functionality of consumer scale machines, often referred to as desktop 3D printers has evolved. Material extrusion (ME) 3D printers are the most popular type of AM machinery, as up to 85 % of consumer level printers are estimated to fall under this category. They are followed with vat photopolymerization (VP) printers in popularity, which gain consumer interest fast as the price gap between VP and ME printers is narrowing quickly. The total number of sold AM units surpassed two million units in 2020. The number includes industrial scale machines which gradually replace traditional manufacturing and tooling technologies. (Hubs B.V. 2021, Wohlers 2021). These statistics describe how the popularity of AM machines and number of people in contact with them has rapidly increased over the past years.

Following the expansion of the AM industry the hazards originating from AM machine operations and processes have been acknowledged, but studied insufficiently (Byrley et al. 2019, Petretta et al. 2019, Min et al. 2021, Stefaniak et al. 2021). Nevertheless, airborne chemical species and ultrafine particles (UFPs) are identified as the most impactful pollutants produced in AM of polymers. Many of the encountered chemicals are identified as carcinogens, irritants, sensitizers, or allergens and the main exposure pathways are inhalation and dermal routes. Inhalation exposure to UFPs and fine particles produced in AM processes is also concerning, as they are linked to adverse pulmonary, cardiovascular, and systemic effects. (Peters et al. 2006, Pope & Dockery 2006, Bakand & Hayes 2016, Creytens et al. 2017, Byrley et al. 2019, Ohlwein et al. 2019, Roth et al. 2019, Dobrzyńska et al. 2021, Min et al. 2021).

Evidence for adverse health effects induced in workers occupied in the plastics processing industries and the presence of hazardous substances therein is irrefutable. Long-term exposure to various gaseous or particulate contaminants are associated with health risks and adverse health outcomes, including increased morbidity and mortality, cancer, reproductive hazards, dermal effects and allergies, central nervous system (CNS) depression, and respiratory symptoms including asthma (Savonius et al. 1993, Tosti et al. 1993, Van Kampen et al. 2000, Minamoto et al. 2002, Vermeulen et al. 2002, Dematteo et al. 2012, Shahnaz et al. 2012, Guillemot et al. 2017, Nett et al. 2017, Lee et al. 2013, Unwin et al. 2013, Christensen

et al. 2018, Darbre 2020, Zulu & Naidoo 2021). Only a little evidence exists about the long-term health hazards within the AM industry, as many adverse health effects have a latency time. The first cases of occupational respiratory illnesses in the AM industry have been documented, however (Johannes et al. 2016, House et al. 2017, Chan et al. 2018), and 3D printer emissions are demonstrated to produce acute hypertension and microvascular dysfunction in rats (Stefaniak et al. 2017a) as well as increase irritation and inflammatory biomarker levels in human subjects after only a short exposure period (Gümperlein et al. 2018). Cell toxicity tests have also revealed that particles produced in 3D printer operations have toxic properties (Farcas et al. 2019, Zhang et al. 2019). Now, these risks are expanding as AM machines penetrate new industries and operational environments. It has been acknowledged that the AM safety research trails behind the march of technology and practically only one of the seven standardized AM technologies, the material extrusion (ME) method, has been focused on in safety and emission studies thus far. However, these studies are focused mostly on the common feedstocks, acrylonitrile butadiene styrene (ABS), and (poly)lactic acid (PLA). (Roth et al. 2019, Dobrzyńska et al. 2021, Leso et al. 2021).

The number of consumers and industrial workers in contact with 3D printers has expanded greatly over the past years with no signs of stagnation. Consumer and hobbyist exposure to air pollutants emitted from 3D printers is a relevant concern as they are not adequately prepared for exposures or exposure control, and even the exposure levels and compositions are mostly unknown. 3D printing is often performed in spaces which are not designed for effective indoor air pollutant control, e.g., homes and offices. On the other hand, industrial workplaces often operate industrial level AM machines whose emissions are studied very scarcely, and complex pre- and post-processing techniques are performed on a regular basis. The pre- and post-processes may be the tasks where exposure levels to chemicals and particles reach the highest levels as these processes can involve solvents, pressurized air, and powder mixers, which can influence exposure levels greatly. Further efforts are needed to identify the occupational and operational hazards within the AM industry so that targeted means of hazard control can be implemented.

2   Review of literature

2.1   Overview of additive manufacturing

AM is a rapid process in comparison to traditional production methods which allows manufacturing of small volumes and customized products at an economical cost technically anywhere. These factors contribute to shortened and altered supply chains and reduced need for storage and tooling machinery, as ready-to-use products can be produced and distributed locally on-demand. However, mass production through AM is not yet as cost-effective as traditional manufacturing methods. (Jasiuk et al. 2018, Wu et al. 2020). Seven standardized AM methods exist up to date as described by the ISO/ASTM 52900:2015 standard, while novel methods are continuously under development (Ngo et al. 2018). The methods relevant in the context of this thesis are described later. Polymers and metals are most used feedstocks in AM production, but niche applications exist for many other alternatives, e.g., sheets, ceramics, and concrete (Ngo et al. 2018). Multi-material (MM) additive manufacturing (MMAM) machines and feedstocks are also developed for the growing demands of the AM industry as they expand the diversity and potential of manufactured objects. MMAM machines can use multiple materials as their feedstocks simultaneously, and henceforth, an object with special and localized properties can be produced in a single process. Additionally, the need for post-processing can be reduced by MMAM methods. (Vaezi et al. 2013, Jasiuk et al. 2018).

AM machines are used for a wide range of purposes, including hobbyist tinkering and spare parts production, model and prototype testing, and the production of customized products and consumer goods. Furthermore, industrial AM machines can manufacture complex high-end parts with excellent mechanical properties for various technical sectors, e.g., electrical, automotive, and aerospace industries. Impressive advances in dental applications, prosthetics, and (bio)medical manufacturing have also been made. (Ligon et al. 2017, Ngo et al. 2018, Karakurt & Lin 2020, Singh et al. 2020, Tang et al. 2020, Wu et al. 2020, Piedra-Cascón et al. 2021, Gülcan et al. 2021, Tyagi et al. 2021, Zhang et al. 2021). Consumer level 3D printers are usually incapable of producing objects with exceptional mechanical properties required for functional parts, but customized products for a wide range of purposes

can be produced with them at a relatively low cost, nevertheless. (Ligon et al. 2017, Jasiuk et al. 2018). However, even the consumer level machines are soon reaching a critical threshold where the parts fabricated with them are competitive with products manufactured through traditional means in both mechanical performance and visual appearance (Jasiuk et al. 2018, Tan et al. 2020).

Various indoor air pollutants are confronted in the AM industry and the operation of AM machinery. Different pollutants have their distinctive sources, while the applied AM method is the main determinant of the produced pollutant profile, along with the used material (Petretta et al. 2019, Roth et al. 2019, Dobrzyńska et al. 2021). Chemical substances are encountered in thermal processing of plastics, which is a characteristic operational principle of certain AM methods but deteriorating for the feedstock. A polymer can't withstand prolonged thermal exposure which results in thermal decomposition where chemical alterations, e.g., polymer chain scissions, cross-linking, and de-polymerization occurs in the polymer matrix. Volatile and semi-volatile chemical species (solvents, catalysts, additives, monomers, or general decomposition products) with varying toxic properties are released in the degradation process. (Lithner et al. 2011, Unwin et al. 2013, Guillemot et al. 2017, Ding et al. 2019, Mikula et al. 2020). Furthermore, volatile chemicals are spontaneously evaporated from photopolymer resin vats, or chemical processing stations used in certain AM methods and the evaporation rate is further amplified by the application of heat or environmental warmth. (Afshar-Mohajer et al. 2015, Yang & Li 2018, Stefaniak et al. 2019). Chemicals are also used to process and finish manufactured products, and items manufactured through certain methods may be coated with unpolymerized feedstock material. Manufactured products can be chemically polished, or removable structures or the excess printing material may be dissolved, resulting in chemical exposure events as these processes are not usually automated. While the exposure often occurs through inhalation, a dermal route exists in the post-processing and resin vat handling tasks.

Fine and ultrafine airborne particulate matters are often encountered in tandem with chemical substances in thermal processing of plastics. These particles are formed in nucleation and coagulation processes involving volatile and semi-volatile chemical species which condensate in the air into solid particles. The particles are initially nano-sized, but they can grow into fine particles over time. The health impacts of these particles are hard to evaluate, as the chemical composition and surface chemistry of the particles play a major role in their functionality. Inhalation

of particles with low interactive potential is considered less hazardous than inhalation of highly reactive particles, which can produce a variety of adverse impacts in the human airways, or systemic effects after absorption. Owing to their small size, UFP and fine particles can penetrate in the deepest regions of the lungs and enter the blood stream, and eventually translocate into vital organs. (Peters et al. 2006, Shahnaz et al. 2012, Lee et al. 2014). Particles can also be directly disintegrated from a polymer when exposed to sufficiently high temperatures (Byrley et al. 2019). Furthermore, exposure to coarse and dust particles is plausible when AM machines which employ powdered materials are loaded, operated, and unloaded, or product surfaces manufactured using these machines are cleaned from excess printing material. The use of shakers, compressed air or other tools used for feedstock preparation or product finishing can produce large amounts of airborne dust and fine particles. Particles are also produced when any manufactured products are sanded. Exposure to UFPs and fine particles is, however, more common than exposure to coarse and dust particles as larger particles are produced in masses only in certain situations, but fine particles and UFPs are formed in a greater number of AM processes (Byrley et al. 2019, Petretta et al. 2019.)

The nature and duration of the exposure events are important factors in exposure and risk assessing. An AM production process can be split into three parts: pre-processing, manufacturing process, and post-processing. Pre- and post-processes are significantly shorter than the actual manufacturing process, but oftentimes a process operator must be physically present in them. Henceforth, these processes can be the most impactful situations in terms of exposure potential. (Short et al. 2015, Du Preez et al. 2018, Zisook et al. 2020, Leso et al. 2021). However, the actual manufacturing process can last from just minutes to up to days, and therefore the operator exposure to the produced contaminants can be low but sustained over multiple working days. This results in prolonged and chronic exposure potential to the encountered contaminants, and the impact of such exposure events on adverse health impact induction is difficult to estimate – especially as the exposure agents are relatively unknown. The diversity of AM technologies, operational environments, and feedstocks produce further challenges for coherent, industry-wide safety evaluation. The main risk characteristics of the most common AM technologies have been, however, identified as described above (Petretta et al. 2019).

Workers occupied in the AM industry are generally protected by occupational safety legislations and obligations. Furthermore, the impact of occupational hazards

and their control, and the relevance of risk assessing are generally acknowledged. As comprehensive research information is scarce, protective measures and safe operation planning may be troublesome to apply and AM operators must rely on the general guidance issued by public authorities, or machine and feedstock manufacturers. The lack of available research data causes issues in the adoption of appropriate safety measures, however, and the existing hazards may be belittled in the absence of available information. Additionally, the protective laws and guidelines are not applicable in domestic environments, and the essential pieces of information may even be beyond a hobbyist's reach. (Bharti & Singh 2017, Wojtyła et al. 2017, Pelley 2018, Roth et al. 2019.) Therefore, an unprofessional 3D printer operator can be left responsible for their own actions. 3D printing machinery and feedstock material manufacturers do, however, provide a necessary safety data sheet or an operation manual, but the requirements for the safe machine operation or material application may be too strict to be met in domestic conditions as they often demand the use of, e.g., technical emission control measures like fume hoods.

Finally, in addition to the various exposure agents encountered in the operation of the various AM technologies, the manufactured products can be a source for chemical emissions and exposures as well. Chemical outgassing and blooming from plastic products have been identified, and the phenomena are also encountered in the AM industry. Outgassing occurs when gaseous compounds entrapped within the polymer matrix during the AM process migrate to the surface of the product and are evaporated. (Gonzalez et al. 2017, Ligon et al. 2017, Du Preez et al. 2018.) Blooming refers to a similar incident which involves the movement of non-volatilized chemical substances within a polymer matrix. Unbound chemical residues, e.g., oligomers, additives, and other molecules can travel across the polymer matrix and emerge to the surface of a product. The use of post-processing solvents has been found to increase the magnitude of outgassing and blooming following solvent absorption into the product, while post-curing or heat treatments can reduce the effect. (Lago et al. 2015, Nouman et al. 2017, Alifui-Segbaya et al. 2020, Krechmer et al. 2021). Surfaced and outgassed chemicals can be a secondary health hazard in addition to the airborne chemicals produced in AM processes, as several plastic monomers and additives possess toxic properties. Products manufactured with photocurable resins may be used for dental or other biological applications, resulting in additional exposure pathways. Compounds emerged via blooming can eventually evaporate into the air as well, given appropriate circumstances are met. (Jorge et al. 2003, Fukumoto et al. 2013, Lago et al. 2015,

Oskui et al. 2016, Nouman et al. 2017, Alifui-Segbaya et al. 2018, Kostć et al. 2020.) Ultimately, the risks and hazards are not limited to the use of AM technologies and the exposure agents encountered therein, but secondary consumer or product user hazards may emerge from improper finishing and incautious use of the manufactured products.

2.2 Relevant polymer additive manufacturing methods

As previously mentioned, seven standardized AM methods exist with their own characterizing operational principles, while numerous other non-standardized methods are developed, or are under development. Each method makes use of specific types of feedstock materials, and the degree of production freedom varies between the AM machines as specific pre- and post-production measures are demanded by each different AM method. All methods, however, follow the same manufacturing principle: the products are manufactured autonomously by the AM machine based on a modeled and sliced 3D design in a layer-on-layer basis. A flowchart describing the AM processing steps required to produce a final product is presented in Figure 1, and the AM methods, materials, and emission products relevant in the context of this thesis are described below in detail.

Figure 1. The additive manufacturing process flowchart.

2.2.1 Material extrusion method

Material extrusion (ME) method, often referred to as fused filament fabrication (FFF) or fused deposition modeling (FDM) makes use of thermoplastic polymer and composite pellets or filaments (rarely slurries or liquids) which are extruded through a heated nozzle (typically at around 200–240 °C) to manufacture a product. The method is widely used for prototyping and small-scale production of objects designed for a wide range of mechanically non-demanding purposes due to the cost-efficiency of the technology, and the relatively poor mechanical properties of the products. However, industrial scale ME machines capable of producing sturdy parts are being used to produce consumer products as well. A wide range of ME printers exist, and the machine properties vary greatly. ME machines are available with open or semi-enclosed build areas or fully enclosed build chambers, different nozzle widths, some have integrated emission filtration systems, and the build volumes range greatly as well. ME printers are used in numerous environments following their economic costs and ease of use, and the diversity of the available machines and feedstocks. (Calignano et al. 2017, Kumbhar & Mulay 2018, Ngo et al. 2018, Tan et al. 2020, Stefaniak et al. 2021.)

The feedstock liquefies as its temperature exceeds the polymer's glass transition temperature or melting point while it's forced through the heated printer nozzle, and rapidly hardens as it cools down. The extruded polymer matter attaches to the previous layer or the build plate and forms a solid structure. Enclosed ME printers are usually designed for higher-end production as the temperature inside the chamber is easier to control and a higher atmospheric temperature can be maintained, resulting in less dimensional inaccuracies. ME method does not require necessary preparations before printing a part apart from material selection, but several means to improve the first layer adhesion on the build plate exist as certain polymers are prone to warping and detaching from the plate. The build plate can be coated with glue, tape, sheet, or slush prepared by dissolving a small amount of the used polymer in a solvent. The build plate is often heated to around 50–90 °C to improve adhesion and reduce warpage. ME printers are unable to print steep or negative angles, e.g., ledges and therefore removable support structures created by the utilized slicing program must be formed during the printing process to enable the production of such shapes. The supports must be removed, usually by cutting or dissolution after the print job is finished. The joining points between the supports and the printed object typically require further smoothing to finish the product.

Additionally, the surface quality of an object printed with ME method is usually crude in comparison to other AM methods and additional post-processing may be required to improve it. The object can be sanded or abraded, or chemically (vapor) polished. No other post processing, e.g., coating is usually required due to the wide feedstock selection. (Calignano et al. 2017, Ligon et al. 2017, Kumbhar & Mulay 2018, Ngo et al. 2018, Karakurt & Lin 2020, Tan et al. 2020, Wu et al. 2020, Stefaniak et al. 2021.)

The main hazards in the use of ME machines emerge from decomposition of plastics in the printing nozzle which results in the production of VOCs and UFPs with various potential adverse effects for human health. Heated build surfaces and hot printing nozzles produce a burn hazard as well. In the absence of necessary post-processing, no further hazards emerge directly from the defining characteristics of the ME method. (Byrley et al. 2019, Petretta et al. 2019, Roth et al. 2019, Stefaniak et al. 2021.)

2.2.2 Vat photopolymerization method

Vat photopolymerization (VP), which covers the stereolithography (SLA) and digital light processing (DLP) technologies is among the earliest developed AM technologies and characterized by an extreme surface precision. In addition to general prototyping and manufacturing at a relatively low cost, VP is used for several (bio)medical and dental applications as well as for casting molds and other purposes where high dimensional accuracy and level of customization are needed, but no special mechanical performance is required. VP printers are available at consumer scale desktop models, all the way up to large industrial machines. The consumer level machines often lack emission control mechanisms apart from a cover which is provided with practically every VP printer, which both contains the produced resin vapors as well as keeps the resin vat safe from dust and other contaminants. Industrial VP machines can, however, be equipped with in-built exhausts or emission control systems. The available VP printer build volumes are typically small, although large industrial printers are also available. (Calignano et al. 2017, Ngo et al. 2018, Pagac et al. 2021, Piedra-Cascón et al. 2021, Zhang et al. 2021).

The VP method makes use of photopolymer resins sensitive to UV or visible wavelengths of light as the feedstock materials. They are most suitable for non-functional part production as the mechanical properties of the resins are generally

inferior in comparison to many other AM feedstocks. The manufacturing platform is traditionally dipped in or lowered to the bottom of a photopolymer-filled vat, from where it is gradually lifted. A light source located beneath the vat cures each layer of the object and thus, the product is formed upside-down. The VP method cannot produce steep or negative angles and therefore removable or dissolvable support structures must be formed during manufacturing if such shapes are included in the product's design. The VP method requires necessary post-processing, as the manufactured object is coated in un-cured resin which must be dissolved or otherwise removed, e.g., by using an ultrasonic bath. The very surface of the object is usually left partly uncured as well. UV-treatment is a second commonly applied post-processing procedure where the surface of the object is completely cured. Further machining or surface improvements through, e.g., abrasive techniques can be applied on the products as well, but such measures are rarely needed. The characterizing features of the VP method, mostly the reliance on liquid resin feedstocks has limited the development of MM VP technologies, but advances on the matter have been made recently. (Vaezi et al. 2013, Calignano et al. 2017, Ligon et al. 2017, Kumbhar & Mulay 2018, Ngo et al. 2018, Karakurt & Lin 2020, Tan et al. 2020, Wu et al. 2020, Pagac et al. 2021, Piedra-Cascón et al. 2021, Zhang et al. 2021). The demand for a dedicated post processing equipment may make the application of VP method unappealing to consumers, as the post-processing can be messy and require solvents and other special devices. If more than one resin blend is used for manufacturing using a single VP machine, the vats must be switched and stored in between the manufacturing processes, which demands a ventilated storage space or an airtight chamber.

The use of liquid resins and the demand for chemical post-processing produce the characteristic hazards of the VP method. Resin components and post-processing solvents can spontaneously evaporate over time and produce a chemical inhalation hazard. Handling and use of the freshly manufactured products, resin vats, and the post-processing machines also produce a dermal chemical hazard. A further hazard emerges from the use of the products through chemical blooming or outgassing where chemical substances emerge from the polymer matrix to the surface of the product and evaporate or transfer to biological tissues via touch. (Creytens et al. 2017, Yang & Li 2018, Roth et al. 2019, Stansbury & Idacavage 2016, Petretta et al. 2019, Zisook et al. 2020, Stefaniak et al. 2021.)

2.2.3 Powder bed and multi jet fusion methods

Powder bed fusion (PBF) method is the most widely used AM method for large-scale production of professional and consumer products, as the PBF method can manufacture large volumes at fast speed but at a relatively high cost. Industrial PBF machines are equipped with in-built exhaust and ventilation systems which help in maintaining desired build chamber conditions, and aids in the elimination of produced manufacturing emissions. However, semi-desktop PBF printer models with small build volumes and no emission elimination systems have been introduced to the market recently. The method makes use of powdered polymer or metal materials as the most common feedstocks, but novel composite materials and alloys are developed for PBF manufacturing purposes. The method is characterized by filling the whole manufacturing area called a powder bed with the feedstock powder over the course of the manufacturing process under an inert atmosphere. The excess, non-fused powder acts as a support for the products and therefore no dedicated support structures are required. The AM process takes place inside an enclosed and protective atmosphere by laser-induced melting or sintering of each layer of the product distributed by a feeder-spreader system. The chamber is often heated almost to the feedstock's melting point or glass transition temperature to achieve the best surface quality. PBF method has several subtypes of which selective laser melting (SLM) and selective laser sintering (SLS) are the most common. SLM operates by applying sufficient energy on the manufacturing material to melt the desired area and thus joining individual layers together. SLS operates by applying less energy into the manufacturing material which does not melt thoroughly, but rather fuses to the layers on a molecular level by binding only the outer molecular layers of the powder. (Calignano et al. 2017, Ligon et al. 2017, Ngo et al. 2018, Singh et al. 2020, Tan et al. 2020, Wu et al. 2020, Dev Singh et al. 2021).

PBF method requires multiple necessary pre- and post-processing steps. The feedstock is usually first de-clumped by sieving, after which the powder feeding system must be manually loaded with the feedstock. The formed powder cake is manually removed from the PBF machine after the manufacturing process is completed. The manufactured objects are excavated from the powder bed and the excess manufacturing powder is brushed or air blasted off. The products are oftentimes chemically infiltrated or coated to achieve desired surface properties or color. Generally, similar surface-finishing processing may be applied on PBF manufactured products as on ME fabricated ones. Additionally, the manufactured

products can experience internal residual stress which can be relieved with heat treatments. (Ligon et al. 2017, Kumbhar & Mulay 2018, Ngo et al. 2018, Karakurt & Lin 2020, Singh et al. 2020).

Multi jet fusion (MJF) is a popular and flexible MMAM method which adopts features from PBF and binder jetting methods (not addressed in this thesis) to produce high-end products. Polyamide (PA) powder or PA-based composites are typically used as the feedstock material for the process, which is distributed on the powder bed in a similar fashion as in the PBF method. The layer fusion is induced by the selective deposition of energy-absorbing fusing agent, applied by ink-jet nozzles attached to a printhead rail. An infrared lamp is used as the energy source which melts the areas coated with the fusing agent. A detailing agent is used around the to-be fused cross-sections to enhance printing accuracy. New layers are spread by a feeder-spreader system after the agents are applied and the layer is fused. The MJF method can use multiple fusing agents concurrently, and thus multi-colored objects and parts with localized properties can be produced using the method. The feedstock preparation and post-processes are analogous to the PBF method. (Tan et al. 2020, Wu et al. 2020).

The greatest hazards emerge from exposure to chemical substances, and especially to particles in PBF manufacturing. Dust and fine particle exposure can reach significant levels in pre- and post-processing stages, given the fact that the feedstock preparation, machine loading, and object excavation are at least partially manual processes where airborne dust is produced. Equipment and tools used in these processes can release high amounts of dust in the air. Dermal exposure to dust can also be high during these processes. The high temperatures (typically 175–275 °C) applied in the AM process allow VOCs and UFPs to be produced as well. (Petretta et al. 2019, Zisook et al. 2020, Stefaniak et al. 2021). The VOC exposure may be higher when a MJF machines are operated, as the fusing and detailing agents can vaporize during and after deposition and exit the machine (Hayes et al. 2021).

2.2.4 Material jetting method

Material jetting (MJ) manufacturing bears resemblance to traditional 2D printing. A printhead nozzle or multiple ink-jet nozzles attached to a printhead rail deposits photosensitive ink-like polymer resin continuously or selectively onto a manufacturing platform layer by layer. The ink resin is hardened by an UV-light

source after deposition. Similar to VP manufacturing, the dimensional accuracy and the surface quality of the MJ method is exceptional, and minute amounts of material waste is produced in the manufacturing process. MJ machines cannot produce steep or negative angles, and removable or dissolvable support structures must be formed to enable the production of such shapes. MJ is used for purposes where exceptional precision is required, e.g., casting molds and dimensionally accurate prototypes. (Yang et al. 2016, Calignano et al. 2017, Ligon et al. 2017, Karakurt & Lin 2020, Tan et al. 2020, Gülcan et al. 2021, Tyagi et al. 2021). MJ printers have enclosed build areas and they are similar or larger in size in comparison to VP and ME printers, and they can be equipped with exhaust systems to eliminate the produced jetting aerosols. The used resins often express poor mechanical properties in comparison to many other AM technologies, and thus MJ can scarcely be used for production of functional parts.

The materials used in MJ and VP manufacturing resemble each other to a great extent. The excess resin, if left on the product, is washed off either by an ultrasonic bath, water, or a solvent, and the surface can be fully cured using a UV-light if needed. Up-to-date MJ machines, however, seldom leave ink residues and therefore post-processes are not always demanded. The resins used in MJ manufacturing are, however, more ink-like and flowing in comparison to VP resins, and usually slightly pre-heated by the manufacturing machine to achieve optimal jetting properties (Gülcan et al. 2021, Hayes et al. 2021, Tyagi et al. 2021). Similar voluntary post-processing techniques may be applied on MJ printed products, as on VP manufactured items.

MJ based MMAM is possible by use of multiple resins if the AM machine is equipped with multiple ink-jet nozzles which are capable of depositing multiple feedstocks simultaneously on-demand. The deposition locations of the feedstocks are determined by a slicing program. The different resins can have unique material and visual properties, and thus multi-colored and multifunctional products with, e.g., stiff sections and flexible joints can be manufactured. (Vaezi et al. 2013, Yang et al. 2016, Calignano et al. 2017, Jasiuk et al. 2018, Karakurt & Lin 2020, Tan et al. 2020, Gülcan et al. 2021).

The hazards and routes of exposure are similar in MJ as in VP manufacturing following the similarity of the used feedstocks. The main VOC exposures are, however, a result of aerosolization of the ink jet stream, in addition to direct evaporation of non-cured resin molecules and the use of solvents. A further dermal chemical hazard emerges from handling, post-processing, and use of the

manufactured products. UFPs may also be formed in the jetting process and through VOC condensation, and these particles, and VOCs, can escape the building enclosure. (Roth et al. 2019, Stefaniak et al. 2019, Zisook et al. 2020, Hayes et al. 2021, Tyagi et al. 2021).

2.3 Polymer materials used in additive manufacturing

Polymeric materials applied in AM machines exist in various forms, including filaments, pellets, liquid resins, and powders (Calignano et al. 2017, Ligon et al. 2017, Jasiuk et al. 2018, Tan et al. 2020, Wu et al. 2020). Some of the used feedstocks are thermoplastic materials which can be repetitively shaped with heat, while materials which can be processed and shaped only once are classified as thermosetting materials. Photosensitive feedstocks which harden after exposure to certain wavelengths of light are applied in certain AM methods as well. A polymer is composed of a repeating base unit, and a mixture of additive substances including pigments or material property enhancers designed to achieve desired material and visual properties. For example, softeners are used to improve the extrudability and flexibility of the polymer, while UV-stabilizers, antioxidants and flame retardants are used to protect the material from external stress factors, and a desired look can be achieved with coloring agents. (Lithner et al. 2011, Ligon et al. 2017, Mikula et al. 2020, Tan et al. 2020, Wu et al. 2020).

2.3.1 Thermoplastic filaments and pellets

Filaments and pellets are both used in ME machines, while the applicable feedstock shape is determined by the machine features. Filaments are usually favored in small-scale ME printers, while pellets are typically applied in industrial ME systems. A wide selection of applicable thermoplastics exists, but the most used polymers in the AM industry are traditional commodity or engineering grades, e.g., polylactic acid (PLA), acrylonitrile butadiene styrene (ABS), or polypropylene (PP), which can be melted and hardened repetitively. The polymer type and used additives determines the properties and behavior of the filament, e.g., the solidification rate, shrinkage, hygroscopicity, and viscosity. Desirable polymer properties include low shrinkage and warpage, good dimensional accuracy, low

thermal expansion, and good flowing and extrudability factors. (Calignano et al. 2017, Jasiuk et al. 2018, Ngo et al. 2018, Mikula et al. 2020, Tan et al. 2020, Wu et al. 2020). Filaments and pellets are sold as ready-to-use units, usually as spools, and bags from which pellets are loaded into an AM machine; pellets are also used as the main feedstocks for filament extrusion, while small polymer shreds and scraps can be applied as well. Thermal processing is detrimental for the polymer which can result in reduced mechanical performance and altered emissions in consecutive extrusion processes. Different polymer blends express variability in their required extrusion temperatures and thermal decomposition resistance, among other extrudability factors, which partly explain the differences in their emission profiles; especially the magnitude of particulate emissions (Azimi et al. 2016, Guillemot et al. 2017, Kwon et al. 2017, Byrley et al. 2019, Ding et al. 2019).

Recycled plastics are applicable raw materials for filament production. However, polymer integrity of such plastics is often compromised. The chemical structure of recycled plastics may have been altered and chemical contaminants may be accumulated in the polymer matrix, functional groups may have been disintegrated, and their functionality and processability are ultimately hindered by repetitive thermal processes. Mechanical performance is also decreased after multiple thermal processing cycles, making them less suitable for production of functional parts. Furthermore, the use of such feedstocks may produce altered airborne emissions in comparison to virgin plastics. (Lithner et al. 2011, Mylläri et al. 2016, Mikula et al. 2020).

2.3.2 Photocurable resins

Photosensitive polymers are liquid, or wax-like resin mixtures used in VP and MJ manufacturing. They are sensitive to UV- or visible light at a particular wavelength which initiates a polymerization reaction called curing within the resin. The resins consist of epoxides or acrylates as functional or structural monomers and oligomers (the main resin body), photoinitiators, inhibitors, sensitizers or retardants, and other additives including solvents (viscosity enhancers). The resin molecules bind together and solidify irreversibly as photoinitiators, the key molecules in the photocuring process, are exposed to light. (Lago et al. 2015, Ligon et al. 2017, Ngo et al. 2018, Stefaniak et al. 2019b, Alifui-Segbaya et al. 2020, Tan et al. 2020, Wu et al. 2020, Pagac et al. 2021, Tyagi et al. 2021, Zhang et al. 2021). A wide selection of resins with

distinctive material properties are available for traditional prototyping and production, while biocompatible resins are available as well. The relatively high cost and weak mechanical properties are the main disadvantages of the resins, but advances in mechanical performance have been made recently as the formulations of technical and composite resins have developed notably. (Petretta et al. 2019, Tan et al. 2020, Wu et al. 2020, Gülcan et al. 2021, Tyagi et al. 2021). Biocompatible resins are used for purposes where the manufactured product is designed to be in contact with biological tissues, e.g., as dental devices, prostheses, or cell and organ matrixes used for tissue repair. (Calignano et al. 2017, Jasiuk et al. 2018, Alifui-Segbaya et al. 2020, Tan et al. 2020, Wu et al. 2020, Gülcan et al. 2021, Pagac et al. 2021, Zhang et al. 2021).

2.3.3 Powders

Powders feedstocks are used in PBF machines and their subtypes, and in certain other AM methods, e.g., binder jetting. Polyamide (PA) is the most widely used polymer type, followed by other thermoplastics with good dimensional stability and a wide sintering window, e.g., polyesters, polyethylene, and polypropene. (Ligon et al. 2017, Ngo et al. 2018, Tan et al. 2020, Wu et al. 2020). The desired particle size range of the powder is around 20-80 µm: the smaller particles fill in the voids between the larger particles, while contact surface area is minimized by the spherical shape of the particles. Stored powder often demands pre-processing where powder clumps are broken down, after which the powder is loaded into an AM machine. A portion of leftover feedstock from a previous manufacturing process is often recycled to reduce waste, at the cost of increased particle size. The powder matter is usually heated close to the polymer's melting point under a controlled atmosphere to enable efficient layer fusion which can produce chemical emissions through thermal decomposition. Powdered AM feedstocks are normally, however, heavily treated with additives to withstand the prolonged thermal load. (Ligon et al. 2017, Tan et al. 2020, Damanhuri et al. 2021, Wang et al. 2021).

2.3.4 Composites

Novel composite and biological particle containing biocomposite (BC) materials have been introduced to the AM consumer markets over recent years. Composite materials refer to a material where at least two insoluble materials with different physiochemical properties are merged into one functional material with special physiochemical properties. The criteria of the source material heterogeneity is the critical separating factor between composite materials and solutions. In AM, the composite term often refers to micro- or nano-reinforced plastics which constitute of a thermoplastic polymer base, to which micro- or nano-scale material, e.g., wood or glass fibers, metals, or carbon nanotubes are added to introduce new properties, e.g., increased mechanical performance or conductivity, or altered visual appearance. Composite materials can be used as filaments, pellets, and powders especially in the ME and PBF methods, but composites for SLA, MJ, and other technologies have been developed as well. (Ligon et al. 2017, Ngo et al. 2018, Alberts et al. 2020, Dickson et al. 2020, Tan et al. 2020, Wu et al. 2020). The introduction of bio-matter, e.g., wood particles into the polymer matrix in the production of BC materials can lead to altered emissions when used as AM feedstocks. Heat-treatment of wood produces various organic compounds, including terpenes, carboxylic acids, and carbonyls which increase the diversity of the produced chemical contaminants in the AM process. (Kim et al. 2006, Höllebacher et al. 2015).

2.4 Indoor air pollutants of interest

Multiple indoor air pollutants which can impair air quality and induce human health hazards are emitted in the various AM processes. These emissions are produced through thermal decomposition of polymer feedstocks, or during storage, handling and processing of feedstocks and manufactured products. It is of particular importance to identify the contaminant compositions and exposure characteristics to determine the need for and type of effective contaminant control measures.

2.4.1 Volatile organic and carbonyl compounds

By definition, a volatile organic compound (VOC) is a carbon-based compound which possess a maximum boiling temperature of 250 °C and a minimum vapor pressure of 0,01 kPa at 20 °C. Due to these characteristics, VOCs can vaporize into air phase under normal room conditions from where they can be absorbed through skin and lungs. VOCs can be expanded to very volatile substances (VVOCs) and semi-volatile substances (SVOCs), which are either more, or less, volatile than generic VOCs, but express similar chemical properties and structure. VOCs are ubiquitous chemicals encountered as mixtures, and many VOC species, including several of those encountered in plastics processing are linked to various adverse effects like discomfort, inflammation, cytotoxic effects, CNS depression, asthma, irritation, oxidative stress, respiratory illnesses, and even cancer. (WHO 2006, Wolkoff et al. 2006, Rumchev et al. 2007, Sarigiannis et al. 2011, Win-Shwe et al. 2013, Unwin et al. 2013). The plausible effects of the complex VOC mixtures are difficult to evaluate, and certain compounds can have an increased effectiveness through synergism when co-exposed to. The likelihood and severity of the various adverse effects grows as the chemical burden of a body increases. (Wolkoff et al. 2006, Rumchev et al. 2007, Win-Shwe et al. 2013).

VOCs can constitute of only carbon and hydrogen atoms, or specific functional groups may be attached to the carbon body. The properties of an individual VOC are usually determined by the number of carbon atoms and the attached functional groups, which are also used for the classification of VOCs under sub-categories. The smaller number of carbon atoms and the presence of functional groups that include oxygen atoms usually contribute to increased biological reactivity and potential for adverse effects induction. (Wolkoff et al. 2006, Win-Shwe et al. 2013). Due to the wide range of existing VOCs, a total VOC (TVOC) concentration can be used to express the total amount of VOC contamination in the air. This total concentration is not suitable for specific health effect estimation as individual compounds can cause very specific effects at different exposure levels, but it can be used to estimate the magnitude of VOC pollution and total exposure levels. The plausible hazards must be assessed through evaluation of individual compounds, their air concentrations or exposure levels, and synergism. It should be also noted that even though various exposure limits have been established for various VOC species, adverse health impacts have been documented to be induced at much lower levels as well. (Wolkoff et al. 2006, Rumchev et al. 2007, Tuomi & Vainiotalo 2014.)

Carbonyl compounds are a sub-group of chemicals under VOCs. Carbonyls are characterized by the functional carbonyl group (an oxygen atom double-bonded with a carbon atom) present in their chemical structure. The main principles and characteristics that apply to VOCs, do so to carbonyls. Some differences exist, however; they always contain the functional carbonyl group and especially carbonyls of low molecular mass are generally more volatile and biologically reactive than generic VOCs with a longer carbon base chain. Principally, they are formed as emission products in similar occasions when VOCs are produced. Carbonyls of low molecular mass are also formed as secondary by-products of chemical reactions in the air phase, especially in the presence of ozone, and other oxidants or reactive species (Zhang 1994, Wolkoff et al. 2000 & 2006, Sarigiannis et al. 2011).

VOCs have numerous sources, and they are formed and encountered as mixtures through a variety of chemical reactions (Wolkoff et al. 2006, Rumchev et al. 2007, Destaillats et al. 2008, Sarigiannis et al. 2011, Win-Shwe et al. 2013). The most important sources in terms of this thesis are thermal decomposition of polymers and direct aerosolization from a source, e.g., a photopolymer vat or a jetting nozzle spray. Thermal polymer degradation occurs in processes where polymers are used as the feedstock material and external heat is applied on the material during manufacturing process, e.g., in ME and PBF manufacturing. A higher processing temperature results in a higher number of produced VOCs, as the degree of depolymerization and decomposition increases in tandem with temperature (Wojtyła et al. 2017, Ding et al. 2019). Additional sources are resin leaks, open or leaking VP or MJ machines, and storage or replacement of resin vats. Furthermore, chemical post-processing of any manufactured object is an occasion where VOC exposures likely reach elevated levels.

2.4.2 Dust and coarse particles (PM$_{15}$, PM$_{10}$)

Dust particles are particulate matter which can be suspended in air phase for a limited period of time and have a size-dependent gravitational settling speed. Inhalable dust particles possess a maximum aerodynamic diameter of 100 μm, with aerodynamic diameter referring to a spherical particle with density of 1 g/cm^3 that has the same settling speed as the true particle in question. This definition disregards the true shape and density of the real particle, as the most important

factor determining the lung penetrability and deposition of a particle is the aerodynamic diameter. Dust particles can be divided further into three categories by their aerodynamic diameter. Inhalable fraction (particle size range 30–100 μm) refers to the largest inhaled particulate matter which deposits readily in the upper airways. Thoracic fraction (particle size 10–30 μm) can penetrate deeper, beyond the larynx and into the thorax and bronchus, while respirable fraction (particle size <10 μm) is poorly deposited into the upper airways, and thus, these particles can reach the ciliated airways. Particles of the respirable fraction are sometimes referred to as PM_{10} particles. PM_{10} particles, however, can also refer to particles in the aerodynamic diameter range between 10 and 2.5 μm. (Brown et al. 2013.) The particles above the aerodynamic diameter of 10 μm are usually of little concern as they readily deposit in the upper airways from where they are quickly eliminated. PM_{15} size fraction, which represents particles with an aerodynamic diameter of 15 μm and below, is rarely used as a substitute to PM_{10} particles. Dust and coarse particle exposure can generally induce both short and long-term effects including allergies, obstruction, inflammation, reduced lung function, and less severe momentary effects including cough, irritation, and wheezing. The smaller particles produce a greater hazard as they penetrate deeper and are cleared at a notably slower pace. (Oberdörster 1988, WHO 1999 & 2021, Carvalho et al. 2011, Brown et al. 2013, Lee et al. 2014). Dust particles are occasionally encountered in the AM industry, and dust is a major exposure agent only in the pre- and post-processes related to the PBF, and similar methods, but also produced in lesser amounts when any manufactured products are sanded or processed abrasively.

2.4.3 Fine particles (PM$_{2.5}$)

Fine particles are a transitional group between coarse and ultrafine particles. They are usually described as particles with an aerodynamic diameter of 2.5 μm and below, sometimes including the ultrafine particle (UFP) fraction as well. Depending on the source, $PM_{2.5}$ can also refer to particles of aerodynamic diameter range between 2.5 and 0.1 μm, thus excluding the ultrafine fraction. Fine particles have a slower settling speed in comparison to dust and coarse particles, with the smallest particles being almost unaffected by gravitational forces. As the impact of gravitational forces reduces, the effectiveness of diffusional and electrical forces increases. This results in altered deposition efficiency, and the non-deposited

portion of the particles are exhaled instead. Fine particles can deposit deep in the lungs, and the smallest particles can reach the alveoli and enter the circulatory system. Airborne fine particle mass concentration is more universally used as an indicator of ambient air quality rather than an occupational exposure parameter, despite the various air quality guidelines being introduced to preserve human health and the quality of life. Fine particles are associated with increased mortality and morbidity, pulmonary and systemic inflammation, reduced lung function, and cytotoxic effects. Fine particles can also translocate across the body and deposit into vital organs, where localized effects can be induced. (WHO 1999, Nurkiewicz et al. 2006, Peters et al. 2006, Pope & Dockery 2006, Carvalho et al. 2011, Lee et al. 2014). Fine particles are documented to be produced in thermal processing of plastics, and plausibly following the aerosolization of ink jet spray (Ryan & Hubbard 2016, Rao et al. 2017, Damanhuri et al. 2019, Byrley et al. 2020, Ding & Ng 2021).

2.4.4 Ultrafine particles

Ultrafine particles (UFPs) are submicron particulate matter with an aerodynamic diameter of and below 0.1 µm. These particles originate from condensation and agglomeration of VOCs and other inorganic and organic airborne substances, including semi-volatile organic compounds, and their surface chemistry and properties are strongly affected by their chemical composition. The particle composition also affects the physiochemical properties of the particles, as well as general toxicity. Particles with different compositions travel and impact human body in very different ways, as inert particles can travel through the body without interactions, while on the other hand, reactive particles can interact with cells and tissues and produce a biological response. (Peters et al. 2006, Shahnaz et al. 2012, Ding et al. 2019). The small size of these particles contributes to their special properties. The effective surface area and area-to-mass ratio of UFPs are very high in comparison to larger particles. Gravitational forces have a negligible impact on them, and they are easily inhaled deep into the lungs and the alveoli where they can be transferred into the blood stream. Deposition occurs mainly through diffusion and electrical forces, and the non-deposited portion of UFPs is exhaled. Ultimately, UFPs can translocate into vital organs and produce systemic and localized adverse effects. The large surface area and effective penetrability enables the deposition of surface-adsorbed chemicals into the lungs and blood, which contribute to the

toxicity of the particles and increased chemical burden of the body. (Oberdörster 2001, Pope & Dockery 2006, Carvalho et al. 2011, Shahnaz et al. 2012, Lee et al. 2014, Bakand & Hayes 2016, Ohlwein et al. 2019). In contrast to larger particles, the number concentration is the most meaningful exposure parameter in the case of UFPs, rather than mass concentration, following the special particle properties (Oberdörster 2001).

Adverse health impacts induced by UFPs include increased cardiovascular morbidity and mortality, cytotoxic effects, systemic and respiratory diseases and inflammation, reduced respiratory function, generation of reactive oxygen species and oxidative stress, localized organ damage, and even DNA damage or alteration of cell cycle regulation. Evidence for the induction of neurodegenerative effects is growing as well. UFPs can be transported across the body and penetrate biological membranes, and ultimately, they can deposit in the brain and other regions of the CNS where inflammatory and cytotoxic effects can be induced, plausibly producing neurodegenerative effects, among other impacts. (Oberdörster 2001, Nurkiewicz et al. 2006, Peters et al. 2006, Pope & Dockery 2006, Shahnaz et al. 2012, Lee et al. 2014, Bakand & Hayes et al. 2016, Ohlwein et al. 2019).

UFPs are formed in thermal AM processes and encountered in situations where substantial amounts of chemical substances are released. These include the use of AM methods where elevated temperatures are used in the manufacturing process, in addition to the use of resin feedstocks and post-processing chemicals which can evaporate and condensate into physical particles. Like VOC emissions, higher processing temperatures are linked to higher emitted UFP concentrations as the higher temperatures are more deteriorating for the feedstock. UFPs are also formed following the aerosolization of MJ ink jet spray. The formed particles are initially nano-sized, but they can grow into fine particles as additional airborne substances condense on their surface. (Pope & Dockery 2006, Chen et al., 2012; Stabile et al. 2017, Wojtyła et al. 2017, Zhang et al., 2017, Chen et al., 2017; Kwon et al., 2017; Rao et al., 2017, Ding et al. 2019.) Furthermore, ozone has been found to increase the rate of UFP formation in the presence of organic aerosols, especially terpenes. Indoor ozone can originate from outdoor sources, and it is generated by electric appliances, and thus, both VOCs and ozone are commonly co-encountered in an AM process, promoting the formation of UFPs. (Sarwar et al. 2004, Destaillats et al. 2008, Fadeyi 2015, Wolkoff 2020).

2.5 Established 3D printer emission literature

The absence of universal methodology for AM machine emission measurements is a recognized limitation for the subject's research. A standard procedure (ANSI/CAN/UL 2904: Standard method for testing and assessing particle and chemical emissions from 3D printers) for desktop ME 3D printer emission determination in a chamber was issued in 2019 by Underwriters Laboratories and Georgia Institute of Technology, however, but no similar standardized procedures have been proposed for other AM systems. The diversity of the AM environments (homes, offices, laboratories, chambers), AM machine technologies and feedstocks, applied research methods (measurement of particles, gases and aerosols, individual chemicals) and instruments (real-time measurements, sample collection for later analysis, particle counting based on optics or particle condensation), and data presentation (results shown in a variety of units, e.g., emission rate, emission per mass unit, mass or number concentration) create difficulties in research evidence and emission comparison (Byrley et al. 2019, Min et al. 2021).

2.5.1 Material extrusion method

ME is the most extensively studied AM method up to date, and it has been currently identified as potentially the highest emitter of VOCs and UFPs of all AM methods following their commonly open design, absence of in-built exhaust systems, and high operation temperatures (Min et al. 2021). ME printers are documented to emit mainly organic compounds and UFPs, while some research documents have also reported elevated fine and coarse particle concentrations. Roth et al. (2019) and Stefaniak et al. (2021) identified VOC and particulate matter exposures as major hazards of the ME technology, in addition to hazards related to plastic additives and machine operation, e.g., burn hazard. Notable variance in the documented emissions can be observed in the relatively comprehensive body of literature following a wide variety of applied research methods and setups. For this reason, a uniform review of literature is difficult to conduct. As an example, TVOC emission rates have been documented to range from as low as 1 µg/min or below limit of detection to up to 10^6 µg/min. The documented UFP emission rates range between the magnitudes of 10^5–10^{12} #/min depending on feedstock and printing parameters. The documented particle morphologies have ranged from singular

nanoscale particles to micrometer-sized soot-like agglomerates. (Roth et al. 2019, Dobrzyńska et al. 2021, Stefaniak et al. 2021). Selected VOC and UFP emission and exposure level research data for PLA, ABS, and biocomposite feedstocks are presented in Tables 1–2. The magnitude and compositions of the produced emissions are identified to be most notably affected by the design of the operated 3D printer and the applied feedstock and processing temperatures, while other 3D printing parameters, e.g., feed rate, influences emissions as well. (Zhang et al. 2017, Zontek et al. 2017, Pelley 2018, Byrley et al. 2019, Davis et al. 2019, Gu et al. 2019a, Poikkimäki et al. 2019, Dobrzyńska et al. 2021, Min et al. 2021). Majority of the recorded contaminant levels, however, are reported to fall below occupational exposure limits (OELs) or other guideline values, albeit some potentially toxic substances, e.g., styrene, acrylates, aromatic hydrocarbons, and low molecular weight carbonyls have been found. Nevertheless, the emissions are complex mixtures and (long-term) co-exposure to the various emission components can possess hazardous characteristics.

Table 1. Chemical compounds and emission rates encountered in material extrusion 3D printing, as documented in selected literature. (1/2)

Reference	Target	Measurement instruments	Study design	Feedstock	Temperature °C (nozzle/bed)	TVOC concentration	TVOC emission rate (µg/min)	Primary compounds
Kim et al. 2015	TVOC, carbonyl compounds, selected VOCs	Real-time sensor, cartridge samples + HPLC, adsorbent tube samples + GC-MS	Chamber, multiple printers	ABS	250/-	1550 ppb (approx. 6000 µg/m³)	n/a	Ethylbenzene, xylene, formaldehyde
				PLA	210–220/-	Below LOD	n/a	Toluene, formaldehyde, acetaldehyde
Azimi et al. 2016	TVOC, individual VOCs	Adsorbent tube samples + GC-MS	Chamber, multiple printers	ABS	230–240/100–110	n/a	40–160	Styrene, propylene glycol, ethylbenzene
				PLA	200–230/20–110	n/a	10–15	Lactide, 2-(2-bytoxyethoxy)ethanol, 2-ethyl-2-hexanal
				Biocomposite	200/65	n/a	50	Caprolactam, 2-ethyl-2-hexanal, acetic acid
Steinle 2016	TVOC, individual VOCs	Real-time sensor, adsorbent tube samples + GC-MS	Chamber, open printer	ABS	-/-	550 µg/m³	10	Styrene, ethylbenzene, cyclohexanone
				PLA	-/-	770 µg/m³	16	Methyl methacrylate, n-butanol, cyclohexanone
Vance et al. 2017	TVOC	Real-time sensor	Chamber, open printer	ABS	-/-	0.8 ppm (approx. 3000 µg/m³)	n/a	n/a
				PLA	-/-	Below LOD	n/a	n/a
Floyd et al. 2017	TVOC, individual VOCs	Real-time sensor, adsorbent tube samples + GC-MS	Chamber, open printer	ABS	210/70	9000 µg/m³	64	Styrene, ethylbenzene, acetophenone
				PLA	210/70	7000 µg/m³	50	Acrylic acid dimer, d-limonene, decane
Mendes et al. 2017	TVOC, individual VOCs	Real-time sensor, adsorbent tube samples + GC-MS, cartridge samples + GC-MS	Chamber, open printer	ABS, PLA	200–250/70–110	*230–270 µg/m³	n/a	Styrene (ABS), low carbonyls (both), *confounding particle counter fumes
			Laboratory, open printer	ABS, PLA	200–250/70–110	*250–520 µg/m³	n/a	Styrene (ABS), low carbonyls (both), *confounding particle counter fumes
Stefaniak et al. 2017b	TVOC, individual VOCs	Real-time sensor, canister samples + GC-MS	Chamber, enclosed printer	ABS	230/110	1600 µg/m³	18–59	Styrene, isopropanol, ethanol
				PLA	215/20	80 µg/m³	<2	Isopropanol, ethanol, acetone
Bravi et al. 2019	TVOC, individual VOCs	Activated carbon vial	Room, enclosed printer	ABS	230/-	391 µg/m³	n/a	Styrene, cyclohexane, acetone
				PLA	215/-	255 µg/m³	n/a	Acetone, hexane, toluene

GC = gas chromatography, HPLC = high performance liquid chromatography, LC = liquid chromatography, LOD = limit of detection, MS = mass spectrometry.

44

Table 1. Chemical compounds and emission rates encountered in material extrusion 3D printing, as documented in selected literature. (1/2)

Reference	Target	Measurement instruments	Study design	Feedstock	Temperature °C (nozzle/bed)	TVOC concentration	TVOC emission rate (µg/min)	Primary compounds
Davis et al. 2019	TVOC, individual VOCs, selected carbonyls	Adsorption tube samples + GC-MS, cartridge samples + HPLC	Chamber, various printers	ABS	230–270/20–110	n/a	14	Styrene, benzaldehyde, ethylbenzene
Gu et al. 2019a	Chemical composition of particles, individual VOCs and carbonyls	Quartz filter collection, adsorbent tube samples + GC-MS	Chamber, semi-open printer	ABS	230–275/80	n/a	15	Plasticizers, organophosphorous compounds, aromatic hydrocarbons incl. styrene, acetaldehyde, acetone, 2-propenal, ethanol
Gu et al. 2019b	TVOC, individual VOCs	Adsorbent tube samples + GC-MS	Chamber, semi-open printer	ABS	-/-	62 µg/m^3	n/a	Styrene, ethylbenzene, benzaldehyde
Stefaniak et al. 2019a	TVOC, individual VOCs	Real-time sensor, adsorbent tube samples + GC-MS	Room, multiple printers	Multiple	190–270/50–80	n/a	3.3×10^6	Acetone, isopropanol
			Room, enclosed printer	ABS	270/100	n/a	1.2×10^5	Acetone, isopropanol
			Laboratory, semi-open printer	PLA	215/25	n/a	1.6–3.1×10^4	-
			Laboratory, open printer	PLA	215/25	n/a	2.1×10^3–4.4×10^4	-
Stefaniak et al. 2019b	TVOC, selected VOCs	Real-time sensor	Occupational setting, enclosed printer	ABS	265/95	n/a	9.4×10^4	Acetone, naphtha, hexane
Chan et al. 2020	TVOC, individual VOCs	Adsorbent tube samples + GC-MS or LC	Occupational setting, semi-open printer	PLA	-/-	270 µg/m^3	n/a	Isopropanol, acetone, formaldehyde
			Occupational setting, multiple printers	PLA	-/-	1700 µg/m^3	n/a	Isopropanol, acetone, ethanol
Zisook et al. 2020	TVOC, selected VOCs	Canister samples + GC-MS, real-time sensor	Laboratory, enclosed printer	ABS	230/-	Below LOD	Below LOD	Isopropanol

GC = gas chromatography, HPLC = high performance liquid chromatography, LC = liquid chromatography, LOD = limit of detection, MS = mass spectrometry.

Table 2. Ultrafine particle concentrations and emission rates encountered in ME 3D printing, as documented in selected literature. (1/2)

Reference	Measurement instruments	Particle size range (nm)	Study design	Feedstock	Temperature °C (nozzle/bed)	Average or peak concentration (#/cm³)	Average emission rate (#/min)
Stephens et al. 2013	SMPS	10–420	Room, multiple printers	ABS	220/118	2.8×10^4	2.0×10^{11}
				PLA	200/18	9.7×10^3	2.0×10^{10}
Kim et al. 2015	SMPS	10–420	Chamber, multiple printers	ABS	250/-	1.7×10^6	1.6×10^{10}
				PLA	210–220/-	$4.6–5.2\times10^4$	$4.3–4.8\times10^8$
Azimi et al. 2016	CPC	10–1000	Chamber, multiple printers	ABS	230–240/100–110	$2.6–9.0\times10^5$	$1.7\times10^{10}–9.4\times10^{10}$
				ABS	200/110	8.6×10^5	1.7×10^{10}
				PLA	230/-	2.1×10^3	1.3×10^8
				PLA	190–200/45–110	$1.5–3.1\times10^3$	$9.2–9.6\times10^7$
				Biocomposite	200/65	2.3×10^3	8.8×10^7
Deng et al. 2016	CPC	2.5–1000	Room, enclosed printer	ABS	200/110	$8.1\times10^4–2.2\times10^5$	n/a
				ABS	220–240/110	5.6×10^3	n/a
				PLA	180–200/60	$3.7–5.3\times10^3$	n/a
				PLA	220/60	3.1×10^4	n/a
Stabile et al. 2016	CPC, SMPS	>4, 6–220	Room, open printer	PLA	220–240	$0.5–4.9\times10^4$	$0.7–1.0\times10^{10}$
				Biocomposite	220–240	$1.5–9.3\times10^4$	$0.6–2.6\times10^{11}$
				Biocomposite	230–240	$7.0–9.5\times10^5$	$1.9–2.8\times10^{12}$
				Biocomposite	210–240	$0.3–9.5\times10^5$	$1.7\times10^{10}–2.7\times10^{12}$
Steinle 2016	Electrical diffusion battery, miniDiSC	7–400	Chamber, open printer	ABS	-/-	1.1×10^4	2.4×10^8
			Room, open printer	PLA	-/-	8.9×10^4	2.1×10^9
				PLA	-/-	$1.7–3.2\times10^3$	n/a
Vance et al. 2017	SMPS	14.6–680	Chamber, open printer	ABS	-/-	$5\times10^5–2\times10^6$	$1.3\times10^{10}–1.1\times10^{11}$
				PLA	-/-	1.8×10^5	1.5×10^{10}
				Biocomposite	-/-	1.2×10^3	1.1×10^8
	CPC, SMPS	14.6–680, 4–700	Laboratory, open printer	ABS	-/-	$2–6\times10^4$	n/a
			Office, open printer	ABS	-/-	$0.2–4\times10^4$	n/a
			Classroom, open printer	ABS	-/-	$1–4\times10^3$	n/a
Bharti & Singh 2017	CPC	20–1000	Library, multiple printers	PLA	215/-	3.9×10^4 (three printers) / 5.3×10^4 (four printers) / 8.7×10^4 (five printers)	n/a

CPC = condensation particle counter, SMPS = scanning mobility particle sizer.

Table 2. Ultrafine particle concentrations and emission rates encountered in ME 3D printing, as documented in selected literature. (2/2)

Reference	Measurement instrument	Particle size range (nm)	Study design	Feedstock	Temperature °C (nozzle/bed)	Average or peak concentration (#/cm³)	Average emission rate (#/min)
Kwon et al. 2017	SMPS	10–420	Chamber, semi-enclosed printer	ABS	230–240/110–120	$1.4–2.1\times10^4$	n/a
				ABS	265/90	$1.1–1.3\times10^5$	
				PLA	220/60	1.5×10^3	
				PLA	265/90	4.2×10^4	
				Biocomposite	215/60	1.4×10^3	
				Biocomposite	265/90	4.5×10^5	
Zhang et al. 2017	CPC, SMPS, OPS	7–3000, 7–300, 300–25000	Chamber, multiple printers	ABS	230–270/-	$10^5–10^6$	$10^9–10^{11}$
				PLA	210–230/-	$10^3–10^4$	$10^7–10^8$
Zontek et al. 2017	CPC	10–1000	Laboratory, enclosed printer	ABS	213/-	2×10^5 inside printer enclosure, 3×10^3 outside printer enclosure	n/a
			Room, enclosed printer	PLA	180–230/-	3.3×10^3	
Gu et al. 2019a	FMPS	5.6–560	Chamber, semi-open printer	ABS	260–275/80	$2.3–4.4\times10^5$	$2.9\times10^{10}–1.3\times10^{11}$
				ABS	230–250/80	$3.3–8.7\times10^4$	$4.2\times10^9–2.3\times10^{10}$
Poikkimäki et al. 2019	CPC coupled with particle size magnifier	1.4–1000	Laboratory, semi-open printer	ABS	240–250/90	$7.1\times10^3–3.7\times10^4$	$1.9\times10^9–1.1\times10^{10}$
				PLA	210–220/60	$1.6–5.7\times10^3$	$4.3\times10^8–1.4\times10^9$
				Biocomposite	210–220/60	$2.7–3.1\times10^5$	$9\times10^{10}–1\times10^{11}$
Stefaniak et al. 2019a	CPC	20–1000	Room, various printers	Multiple	190–270/50–80	n/a	9.7×10^{10}
			Room, enclosed printer	ABS	270/100	n/a	7.3×10^{10}
			Laboratory, semi-open printer	PLA	215/-	n/a	$1.9\times10^9–2.1\times10^{11}$
			Laboratory, open printer	PLA	215/-	n/a	$5.5\times10^9–9.0\times10^{10}$
Zisook et al. 2020	CPC	20–1000	Laboratory, enclosed printer	ABS	230/-	1.5×10^4	n/a
Ding & Ng 2021	SMPS	10–420	Office, open printer	ABS	260/-	3.3×10^4	n/a
				PLA	220/-	Below LOD	
			Laboratory, enclosed printer	ABS	260/-	Below LOD	

CPC = condensation particle counter, FMPS = fast mobility particle sizer, LOD = limit of detection, OPS = optical particle sizer, SMPS = scanning mobility particle sizer.

The identified major compounds emitted in ME 3D printing are often known plastic decomposition products, low molecular weight carbonyls, alcohols, and aromatic hydrocarbons (Mendes et al. 2017, Du Preez et al. 2018, Stefaniak et al. 2019b, Secondo et al. 2020.) Azimi et al. (2016) documented that the VOC emissions are dominated by the relatively well-known main decomposition products of the used filament type, e.g., styrene in the case of ABS, and lactide in the case of PLA. Inorganic gases have also been included in multiple studies, but they have not been found at concentrations above their limits of detection. Davis et al. (2019) detected a total of 216 individual VOCs, including multiple carcinogens and substances which can induce reproductive toxicity in their study using multiple filament types. ABS was documented to produce the most complex VOC emissions, as up to 177 individual compounds were identified during its use, whereas PLA was documented to emit up to 57 chemical substances. The 3D printer type had a surprisingly great impact on the produced emissions, even when the exact same feedstock was used in the printers. Filament color had an influence on the emissions as well, suggesting that additives play a part in the production of 3D printer emissions. Floyd et al. (2017) documented very similar levels of TVOC emissions from the use of multiple filaments when printed at a static temperature using a single 3D printer, although the chemical compositions were different between the feedstocks, emphasizing the impact of the nozzle temperature and feedstock choice on the 3D printer emissions. Stefaniak et al. (2017b) also found in their study that the TVOC emission rate was almost doubled during a printer malfunction.

Chemical post-processing tasks are identified as situations where workers can be exposed to volatile solvents at relatively high concentrations, as well as dermally. Acetone peaked at 900 mg/m^3 during acetone polishing in a study by Du Preez et al. (2018), while 100–250 mg/m^3 levels of chloroform was recorded during chloroform polishing. These concentrations, however, declined quickly and the exposures were short-term. Stefaniak et al. (2017b) and Du Preez et al. (2018) also documented that ME manufactured products continued outgassing VOCs after production, plausibly resulting in unexpected secondary VOC exposures. Gonzalez et al. (2017) also identified free chemical substances in PLA polymer matrix that could spontaneously travel to the product's surface and evaporate or transfer to surfaces in contact with the product.

ME printers using ABS and PLA feedstocks have been recorded to produce UFPs mostly in the 15-70 nm size range, with ABS feedstocks producing slightly larger particles than PLA feedstocks (Byrley et al. 2019). Zhang et al. (2017) stated that

vapor condensation is the main mechanism behind UFP formation, and that greater concentrations of organic vapors allows the production of a greater number of particles, which can grow larger in size as well. They also documented that UFPs dominated particle number concentrations, but 200–500 nm particles dominated particle mass concentrations. Kim et al. (2015), Zontek et al. (2017) and Secondo et al. (2020) reported in their research articles that up to 99 % of particles produced by ME 3D printers are nanoscale. The UFP emissions are documented to be influenced by the same factors as VOC emissions. These include the feedstock and printer types, and the printing parameters, especially nozzle temperature. (Deng et al. 2016, Stabile et al. 2016, Mendes et al. 2017, Zhang et al. 2017, Byrley et al. 2019, Jeon et al. 2020). Jeon et al. (2020) documented an analogous finding as Floyd et al (2017), but on behalf of UFPs: when printed at similar temperatures the emissions produced by different feedstocks are at very similar levels with each other, promoting the importance of appropriate temperature settings as a 3D printer emission control measure. This is not a universally consistent finding, however, as Deng et al. (2016) recorded ABS to produce more particles than PLA at the same 3D printer settings. Vance et al. (2017) identified additional factors which influence the UFP formation in ME 3D printing: Semi-VOCs likely contribute for the UFP formation and growth, as these compounds are volatilized as they pass through the printer nozzle, but quickly condense at atmospheric temperature. Certain additive substances were speculated to behave similarly, and the additive pigments have been documented to influence the magnitude of produced particle emissions.

Several researchers, including Yi et al. (2016) and Mendes et al. (2017) have documented that printer malfunctions, where the filament is suspect for burning, produce a large burst of particles. The UFP emission rates and concentrations can increase by multiple orders of magnitude in such scenarios. Multiple other researchers, including Deng et al. (2016), Steinle (2016), Jeon et al. (2020), and Alberts et al. (2021) have also documented that ME printers produce an initial UFP burst as the 3D print job starts following thermal filament residue decomposition in the nozzle, and the particles are found to grow gradually as the print job continues, suggesting that the UFPs agglomerate into larger particles which are occasionally detected with fine and coarse particle measurement devices at low concentrations (Yi et al. 2016, Rao et al. 2017, Jeon et al. 2020).

According to Farcas et al. (2019) and Zhang et al. (2019), both PLA and ABS particles expressed cytotoxic properties, with PLA being, surprisingly, more toxic than ABS, which contradicts the chemical characterization of 3D printing fumes.

ABS, however, produced more and larger particles per mass unit of printed material. Additives, including metal pigments, were speculated to have a major impact on the toxicity and particle formation efficiency, which could explain the unpredicted results. The impact of filament color on the magnitude of particle emissions, and the presence of metal components has been documented in other studies as well. Generally, the particles collected during ME printer operations mostly consist of carbon and oxygen. (Steinle 2016, Yi et al. 2016, Rao et al. 2017, Stefaniak et al. 2017b, Gu et al. 2019, Stefaniak et al. 2019b, Kim et al. 2020a, Zisook et al. 2020, Alberts et al. 2021).

Larger particles have been documented in multiple studies to be produced in ME 3D printing in small amounts. The documented micrometer-scale particle mass concentration levels have ranged from below 1 µg/m^3 to around 0.1–1 mg/m^3 (Kim et al. 2015, Steinle 2016, Chan et al. 2020, Ding & Ng 2021). Coarse particle number concentrations have been documented to range around 5–50 #/cm^3 (Zhou et al. 2015, Gu et al. 2019a). Rao et al. (2017) displayed in their study that PM$_{2.5}$ particle emissions were affected by ambient relative humidity (RH), with higher humidity levels increasing the particle emissions. This is a consistent finding with VOC emissions in general (Manoukian et al. 2015). The increased VOC emissions following a higher RH level supposedly increased the particle formation efficiency, resulting in a greater number of particles which were also found to be physically larger at higher RH levels.

The introduction of commercial filament extruders into the consumer markets has made them a relevant research subject as well, given their capability to produce ME printer feedstocks from virtually any thermoplastics, including household waste plastics (HWPs). They resemble ME printers by their operational principle as they heat the feedstock material up until it can be extruded through a nozzle, and pulled into a filament form. (Byrley et al. 2020, Mikula et al. 2020). The emissions from these machines have been documented in one study by Byrley et al. (2020). A filament extruder using ABS and PLA feedstocks produced similar UFP and PM$_{2.5}$ emissions as desktop ME 3D printers. UFPs peaked at 2×10^6 #/cm^3 when ABS pellets were extruded, and the particles were around 50–100 nm in size. An emission rate of 3.5×10^{11} #/min was calculated for these particles. 11 individual VOCs, including styrene, aromatic hydrocarbons, and acetophenone were identified from air samples. The extrusion of PLA pellets produced an UFP peak of 2×10^4 #/cm^3, with particles ranging around 90–200 nm in size. The corresponding emission rate for UFPs was 1.7×10^9 #/min. 15 individual VOCs were found, including lactide, aromatic

hydrocarbons, toluene, and diethyl phthalate. Pulverized PLA, surprisingly, produced mostly 50–80 nm sized UFPs at up to 3.5×10^5 #/cm^3 concentration level. The identified VOCs were similar to those encountered using granulated PLA, with the addition of over 10 compounds including butyl lactate and styrene.

Filament extruders also make it plausible to recycle failed prints into new feedstocks. Thermal recycling has, however, been found to influence the emission profiles of plastics. The current research literature suggests that chemical emissions are reduced after repetitive thermal processing as readily volatilized substances are reduced in the polymer matrix. This is expected to reduce UFP emissions as well, as less matter that enables UFP formation is released into the air phase. The chemical emission profile is suspect to alter after thermal recycling as well, as impurities, contaminants, and chemical reaction products which can be potentially hazardous can accumulate into the polymer matrix. Recycling is, therefore, expected to reduce the magnitude of emissions, but also alter the chemical emission profile. (Mylläri et al. 2016, Cabanes et al. 2020).

2.5.2 Vat photopolymerization method

According to Roth et al. (2019) and Stefaniak et al. (2021), the major hazards originating from VP manufacturing process are inhalation exposure to VOCs, dermal exposure to manufacturing resins, and (UV) laser exposures. Photocurable resins, including the ones designed for biomedical applications, have been identified to induce allergic dermatoses and inflammation in dental personnel, and more recently, AM personnel as well. (Savonius et al. 1993, Chang et al. 2004, Creytens et al. 2017.) The resins components include compounds with toxic properties (Jorge et al. 2003, Fukumoto et al. 2013, Kostić et al. 2020), and novel chemical compounds, including free radicals and compounds of low molecular weight are produced within the resin in the photocuring process (Lago et al. 2015, Ligon et al. 2017) as supported by the findings by Alifui-Segbaya et al. (2020) who found that up to 25 % of the components in analyzed resin feedstocks were not listed in the resin component description. These compounds, in addition to the resin base units, e.g., acrylates and epoxies, can spontaneously evaporate into the 3D printer premises during manufacturing. (Alifui-Segbaya et al. 2020, Tan et al. 2020, Wu et al. 2020). Further chemical exposure hazards, including dermal exposure to solvents and resins originate from pre- and post-processing tasks which can involve resin handling and

mixing. Vapors can be formed and inhaled during these processes, and spills and splashes can produce environmental contamination and further dermal exposure hazards. Post-processing is expected to be the most hazardous process as solvents are used to remove resin residues from product surfaces, causing exposures to both solvents and resins. The resins are also listed to contain toxic compounds and potent irritants or sensitizers, underlining their plausible adverse impacts for human health once exposed to.

Concerns regarding patient or consumer exposure to uncured resin residues emerge from the use of products manufactured with the VP method, as chemical blooming and resin biodegradation can lead to unwanted exposure to toxic resin components or associated degradation products, e.g., acrylic acids. These products express toxic properties, including cytotoxicity, inflammatory and allergenic potential. (Jorge et al. 2003, Lago et al. 2015, Nouman et al. 2017, Alifui-Segbaya et al. 2018 and 2020, Tan et al. 2020, Krechmer et al. 2021).

Chemical exposure can occur through several routes when VP method is applied. The AM process is identified as a VOC source, while open resin containers and leaks or spills serve as additional origins of VOC contamination. Skin exposure may occur when resin vats are handled, or through resin leakages and contaminated surfaces. UFPs are also formed in VP manufacturing process, mostly due to direct evaporation and condensation of VOCs as the manufacturing process occurs at near room temperature, despite some machine models heating the resin vats to an elevated target temperature. However, the photocuring is an exothermic process, which can further promote VOC evaporation. The photocuring process can also produce novel chemical reaction compounds within the resin, resulting in exposure to unpredictable substances once they evaporate. (Short et al. 2015, Yang & Li 2018, Stefaniak et al. 2019b & 2021). Additional post-manufacturing hazards emerge from the biological compatibility of the resins and chemical blooming or outgassing.

Yang & Li (2018) found in their laboratory study using a real-time VOC sensor that the production of larger objects produced more VOC emissions than the production of smaller products, suggesting that volatile substances are produced in the photocuring process, and the magnitude of VOC emissions is surface area dependent. VOCs were emitted by an idle machine at lower quantities, at a concentration level of ca. 120 $\mu g/m^3$. The corresponding mean TVOC value during 3D printing was 1050 $\mu g/m^3$, while a concentration level of 1770 $\mu g/m^3$ was recorded during product post-processing. The highest TVOC level peak (up to 6000 $\mu g/m^3$) was detected when 3D printing started after an initial resin heating period.

Stefaniak et al. (2019b) studied multiple resin and VP printer combinations in a chamber. UFPs were recorded to be emitted at rates of 1.3–9.2×10^8 #/g material printed using a P-Trak particle counter (particle size range 20–1000 nm). A FMPS instrument (particle size range 5.6–560 nm) yielded higher particle emissions, between 7.6×10^9–4.0×10^{10} #/g material printed. The mean particle sizes ranged between 15 and 45 nm. The emission rates for TVOCs, measured using a real-time TVOC detector, ranged between 160–1930 μg/g printed, and higher particle emission rates were associated with higher TVOC emission rates. In fact, the printers which produced the highest emissions were based on the DLP technology, which is an adaptation of the VP method which operates at a faster production speed, thus, producing emissions at a faster pace than the traditional VP technology. Collected particles contained various metals as well, which were expected to be photoinitiators or additive substances. Three compounds with identified health hazards were found from collected air samples at parts per billion in air volume (ppb) levels during 3D printing and post-processing. The detected compounds were acetone (0.7–26 ppb, approx. 2–62 μg/m^3), benzaldehyde (1–13 ppb, approx. 4–56 μg/m^3) and 4-oxopentanal (0.1 ppb, below 1 μg/m^3). The findings by Kim et al. (2020) were very similar, as they reported elevated VOC concentrations during VP 3D printing and the identified compounds included ethanol, isopropanol, and acetone. Multiple metals were found from collected air samples as well.

Zisook et al. (2020), on the other hand, found no elevated TVOC levels in an industrial laboratory environment using a real-time TVOC monitor. Only acetone and isopropanol were found from air samples at levels exceeding their limit of detection during the 3D printing process, but these compounds were present in the background as well at similar, or slightly lower levels. Hayes et al. (2021) found no elevated particle levels in their study although ultrafine, fine, and coarse particle fractions were sampled. However, VOCs were documented to be produced in both the AM process and post-manufacturing tasks when one and two-component resins were used. A real-time TVOC detector recorded TVOC peaks which ranged between 1700–5940 ppb (roughly equivalent to the concentration of 7000–24,000 μg/m^3) when a printer was loaded; no elevated TVOCs were detected during the actual AM process, as the operated printer was mechanically ventilated. Higher, up to 20,000 ppb TVOC (approx. 82,000 μg/m^3) levels were recorded during post-processing, while isopropanol was measured at a level of 5000 μg/m^3 and acetone was found at up to 2000 μg/m^3 concentration level. Additionally, multiple other compounds including d-limonene, glycidol, and aromatic hydrocarbons were found at lower

concentration levels. The composition of the two-component resin was complex, and it produced higher and more diverse VOC emission than the one-component resin. The researchers concluded that post-processing tasks may be more hazardous than the actual 3D printing phase in terms of exposure levels.

Medical and dental devices which are used in direct contact with a patient can be produced using the VP method and specially formulated resins. However, chemical blooming is a documented incidence regardless. Krechmer et al. (2021) documented chemical blooming of various VOCs including formaldehyde, aromatic hydrocarbons, and acrylates from traditional and surgical grade resins, and that the magnitude of the blooming effect is lower from post-cured products. Alifui-Segbaya et al. (2020) reported that the solvents used in product post-processing are absorbed into and outgassed from the products over time. Lago et al. (2015) and Nouman et al. (2017) also documented that even fully cured resins secrete VOCs or SVOCs, including monomers and additives, and the effect was much stronger in the case of incompletely cured resins. These findings indicate that appropriate post-processing of the manufactured products matters most in making the use of VP products safe, and in reducing the post-production emissions released by the products.

Oskui et al. (2016) and Alifui-Segbaya et al. (2018) performed resin toxicity tests using zebrafish. Both research groups found that both accordingly post-processed and non-processed products induced lethal effects, lethargy, and behavioral disturbances in zebrafish, and malformations were observed in spawned fish embryos. Various acrylates are documented to have teratogenic effects and to be toxic to fetuses, and so those findings were in accordance with that. Appropriate post-processing did reduce toxicity of the manufactured products significantly, but biocompatibility of the resins remains a real issue in their biomedical applications and related touch exposure hazards.

2.5.3 Powder bed and multi jet fusion methods

PBF machine emission investigations are currently focused on metal and polyamide feedstocks. The available data is limited, regardless. Principally, the emissions produced during the actual AM process are not as relevant concern as exposures to particles produced during pre- and post-processes as PBF machines are enclosed and typically equipped with powerful ventilation and exhaust systems.

The major occupational hazards identified by Roth et al. (2019) and Stefaniak et al. (2021) include exposure to the powder feedstocks and their thermal decomposition products, while laser and radiation exposure, and powder explosion hazards exist as well. Only few factors are known to influence the emissions produced during manufacturing, as the AM machines are enclosed systems and operate under a controlled atmosphere. The feedstock type has an obvious effect as different polymers produce distinctive thermal decomposition products. However, pre-, and post-processing practices and used processing equipment, as well as particle control systems, play major roles in particle contaminant release and control during those stages.

$PM_{2.5}$, TVOC, and formaldehyde concentrations were studied during PBF machine operations under laboratory conditions by Damanhuri et al. (2019). The operations were documented to produce only particulate emissions, as only $PM_{2.5}$ concentration levels were increased. The concentration peaked at around 1100 µg/m^3 during the pre-processing stage (powder preparation), followed by a gradual decline to the level of ca. 100 µg/m^3 over the AM process. The concentration increased again up to 600 µg/m^3 level during post-processing. Real-time VOC monitoring by Zisook et al. (2020) revealed that no TVOCs at concentrations exceeding the background were produced in PBF manufacturing in an industrial laboratory environment. Only isopropanol and propylene were identified from canister air samples at levels above their limit of detection, but the same compounds were present in a background sample at similar concentration levels. No elevated levels of inorganic vapors were found, either. The average respirable dust concentrations reached up to 1.8 mg/m^3 level during post-processing, where PA powder was transferred and the manufactured parts were cleaned with pressurized air, and sandblasted. Momentary total dust concentration reached the used instrument's upper limit of detection, 150 mg/m^3, during these processes. The dust concentrations were close to the background level during the AM process, emphasizing the importance of the auxiliary production steps on risk evaluation in AM. Damanhuri et al. (2021) also concluded that 3D printer operators face the greatest exposure risks during pre- and post-processing steps in PBF manufacturing. Respirable particle concentrations were documented at the lowest concentrations (ca. 0.1 mg/m^3) during 3D printing in a laboratory environment. In contrast, the concentrations were between 0.2–0.4 mg/m^3 during pre- and post-processing stages (weighing, mixing, loading, powder cake breaking, parts cleaning). Virgin and recycled powders were studied successively in this study, and only minor

alterations in the powder properties and measured particle concentrations were observed. A thermal gravimetric analysis also revealed that the used PA powder withstood the upheld atmospheric temperature of 220 C° without significant degree of thermal decomposition, indicating that no excess thermal decomposition emissions are produced during the AM process.

Hayes et al. (2021) documented only low particle concentrations during MJF printer operations, despite ca. 180 C° atmospheric temperature being sustained inside the AM machine. The documented UFP concentrations were at background level (ca. 1.5×10^3 #/cm^3) throughout the experiment. The obtained PM$_{10}$ and PM$_{2.5}$ particle concentrations peaked at 15 and 5 µg/m^3, respectively, during the AM process. The corresponding peak values were unexpectedly low, 15 and below 5 µg/m^3 during post-processing. Multiple VOCs were identified to be produced in the AM process, with 2-pyrrolidone reaching the highest concentration value (21,200 µg/m^3). Other major compounds were triethylene glycol (5100 µg/m^3) and isopropanol (3000 µg/m^3), while aromatic hydrocarbons and other VOC species were also identified. 2-Pyrrolidone was known to be originated from the detailing and fusing agents, while triethylene glycol was identified to be an additive agent used in the PA feedstock. The other compounds were theorized to originate from thermal decomposition of the feedstock. TVOC value peaked at ca. 520 ppb (approx. 2000 µg/m^3) right after the manufacturing process began, after decaying close to the background value of 360 ppb (approx. 1500 µg/m^3). 2-Pyrrolidone, triethylene glycol, and isopropanol were also detected during post-processing at levels of 1300 µg/m^3, 450 µg/m^3, and 280 µg/m^3, respectively, along with multiple other VOC species including dimethylperoxide, 2-methylbutane, and aromatic hydrocarbons. These emissions were speculated to be ink and gas remnants which slowly evaporated from the powder.

Studies investigating particulate emissions using metal feedstocks provide further particle emission data in the absence of adequate amount of research literature on the emissions during the use of thermoplastic feedstocks in PBF and MJF systems. Azzougagh et al. (2021) measured multiple particle fractions and parameters in their study. Inhalable particle mass concentration of ca. 2.4 mg/m^3 was measured from inside a PBF machine, while UFPs were found concurrently at the level range of 2×10^4–2×10^5 #/cm^3, which was roughly an order of magnitude above the background level. The concentrations measured from outside the PBF machine were slightly above the background levels as well, but not by a large margin. Larger particles were documented at low quantities outside the PBF

machine. Personal sampling yielded ca. 1.7 mg/m^3 respirable particle exposure level during post-processing, while the UFP concentration was increased during this stage by two-fold in comparison to the background. Metal exposures in PBF machine operations were high enough to be detected via biomonitoring in a study by Ljunggren et al. (2019). Additionally, while elevated UFP and PM$_{10}$ particle concentrations were found, they were far below the concentrations obtained from welding works. The cell toxicity test findings by Wang et al. (2021) and Vallabani et al. (2022) are very analogous, despite multiple metal and alloy powders with varying compositions being used in both studies. The collected metal particles expressed no particular toxicity in cell culture tests performed in these studies, suggesting low acute toxicity. Long-term exposure may pose greater hazards, as DNA breaks were documented to increase slightly.

The PBF manufactured products typically contain voids where chemical substances can be trapped during the AM process. These compounds can eventually be freed from the product, and thus, the manufactured products can be a source for outgassed VOCs.

2.5.4 Material jetting method

The available literature regarding the emissions and contaminants originated from MJ operations is limited. The emissions are principally produced in the jetting spray aerosolization, where both VOCs and UFPs are released into the air. These emissions can escape the AM machine if not immediately eliminated with an exhaust ventilation system. Feedstock handling is not much of a concern, as the resin inks are stored inside cartridges or ink bags, but post-processing tasks can result in similar hazard scenarios as post-processing of VP manufactured products does if such measures are needed. The available research literature suggests that the machine and feedstock properties have a main role in the production of emissions, with local exhaust systems having the most important role in emission control. (Roth et al. 2019, Stefaniak et al. 2019b & 2021, Ding & Ng 2021).

Ryan & Hubbard (2016) performed perhaps the first MJ emission study in a production facility and documented diverse, but low VOC emissions. The compounds identified at levels below 15 μg/m^3 from air samples were acetone, low molecular weight alcohols, butane, 2-butanone, and toluene. Additionally, 1,4-dioxane was found as well at ca. 100 μg/m^3 concentration level. PM$_{10}$ and PM$_{2.5}$ levels

were only slightly elevated, but below 0.01 mg/m^3 outside the AM machine. A further hazard was identified to emerge from product post-processing, as corrosive sodium hydroxide was used to dissolve the produced support structures.

Stefaniak et al. (2019b) conducted a study under occupational setting and measured UFP, coarse particle, and VOC emissions. Two MJ printers produced mean UFP emissions at rates of 1.5×10^9–2.3×10^{10} #/min, while the corresponding coarse particle emissions were at 8.5×10^3–1.1×10^5 #/min level. The particle emissions were increased by roughly an order of magnitude when the printer lid was open. TVOC emission rates, unaffected by the lid position, were between 2.5–4.5×10^4 μg/min. Acetaldehyde, acetone, benzene, ethanol, toluene, and xylene were identified from the collected air samples at low concentrations, below 1.5 % of their representative OELs. Acetaldehyde was found at up to 215 μg/m^3 level (specified as no applicable OEL was available). Ethanol was used to clean the surfaces in the 3D printing area, and it was found at above 10 mg/m^3 level, promoting the importance of non-manufacturing tasks in risk assessing. Ozone was found to be produced in the AM processes as well, but surprisingly, no elevated carbonyl levels were documented.

Ding & Ng (2021) found elevated UFP concentrations only when measured from the inside of a machine equipped with mechanical exhaust ventilation, while no particles were observed outside the machine. Kim et al. (2020) documented low, but elevated TVOC concentrations and identified multiple VOC species, including ethanol, isopropanol, and toluene from air samples. Multiple metals, plausibly pigments or reactive resin components were found in collected filter samples. The findings obtained by Zisook et al. (2020) under industrial AM laboratory conditions were similar. Real-time VOC monitoring could not find elevated TVOC levels and only isopropanol, propylene, and toluene could be identified by canister air sampling. Post-processing utilizing soapy water and a lye bath did not produce VOCs either. The research paper by Hayes et al. (2021) principally fortifies the previous findings. The UFP concentrations were documented to raise above the background only slightly, while minute amounts of larger particles were observed. However, TVOC concentration was found to increase from ca. 2500 ppb level up to 6600 ppb (which roughly equals the increase from 10,000 μg/m^3 to 27,000 μg/m^3) in a warehouse-like environment, while acetone, hexafluoroethane, and d-limonene were identified as the main VOC emission products.

There is no available research data on chemical blooming or outgassing of MJ manufactured products. The feedstocks are, however, very similar to VP feedstocks,

which suggests that products manufactured using the MJ method may produce similar hazards for an end-user as products manufactured using the VP method do.

2.6   Important exposure influencing factors in AM works

AM technologies differ from many traditional manufacturing methods fundamentally, and 3D printer operators have the option not to be present during the AM process, and AM machines can be isolated from their surroundings. Pre- and post-processes still require manual labor, however. Furthermore, certain AM methods with special process characteristics exist which require more manual labor than the operation of other AM methods. Personal protective equipment and good work practices can reduce exposures significantly in these situations where manual labor is needed.

The different 3D printer and feedstock types can result in the production of very diverse emissions. UFPs and thermal decomposition compounds are expected to dominate the emissions when heat is used in the feedstock processing, while spontaneous evaporation products and UFPs following VOC condensation are assumed to be produced when photocurable resins are used. Use of powders can also lead to dust and fine particle exposures, especially during manual processing tasks.

Different 3D printer types have a varying degree of process parameter tuning options which can influence emissions, as e.g., higher processing temperatures correlate with increased emissions. AM machines also come as open, semi-open, or enclosed models, and the type of an AM machine is a substantial emission influencing factor. Furthermore, only industrial scale AM machines have built-in emission elimination systems, e.g., exhaust ventilation systems, and therefore most of the available printers lack any means of emission control.

Operational environment has an obvious impact on the concentration levels produced by the 3D printers. Space volume and ventilation rates potentially have the greatest impact, in addition to existing local emission control systems. Enclosures and local exhausts and can capture the emission produced in 3D printing process, given the fact that majority of the emissions are chemicals or nanosized particles and thus follow air flow paths. (Azimi et al. 2017 & Kwon et al. 2017.)

3   Aims of the thesis

This thesis is aimed to provide further information regarding the potential exposure levels to airborne chemical and particulate contaminants when different types of 3D printers are operated using various forms of polymeric feedstocks. The obtained results are examined with occupational hygiene and consumer safety in mind. The main aims of this thesis were the identification of the main pollutants encountered in AM of plastics using different methods and to document the exposure levels of the identified exposure agents. Furthermore, the obtained exposure levels were compared to established occupational exposure limits (OELs) and other guidelines or threshold values to help the identification of plausible hazards related to chemical or particle exposures. Lastly, the main exposure agents and important exposure and emission situations per each AM method were identified, and differences in the produced hazards and the potential exposure levels are compared between the different studied AM methods. The hypothesis of this work is that the use of different AM technologies and feedstocks produce different, varying emission profiles, given the distinctive emission production pathways and principal differences in product manufacturing and the chemical compositions of the applied feedstocks.

4 Experimental

The main emission products were identified, and air concentrations and emissions of the produced indoor air pollutants were sampled in this thesis when multiple different AM machines were operated using several different feedstocks. The parameters targeted in each original publication are presented in the Table 3, in addition to the used AM machinery and feedstocks, and the classification of the operation environment. Majority of the samples were collected from stationary points. The stationary points were located near (1–2 meters) an emission source of interest, and the samples were collected from the height of the breathing zone (ca. 1.5 meters from the floor). Some personal samples were also collected in original publications I and IV directly from the breathing zone of a process operator.

All the results presented in this work are background-corrected values. Background samples were always taken before any work was performed at the sampling site, and thus, the interference of e.g., passive emissions from construction materials and supply air were eliminated from the results. The average background sampling values are subtracted from the results obtained during the different AM processes.

Table 3. Description of research used AM machinery and feedstocks, research environments, and study parameters, by publication.

Publication	Method	3D printer	Feedstocks	Environments	Research parameters
I	Material extrusion	Zmorph: ZMorph 2.0 SX (semi-open)	Formfutura: ABSPro Flame Retardant and EasyWood (PLA-based BC) filaments	University laboratory, 195 m³, mechanical ventilation	Airborne and personal VOC* mass concentrations, carbonyl mass concentrations, UFP number concentrations, airborne and personal** inhalable dust mass concentrations, PM$_{15}$ mass concentrations
	Vat photo-polymerization*	Formlabs: Form 2 (enclosed, two machines operated simultaneously)	Formlabs: Grey and Castable Wax resins		
		Bego: Varseo (enclosed)	Bego: VarseoWax CAD/Cast resin	Apartment room, 55 m³, natural ventilation inlet and mechanical outlet	
	Material jetting	3D Systems: Projet MJP 2500 (enclosed)	3D Systems: Visijet M2R-CL ink resin	Office, 48 m³, natural ventilation inlet and mechanical outlet	
	Powder bed fusion**	EOS: Formiga P110 and P396 (enclosed and ventilated, operated simultaneously)	Glass-fiber reinforced polyamide 2200 powder	Industrial hall, 1776 m³, mechanical ventilation	
	Multi jet fusion**	Hewlett-Packard: Multi Jet Fusion 4200 (enclosed)	Glass-fiber reinforced polyamide 12 powder	Industrial hall, 991 m³, mechanical ventilation	
II	Material extrusion	ZMorph: ZMorph 2.0 SX (semi-open)	Formfutura: Premium PLA Grey and PLA ReForm, Verbatim: PP Transparent, and custom waste polypropylene filaments, additional recycled corresponding filaments	University laboratory, 195 m³, mechanical ventilation	Airborne VOC mass concentrations, UFP number concentrations
III	Material extrusion	Creality: Ender-3 (open), 3devo: Filament Composer 450 (an open filament extruder)	UPM: PLA-based Formi 20 and Formi 40 BC filaments, and custom PLA-based BC filaments with 15 % and 30 % wood content	Office, 104 m³, mechanical ventilation	Airborne and personal VOC mass concentrations, carbonyl mass concentrations, UFP number concentrations, PM$_{10}$ and PM$_{2.5}$ mass concentrations
IV	Vat photo-polymerization	Formlabs: Form 2 (enclosed) Nexa3D: NXE400 (enclosed)	Formlabs: Clear and Castable Wax resins Nexa3D: xGPP Translucent resin	University laboratory, 52 m³, mechanical ventilation	Airborne VOC and carbonyl mass concentrations, UFP number concentrations, UFP size distributions, VOC outgassing
		Bego: Varseo (enclosed)	Bego: VarseoWax Model and VarseoWax Tray resins		
		Ivoclar Vivadent: PrograPrint PR5 (enclosed)	Ivoclar Vivadent: ProArtPrint Model and ProArtPrint Splint resins	Dental laboratory 70 m³, mechanical ventilation	
	Material jetting	Stratasys: J735 (enclosed and ventilated)	Stratasys: VeroBlackPlus, VeroCyan-V, VeroMagenta-V, VeroYellow-V, VeroPureWhite, and VeroClear ink resins	University laboratory, 36 m³, mechanical ventilation	

4.1 VOC sampling and GC-MS analysis

Volatile organic compound (VOC) samples were collected with Tenax® TA adsorption tubes (Markes Inc., Sacramento, CA) at a calibrated flow rate of 200 mL/min using AirChek 3000 pumps (SKC Inc., Eighty Four, PA) in all the original publications I–IV. The tubes contained 200 mg of sorbent and a mini-BUCK M-5 Calibrator (A. P. BUCK Inc., Orlando, FL) was used for pump calibration. The samples were analyzed according to ISO 16000-6:2011 standard toluene equivalent method using a TD100 thermal desorber (Markes Inc.), 7890A gas chromatography system and 5975C mass selective spectrometer (both manufactured by Agilent Technologies Inc., Santa Clara, CA). The gas chromatograph was equipped with an HP-5ms column (50 meters of length, 200 µm inner diameter and 0.33 µm film thickness) in original publications I–II, while an updated HP-5ms column (60 meters of length, 250 µm inner diameter and 0.25 µm film thickness, both manufactured by Agilent Technologies Inc.) was used in the original publications III–IV. The mass spectrometer was operated using scan mode which enabled the identification of every captured compound. An MSD ChemStation software program (version F.01.00.1903, Agilent Technologies Inc.) and National Institute of Standards and Technology mass spectrometer libraries were used for compound identification based on compound retention times and the produced ion fingerprints. The compound concentrations were calculated as toluene equivalents. Toluene standard curves were produced by injecting HC 48 component 40353-U standard solution (Supelco Inc., Bellefonte, PA) samples into Tenax® TA tubes with the assistance of nitrogen carrier gas. This method is best suitable for the analysis of compounds with 6 to 16 carbon atoms in their structure. Compounds with a lesser amount of carbon atoms in their structure partially pass through the adsorption tubes, resulting in underestimated air mass concentrations. On the other hand, the quantification of compounds with a greater carbon number is interfered by the background noise of the mass spectrometer.

Additionally, VOCs outgassed by 3D printed resin objects were sampled in the original publication III. Manufactured sample cubes (3×3×3 cm) were placed inside a Micro-Chamber/Thermal Extractor M-CTE250 apparatus (114 mL chamber volume, Markes Inc.) from which Tenax® TA samples were collected from at a calibrated flow rate of 75 mL/min. Nitrogen was used as the carrier gas in the chambers.

4.2 Collection and analysis of carbonyl compounds

Short-chained carbonyl compound samples were collected and selectively analyzed according to ISO 16000-3:2011 standard using Sep-Pak 2,4-dinitrophenyl-hydrazine (DNPH) Silica cartridges (Waters Corp., Milford, MA) containing 350 mg of sorbent, and Laboport vacuum pumps (KNF Neuberger Inc., Trenton, NJ) at a calibrated flow rate of 1.5 L/min. The pumps were calibrated with the mini-BUCK M-5 Calibrator.

The compounds were analyzed using a high-performance liquid chromatography (HPLC) system in the original publication I. An HP 1090 LC liquid chromatography system (Hewlett-Packard, Palo Alto, CA) connected to Zorbax XDB-C8 column (Agilent Technologies Inc.) was operated using water, acetonitrile, and tetrahydrofuran as eluents at a 1.3 mL/min flow rate. A standard solution was produced by dissolving hydrazine derivates of the following carbonyl compounds in acetonitrile: formaldehyde, acetaldehyde, acetone, propanal, butanone, and butanal. The standard solution was further diluted with acetonitrile to prepare a dilution series used to construct standard curves with. The mass concentrations of the captured compounds were calculated based on the compound-specific standard curve response factors, and the collected compounds were identified by matching their retention times with the retention times of the compounds present in the standard samples. This analysis method was selective for the compounds used in the standard solution and any other compounds present in the samples could not be identified.

Liquid chromatography coupled with tandem mass spectrometry (LC-MS/MS) analysis was performed in original publications III–IV using an LCMS-8040 triple quadrupole mass spectrometer (Shimadzu Corp., Kyoto, Japan) equipped with Kinetex® reversed phase C18 column (Phenomenex Inc., Torrance, CA) with 100 mm length, 3 mm internal diameter and 1.7 µm pore size. The eluent flow consisted of water and acetonitrile. Standard curves used for compound identification and quantification were constructed with Carbonyl-DNPH Mix 1 certified reference samples (Sigma-Aldrich Corp., Saint Louis, MO). The reference material contained DNPH-derivates of 2-butanone, acetaldehyde, acetone, acrolein, benzaldehyde, butyraldehyde, crotonaldehyde, formaldehyde, hexaldehyde, methacrolein, propionaldehyde, tolualdehyde and vareladehyde, and therefore the analysis method was selective for these compounds and any other substances captured in

the samples evaded the analysis. The compounds were identified based on their ion fingerprints and retention times.

4.3   Dust, coarse (PM$_{15}$, PM$_{10}$) and fine (PM$_{2.5}$) particle sampling

Particle mass concentrations were sampled using two different methods and multiple different instruments. Real-time mass concentration of coarse particles (PM$_{15}$) with 0.3–15 µm aerodynamic diameter were monitored with a desktop (stationary) DustTrak DRX Aerosol Monitor 8533 instrument (TSI Inc., Shoreview, MN) using a 30-sec logging interval in original publication I. Arizona road dust factory calibration was performed on the instrument according to the ISO 12103-1 standard, and zero filter calibration was performed before each sampling session. Real-time mass concentration of PM$_{10}$ particles were monitored in a similar fashion with a desktop Optical Particle Sizer 3330 (OPS, aerodynamic diameter range 0.3–10 µm, TSI Inc.) in original publications III–IV using 10 or 30-sec logging intervals. Furthermore, the mass concentration of PM$_{2.5}$ particles (aerodynamic particle diameter 0.3–2.5 µm) was monitored in the original publication IV in tandem with PM$_{10}$ particles using a 30-sec logging interval. The OPS instrument was factory calibrated accordingly, as well as zero-filter calibrated before each measurement session. Both particle monitors were optical instruments, and thus, a degree of measurement inaccuracy exist in the resolved particle mass concentration levels.

Total inhalable dust samples were collected at a calibrated flow rate of 2 L/min with IOM samplers (SKC Inc.) equipped with metal cassettes according to the EN 481 standard in the original publication I. AirChek 224 pumps (SKC Inc.) calibrated with the mini-BUCK Calibrator M-5 were used in the sample collection. Mixed cellulose esters membranes (Millipore Corp., Burlington, MA) with pore size of 0.8 µm were used in the IOM cassettes. The membrane cassettes were equilibrated in a condition regulated room for 24 hours before each weighing. The limit of detection was set as exceeding the standard deviation of the weight of the blank membranes by five-fold. IOM samples were collected from both stationary points and process operators' breathing zones.

4.4 UFP sampling

Number concentrations of ultrafine particles (UFPs) with an aerodynamic diameter of 20–1000 µm were monitored with a hand-held (portable) P-Trak Ultrafine Particle Counter 8525 instrument (TSI Inc.) using 10 or 30-sec logging intervals in original publications I, II and IV. The instrument was factory calibrated accordingly, and further zero-filter calibrated before each sampling session. A desktop condensation particle counter (CPC) model 3022A (TSI Inc.) was used in the original publication III for UFP number concentration monitoring (aerodynamic diameter range 7–3000 nm) using a 10-sec logging interval. A fast mobility particle sizer (FMPS) model 3091 (TSI Inc.) was used in tandem with the CPC instrument in the original publication III to resolve size distributions of UFPs within the aerodynamic diameter range of 5.6–560 nm using the instrument's 32 standard size channels using 10-sec logging interval. The P-Trak device used isopropanol as its operational fluid, while butanol was used as the operational fluid in the CPC 3022A instrument. UFP and chemical substance sampling were not performed at the same time to prevent chemical sampling from being affected by operational fluid leaks.

4.5 Air quality monitoring

Indoor air quality parameters were monitored with IAQ-Calc 7535 instrument (TSI Inc.) using 30-sec logging interval in original publications I–II and IV. The parameters included carbon dioxide (CO_2), carbon monoxide (CO, monitored only in the original publication I), temperature (T) and humidity (RH). The instrument was factory calibrated accordingly, and the CO parameter was further zero-calibrated in a clean space with the zero-calibration function of the instrument.

5 Results and discussion

All the relevant exposure agents present during manufacturing using AM machines based on different technologies were sampled in the original publication I, and the follow-up studies were planned based on the initial findings.

The concentrations of VOCs and carbonyl compounds are compared to their official Finnish occupational exposure limits (OELs, FMSAH 2020), the European lowest concentrations of interest (LCIs, EC 2020), and the German maximum permissible workplace or biological tolerance concentrations (MAK and BAT values). The Finnish OELs are official values which may not be exceeded in occupational settings within Finnish workplaces. The values are given for 8-hour time-weighted average (TWA, which means an average exposure level over 8 hours) by default, but a secondary exposure limit is often given for acute, 15-minute exposure as well. In rare cases only a 15-minute TWA limit value is available. (FMSAH 2020).

The LCI values are reference values for inhalation exposure to indoor emissions from construction materials. While these values are not used for the evaluation of health risks of chemical exposure under occupational settings, they are derived from available toxicological data and meant to preserve human health. (EC 2020). MAK and BAT values represent concentrations that may not be exceeded under an occupational setting and include maximum permissible concentrations in the air (MAKs), or biologically tolerable concentration levels (BATs). (DFG 2021.) TVOC guideline values are proposed by Tuomi & Vainiotalo for Finnish occupational environments (300 $\mu g/m^3$ general target, and guideline value of 3000 $\mu g/m^3$) following the as-low-as-reasonably-achievable (ALARA) principle.

Dust particle concentrations are evaluated based on the Finnish OEL for organic dust, as plastic dust is considered organic. The obtained PM_{10} (and PM_{15}, given that no reference value exists for this fraction) and $PM_{2.5}$ concentrations are compared to available long-term ambient air particle guideline values of 20 and 5 $\mu g/m^3$ (EU 2008, WHO 2021.) UFP concentrations are compared to the proposed UFP reference value of 4×10^4 #/cm^3 given for exposure to manufactured light-weight nanoparticles (Van Broekhuizen et al. 2012) as the densities of plastics are less than the threshold density of heavyweight UFPs, and the currently issued long-term ambient UFP guideline value of 2×10^4 #/cm^3 (WHO 2021). To be noted is that the guideline values issued by WHO also apply for indoor environments.

Majority of the utilized reference values are given for 8-hour exposure. For this reason and the sake of simplicity, the exposure agent levels obtained in this work are treated as average values for 8-hour exposure after subtraction of background levels of the measured exposure agents, and thus, the presented exposure levels represent the exposure potential produced by the AM machines, feedstocks, and processes.

5.1 Methods utilizing thermoplastic feedstocks

The emissions from the application of thermal 3D printing methods differ from the use of other methods as diverse chemical species and substantial amounts of UFPs can be produced in thermal decomposition of polymers. The measured concentration levels of VOCs, carbonyl compounds, and the different measured particle sizes are presented in Tables 4–6. Particulate contaminants were produced at rather constant rates, and the peak values were typically within an order of magnitude from the average concentration. Therefore, no separate time-series data is presented.

5.1.1 Material extrusion method and a filament extruder

An ME 3D printer was operated in a laboratory environment in the original publication I using two filaments: an ABS filament doped with flame retardant additives, and a PLA-based EasyWood BC filament. Due to the relatively large base of knowledge behind generic PLA and ABS feedstocks, these filaments provided more information on the contaminants produced in the use of less studied materials and thus expanded the base of knowledge. Considering the environmental issues related to energy conservation and plastics, some environmentally sustainable filaments and a filament extruder were studied in laboratory and office environments in original publications II and III to provide data for safety evaluation of alternative filaments and a custom filament maker.

The main chemical compound results are presented in Tables 4–5, while particulate matter findings are listed in Table 6. Overall, the ME 3D printers and filaments produced the widest range of VOCs (yet not the highest TVOC concentrations) and the highest number concentrations of UFPs of all studied

methods and printers. The ABS filament produced both the most individual VOCs (n = 29) in this thesis, and the highest mean UFP levels (ca. $8×10^4$ #/cm^3), but only few PM$_{15}$ particles (10 µg/m^3 mean). The filament also produced the highest TVOC level among all filament feedstocks (ca. 240 µg/m^3). This is likely attributed to the highest applied processing temperature (250 °C) in this thesis and the polymer type, as ABS has been documented on multiple occasions to be more polluting than, e.g., PLA (see Table 1). The identified compounds included styrene as a major emission product (20 µg/m^3), and some halogenated substances, despite the filament being marketed as halogen-free. This suggests that used additives can influence and be integrated into the airborne emissions produced during a 3D printing process, as documented before by Yi et al. (2016), Stefaniak et al. (2017b and 2019b), Zontek et al. (2017), Gu et al. (2019), Zhang et al. (2019), and Alberts et al. (2021). Multiple carbonyl compounds were found as well, with acetone being detected at the highest concentration level (70 µg/m^3), followed by formaldehyde (20 µg/m^3) and various others at lower levels, which added up to a total carbonyl level of 110 µg/m^3. No combustion-related CO was detected during extrusion of these filaments, which suggests that it is not produced under normal ME 3D printing conditions.

The EasyWood BC filament produced TVOCs at ca. 90 µg/m^3 level, total carbonyls at 40 µg/m^3 concentration, UFPs at $5×10^3$ #/cm^3 mean level, and low PM$_{15}$ levels (10 µg/m^3 mean) even though it was 3D printed at almost the same temperature (245 °C) and under the same conditions as the ABS filament. Lactide (25 µg/m^3) and furfural (10 µg/m^3) were identified as the main produced VOCs, while acetone (15 µg/m^3), 2-butanone (15 µg/m^3), and formaldehyde (10 µg/m^3) were the main emitted carbonyls. Many of these compounds are associated either with thermal processing of PLA, or wood. A 3D printer malfunction (nozzle clogging) produced substantially elevated number concentrations of UFPs (up to ca. $5×10^5$ #/cm^3). Despite the AM machines operating independently, any 3D printer should be supervised regularly to resolve any disturbances in the 3D printing process which can produce massive amounts of unexpected emissions, and even a fire hazard.

In the original publication I the build plate was coated with glue to improve adhesion of the first layer onto it. VOCs released by the glue over a heating period was sampled individually, and the glue emitted mostly propylene glycol (20 µg/m^3) and 2-(2-butoxyethoxy)ethyl acetate (15 µg/m^3), as well as isopropyl alcohol (10 µg/m^3) and hexane (10 µg/m^3), and six additional VOCs at trace concentrations. The use of glue, or other means of adhesion improvement like tapes and slurries can

release additional VOCs into the air especially at the starting phase of a 3D print job, which can increase the initial TVOC exposures.

The use of generic PLA and PP filaments produced TVOCs at 100–180 µg/m^3 mean levels, and UFP at 5×10^2–1×10^3 #/cm^3 average levels under the same conditions as the previous two feedstocks. However, after being 3D printed and recycled back into a filament form multiple times these feedstocks produced lesser amounts of VOCs, which was seen as both a lower number of detected compounds, and reduced TVOC concentrations (50–60 µg/m^3 mean levels). The UFP levels emitted by the recycled filaments were also diminished down to 5×10–5×10^2 #/cm^3 average level. It is likely that portions of the most readily volatilized filament components departed the polymer matrix during repetitive thermal processing, and less volatile substances persisted within the feedstocks. This reduced both the number and concentration levels of VOCs, and secondarily UFPs as less building blocks for UFP formation was produced. A conflicting finding was observed using a recycled HWP PP filament. Its use was found to produce lesser amounts of VOCs (60 µg/m^3 mean) than its virgin counterpart (150 µg/m^3 mean), but it did emit higher amounts of UFPs after recycling (3×10^3 vs. 7×10^3 #/cm^3 average). The HWP filament was produced from bottle caps and no additives were used to enhance its 3D printing properties. Henceforth, it is likely that the 3D printability of the plastic was poor to begin with and reduced further after recycling which resulted in extrusion difficulties, and perhaps, overheating or burning. The UFP emissions were therefore increased, even though the VOC emissions were reduced in similar fashion as they were reduced in the case of commercial 3D printing filaments. The poor 3D printability and the plausible overheating are supported by identification of the airborne compounds: multiple cyclic hydrocarbons were found, suggesting overheating. Nevertheless, the use of recycled 3D printing polymers as feedstocks may produce reduced chemical and UFP emissions, while especially HWPs are to be used cautiously as 3D printer feedstocks. An increased fire hazard may emerge from their use, and there can be residues from foodstuffs, household chemicals, or other substances which can burn or be volatilized during 3D printing, resulting in altered chemical exposures in comparison to commercial feedstocks (Yamasita et al. 2012).

The accumulation of 1,4-dioxane was observed during repetitive thermal processing of PLA feedstocks in the original publication II. This compound was the only emission product found at higher concentration levels as the number of thermal cycles increased. 1,4-dioxane shares a similar base structure with lactide, an esterification product of lactic acid, the base unit of PLA. There is a similar finding

by Mylläri et al. 2016, where 1,4-dioxane was also found to accumulate in thermally recycled household plastics. Although no similar accumulation of any single compound was found with the PP filaments, this finding indicates that impurities or chemical alteration products can be accumulated in the polymer matrix, which result in altered emission products during 3D printing. This can produce novel and unforeseen 3D printer operator hazards regardless of the reduced total chemical exposure. These fundamental findings are expected to apply on other thermal 3D processes as well, e.g., the PBF method. Partially recycled powders are commonly used in PBF 3D printing to minimize material waste and doing so may affect the overall VOC and UFP emissions.

The measured TVOC concentration levels recorded in the original publication III using PLA-based BC filaments were identical between the stationary and personal samples, which ranged between 40–50 $\mu g/m^3$. This indicates that the VOCs readily dispersed in an office environment. The TVOC levels also corresponded with the concentration levels obtained using a pure PLA filament (60 $\mu g/m^3$ mean). Chemical characterization of the 3D printing fumes revealed that the chemical profiles were, however, different between the two material types. Certain compounds associated with thermal treatment of wood (Höllebacher et al. 2015, Pohleven et al. 2019), including acetic acid, furfural, and terpenes were identified in the use of every BC filament. Terpenes contributed to roughly an equal amount of the TVOC levels as the filament's wood content did, and the concentrations of non-terpene VOCs detected during 3D printing using a pure PLA feedstock were equally lower. The TVOC emissions produced by the BC filaments were, therefore, equal in comparison to other PLA feedstocks, but their chemical compositions were different. Furfural (not listed in Table 4) was also found at low concentration levels. It was a compound of high interest due to its hepatotoxic properties (WHO 1995, EC 2020), while some terpenes are associated with inflammatory effects or sensitization, and indoor UFP formation (Kasanen et al. 1999, Sarwar et al. 2004, Kim et al. 2013, Wolkoff 2020), but also with plausible health benefits, including anti-inflammatory potential (Kim et al. 2020b). The use of filaments reinforced with wood particles are therefore not unambiguously more hazardous to use than pure feedstocks, given that polymer degradation products and several carbonyls were present at slightly higher concentrations during the extrusion of pure PLA. Total carbonyl levels were also surprisingly high during extrusion of all four BC filaments (190–230 $\mu g/m^3$) and the reference PLA (250 $\mu g/m^3$) in comparison to the other studied filament feedstocks. Acetone (55–80 $\mu g/m^3$), 2-butanone (50–75 $\mu g/m^3$), formaldehyde (30–40 $\mu g/m^3$),

and hexanal (10–20 µg/m^3) were the dominant carbonyls each time. Minute concentrations (≤5 µg/m^3) of PM$_{10}$ and PM$_{2.5}$ particles were also recorded.

Emission rates for TVOC and UFPs were also calculated in the original publication III for the PLA and the four BC feedstocks under office conditions with 3.6 air exchanges per hour using the following equations:

$$S = ((C_{out} - C_{in}) \times Q)/60$$

where S is emission rate per minute, C_{out} equals the average UFP or TVOC concentration in the air, C_{in} represents the corresponding background level of UFPs or TVOC, and Q is the air flow rate (m^3/h) of exhaust air. The equation can be simplified into the following form:

$$S = C_{average} \times Q)/60$$

where $C_{average}$ is the average number or mass concentration of UFPs or TVOC as measured after background correction. The 3.6 air exchanges per hour was calculated using the equation:

$$ACH = \frac{CFM \times 60}{A \times h}$$

where ACH is air exchanges per hour, CFM equals the volume of exhaust air flow rate measured using a 3000 md micromanometer (Swema AB, Farsta, Sweden), while A and h represent the area and height of the room.

The calculated rates were 3×10^2 µg/min for TVOC, and 4×10^9–1×10^{10} #/min for UFPs during 3D printing. As seen, the emission rates varied only mildly, and no distinctive differences can be seen between the material types. These yields fall within the middle or the lower end of the range of the previously recorded emission rates (see Tables 1 and 2), indicating moderate emissions. As an additional note, BC feedstocks are also produced in powdered form to be used in PBF, and its sub-methods. The fundamental findings involving the alterations in chemical composition and the unaltered UFP emissions in the use of BC filaments instead of pure plastics are expected to apply when BCs are used in other thermal processes as well.

As seen from the Table 4, many of the compounds identified at the highest concentration levels lacked any official exposure or concentration level regulations.

However, the recorded concentrations fell coherently below any regulative limit values if such value was given for the compound, suggesting moderate exposure levels. Only furfural exceeded its regulatory values, in this case the LCI value, during extrusion of the EasyWood BC filament. Also, the proposed occupational TVOC target value of 300 µg/m^3 for Finnish workplaces was not exceeded, either. However, multiple compounds with an association to cancer risk, e.g., formaldehyde, acetaldehyde, styrene, and cyclic hydrocarbons (WHO 2006, Unwin et al. 2013) were also identified at low concentrations in comparison to their OELs. It is always advisable to control exposures to 3D printing fumes given the hazardous properties of many identified compounds. Several compounds were known thermal decomposition products, which were also found in previous studies (see Table 1.) The feedstock type had a major impact on the airborne chemical compositions, as certain plastics tend to break down into particular chemical species during thermal decomposition and additives or fillers, like wood particles, produce specific chemical emissions when heated.

The use of thermal 3D printing methods is expected to be the only occasion where substantial amounts of UFPs are produced into the surrounding environment. Vice versa, the absence of thermal decomposition mechanisms in non-thermal 3D printing methods result in lesser UFP yields. However, the recorded number concentrations were drastically elevated above the background only during 3D printing using the ABS filament, and 3D printer malfunction, albeit lower UFP concentrations were detected during 3D printing with all the used filaments, and all 3D printing scenarios overall. The factors which contributed to the substantially elevated UFP levels were the high operation temperature (ABS) and the printer malfunction (BC). The concentration levels exceeded the UFP reference values of 1–4×10^4 #/cm^3 given for manufactured lightweight nanoparticles and ambient UFP pollution in these cases (Van Broekhuizen et al. 2012, WHO 2021). The other recorded UFP concentration levels were low or moderate in comparison to existing literature (see Table 2). Also, no remarkable concentrations of PM$_{15}$, PM$_{10}$, or PM$_{2.5}$ particles were documented to be produced during the operation of ME 3D printers. The corresponding reference values of PM$_{10}$ and PM$_{2.5}$ particles were both above the obtained average concentrations.

The ME 3D printers were operated under multiple environments, but their emissions were sampled at a similar distance on each occasion. There are no major differences between the obtained results, however, as all individual results are within the same order of magnitude. This suggest that the exposure levels at a close

distance to a 3D printer are at best moderately affected by the environment. The measured concentration levels during extrusion of multiple BC filaments under different conditions were all very similar despite notable differences between the environments (a university laboratory vs. an office). Obviously, there was a larger space for the contaminants to disperse in in the laboratory, and it very likely had more powerful ventilation, but nevertheless, the concentrations near the 3D printers were almost equal. The air conditions were also very similar during all these measurements and therefore, they did not act as confounding factors. The operation environment's properties may affect the concentration and exposure levels in prolonged 3D printing, but not as much during short 3D prints as the contaminants have no time to accumulate in the air.

A filament extruder produced similar emissions in comparison to a 3D printer when the same feedstocks were used in both machines (one PLA and multiple BC materials). The contaminant compositions were equal, and the contaminant concentration levels produced by the filament extruder were mostly similar or minutely lower than those measured during the operation of the 3D printer. Only carbonyl concentrations (25–55 $\mu g/m^3$ for acetone, 15–25 $\mu g/m^3$ for 2-butanone, and >10 $\mu g/m^3$ for formaldehyde and acetaldehyde, and their total concentration ranging between 60–90 $\mu g/m^3$) measured during the operation of the filament extruder were notably lower than what was recorded during 3D printing using the same feedstocks (total carbonyls ≥190 $\mu g/m^3$). The measured mean UFP levels ranged between $9\times10–1.1\times10^3$ #/cm^3 and mean PM_{10} levels were at 20 $\mu g/m^3$ and below, while mean $PM_{2.5}$ concentrations never exceed 5 $\mu g/m^3$. Only negligible differences between the contaminant concentration levels were observed among the used feedstocks, and the concentration levels were low in comparison to established contaminant OELs and other available guideline values, as well as in comparison to the existing ME 3D printer emission literature. The results are also in line with the findings of a study by Byrley et al. (2020), where VOC and particulate matter emissions from a filament extruder were investigated.

To summarize, the emission profiles produced by a desktop filament extruder accurately correspond with a desktop 3D printer. The slightly lower recorded concentration levels were most likely attributed to the lower operation temperature of the filament extruder. Similar exposure hazards are present, however, and the operation environment and extrusion process specifications and placement of the extruder play important roles on contaminant production and exposures.

Table 4. (1/2). TVOC and individual VOC compound concentrations, and the number of detected compounds encountered using thermal 3D printing methods, in comparison to their official reference values, and air quality parameters during the measurements.

Method	Printer	Feedstock	T (°C)	TVOC (µg/m³)	N of VOCs	Top compounds	Conc. (µg/m³)	Finnish OEL (µg/m³)	MAK/BAT (µg/m³)	LCI (µg/m³)	Air quality parameters
Material extrusion	Zmorph: ZMorph 2.0 SX	Formfutura: ABSPro Flame Retardant filament	250	240	29	Styrene; ethyl 2-(3,4-dimethylanilino)-2-oxoacetate; decanal; benzoic acid; sebacic acid, 3-methylbut-2-enyl propyl ester	19; 19; 14; 14; 14	86,000 (styrene); n/a; n/a; n/a; n/a	86,000 (styrene); n/a; n/a; n/a; n/a	250 (styrene); n/a; 900 (decanal); n/a; n/a	CO₂: 470 ppm, T: 26.5 °C, RH: 37 %
		Formfutura: Premium PLA Grey filament	205	180	23	Lactide; 2-hydroxypropyl methacrylate; propanoic acid propyl ester; decanal; benzoic acid	26; 21; 21; 12; 8	n/a; n/a; n/a; n/a; n/a	n/a; n/a; n/a; n/a; n/a	n/a; 110 (2-hydroxypropyl methacrylate); n/a; 900 (decanal); n/a	CO₂: 800 ppm, T: 20.8 °C, RH: 31 %
		Recycled (x5) Formfutura: Premium PLA Grey filament	205	60	13	2-Hydroxypropyl methacrylate; lactide; 1,4-dioxane; decanal; decane	11; 11; 8; 6; 5	n/a; n/a; 36,000 (1,4-dioxane); n/a; n/a	n/a; n/a; 73,000 (1,4-dioxane); n/a; n/a	110 (2-hydroxypropyl methacrylate); n/a; 400 (1,4-dioxane); 900 (decanal); 6000 (decane)	CO₂: 800 ppm, T: 21.3 °C, RH: 30 %
		Formfutura: PLA ReForm filament	205	150	22	2-Hydroxypropyl methacrylate; lactide; decanal; benzoic acid; propanoic acid propyl ester	20; 18; 14; 11; 11	n/a; n/a; n/a; n/a; n/a	n/a; n/a; n/a; n/a; n/a	n/a; n/a; 900 (decanal); n/a; n/a	CO₂: 730 ppm, T: 21.5 °C, RH: 27 %
		Recycled (x5) Formfutura: PLA ReForm filament	205	59	13	Lactide; 1,4-dioxane; 2-hydroxypropyl methacrylate; decanal; propanoic acid propyl ester	8; 7; 6; 5	n/a; 36,000 (1,4-dioxane); n/a; n/a; n/a	n/a; 73,000 (1,4-dioxane); n/a; n/a; n/a	n/a; 400 (1,4-dioxane); 110 (2-hydroxypropyl methacrylate); 900 (decanal); n/a	CO₂: 750 ppm, T: 21.9 °C, RH: 30 %
		Verbatim: PP Transparent filament	230	100	22	Propylene glycol; 2-ethylhexanol; methacrolein; propionaldehyde	23; 10; 10; 8; 7	n/a; 5400 (2-ethylhexanol); n/a; 48,000 (propionaldehyde)	n/a; 54,000 (2-ethylhexanol); n/a; n/a	2100 (propylene glycol); 300 (2-ethylhexanol); n/a; n/a	CO₂: 760 ppm, T: 20.9 °C, RH: 33 %
		Recycled (x5) Verbatim: PP Transparent filament	230	54	16	Propionaldehyde; propylene glycol; decanal; methacrolein; 2-ethylhexanol	8; 6; 4; 4; 3	48,000 (propionaldehyde); n/a; n/a; n/a; 5400 (2-ethylhexanol)	n/a; n/a; n/a; n/a; 54,000 (2-ethylhexanol)	n/a; 2100 (propylene glycol); 900 (decanal); n/a; 300 (2-ethylhexanol)	CO₂: 780 ppm, T: 21.1 °C, RH: 34 %
		Custom HWP PP filament	235	150	27	Propylene glycol; ethylbenzene; n-xylene; isobornyl acrylate; n-butyl acetate	20; 8; 7; 5; 4	n/a; 220,000 (ethylbenzene); 220,000 (n-xylene); n/a; 240,000 (n-butyl acetate)	n/a; 88,000 (ethylbenzene); 440,000 (n-xylene); n/a; 480;000 (n-butyl acetate)	2100 (propylene glycol); 850 (ethylbenzene); 500 (n-xylene); 110 (isobornyl acrylate); 4800 (n-butyl acetate)	CO₂: 740 ppm, T: 21.0 °C, RH: 33 %
		Recycled (x3) custom HWP PP filament	235	56	20	Propylene glycol; ethylbenzene; n-xylene; decanal; propionaldehyde	11; 7; 7; 4; 4	n/a; 220,000 (ethylbenzene); 220,000 (n-xylene); n/a; 48,000 (propionaldehyde)	n/a; 88,000 (ethylbenzene); 440,000 (n-xylene); n/a; n/a	2100 (propylene glycol); 850 (ethylbenzene); 500 (n-xylene); 900 (decanal); n/a	CO₂: 690 ppm, T: 21.2 °C, RH: 34 %

Table 4. (2/2). TVOC and individual VOC compound concentrations, and the number of detected compounds encountered using thermal 3D printing methods, in comparison to their official reference values, and air quality parameters during the measurements.

Method	Printer	Feedstock	T (°C)	TVOC (µg/m³)	N of VOCs	Top compounds	Conc. (µg/m³)	Finnish OEL (µg/m³)	MAK/BAT (µg/m³)	LCI (µg/m³)	Air quality parameters
	Zmorph: ZMorph 2.0 SX	Formfutura: EasyWood BC filament	245	91	13	Lactide; furfural; hexadecane; hexamethylcyclotetra-siloxane; octamethylcyclotetra-siloxane	24; 11; 11; 8; 7	n/a; 8000 (furfural); n/a; n/a; n/a	n/a; n/a; n/a; n/a; n/a	n/a; 10 (furfural); 6000 (hexadecane); n/a; 1200 (octamethylcyclo-tetrasiloxane)	CO₂: 660 ppm, T: 27.1 °C, RH: 43 %
Material extrusion	Creality: Ender-3	3Devo: PLA Transparent, custom filament	200	55	11	Lactide; 1-nonanol; decanal; 1-propanol; acetic acid	15; 8; 6; 5; 5	n/a; n/a; n/a; 500,000 (1-propanol); 13,000 (acetic acid)	n/a; n/a; n/a; n/a; 25,000 (acetic acid)	n/a; n/a; 900 (decanal); n/a; 1200 (acetic acid)	CO₂: 810 ppm, T: 20.2 °C, RH: 29 %
		UPM: PLA-based Formi 20 BC, custom filament	200	49	15	Lactide; alpha-pinene; 1-propanol; ethyl acetate; 1-nonanol	7; 5; 5; 4	n/a; n/a; 500,000 (1-propanol); 730,000 (ethyl acetate); n/a	n/a; n/a; n/a; 1,500,000 (ethyl acetate); n/a	n/a; 2500 (alpha-pinene); n/a; n/a; n/a	CO₂: 770 ppm, T: 20.4 °C, RH: 34 %
		UPM: PLA-based Formi 40 BC, custom filament	200	45	15	Lactide; d-limonene; 1-nonanol; 1-propanol; alpha-pinene	8; 6; 4; 3; 3	n/a; 140,000 (d-limonene); n/a; 500,000 (1-propanol); n/a	n/a; 28,000 (d-limonene); n/a; n/a; n/a	n/a; 5000 (d-limonene); n/a; n/a; 2500 (alpha-pinene)	CO₂: 830 ppm, T: 20.3 °C, RH: 28 %
		Custom PLA-based BC filament (15 % wood content)	200	48	16	Lactide; 1-nonanol; d-limonene; decanal; 1-propanol	8; 5; 4; 4; 3	n/a; n/a; 140,000 (d-limonene); n/a; 500,000 (1-propanol)	n/a; n/a; 28,000 (d-limonene); n/a; n/a	n/a; n/a; 5000 (d-limonene); 900 (decanal); n/a	CO₂: 830 ppm, T: 20.3 °C, RH: 28 %
		Custom PLA-based BC filament (30 % wood content)	200	42	13	Lactide; d-limonene; 1-nonanol; ethyl acetate; alpha-pinene	6; 5; 4; 4	n/a; 140,000 (d-limonene); n/a; 730,000 (ethyl acetate); n/a	n/a; 28,000 (d-limonene); n/a; 1,500,000 (ethyl acetate); n/a	n/a; 500 (d-limonene); n/a; n/a; 2500 (alpha-pinene)	CO₂: 780 ppm, T: 20.4 °C, RH: 33 %
Powder bed fusion	EOS: Formiga P110 and P396	Glass-fiber reinforced PA 2200 powder	~175	26	4	Cyclododecanone; decamethylcyclopenta-siloxane; ethanol	12; 8; 4	n/a; n/a; 1,900,000 (ethanol)	n/a; n/a; 960,000 (ethanol)	n/a; n/a; n/a	CO₂: 450 ppm, T: 25.3 °C, RH: 29 %
Multi jet fusion	Hewlett-Packard: Multi Jet Fusion 4200	Glass-fiber reinforced PA 12 powder	~175	780	8	2-Pyrrolidone; triethylene glycol; alpha-pinene; isopropanol; 1,2,3-trimethyl benzene	480; 190; 47; 18; 14	n/a; n/a; n/a; 500,000 (isopropanol); 100,000 (1,2,3-trimethyl benzene)	n/a; 1,000,000 (triethylene glycol); n/a; 500,000 (isopropanol); 100,000 (1,2,3-trimethyl benzene)	n/a; n/a; 2500 (alpha-pinene); n/a; 450 (trimethyl benzene)	CO₂: 680 ppm, T: 21.4 °C, RH: 29 %

Table 5. Cumulative and individual concentrations of the analyzed carbonyl compounds encountered using thermal 3D printing methods, in comparison to their official reference values.

Method	Printer	Feedstock	T (°C)	Total carbonyls (µg/m³)	Top carbonyls	Conc. (µg/m³)	Finnish OEL (µg/m³)	MAK/BAT (µg/m³)	LCI µg/m³
	ZMorph: ZMorph 2.0 SX	Formfutura, ABSPro Flame Retardant filament	250	110	Acetone; formaldehyde, acetaldehyde; 2-butanone	74; 18; 8; 8	1,200,000; 370; 46,000; 60,000	1,200,000; 370; 91,000; 600,000	120,000; 100; 300; 20,000
		Formfutura, EasyWood BC filament	245	43	Acetone; 2-butanone; formaldehyde	17; 15; 11	1,200,000; 60,000; 370	1,200,000; 600,000; 370	120,000; 20,000; 100
Material extrusion	Creality: Ender-3	3Devo: PLA Transparent custom filament	200	250	Acetone; 2-butanone; formaldehyde; acetaldehyde; hexanal	83; 70; 40; 27; 16	1,200,000; 60,000; 370; 46,000*; 42,000*	1,200,000; 600,000; 370; 91,000; n/a	120,000; 20,000; 100; 300; 900
		UPM: PLA-based Formi 20 BC custom filament	200	230	2-Butanone; acetone; formaldehyde; acetaldehyde; hexanal	73; 69; 37; 24; 13	60,000; 1,200,000; 370; 46,000*; 42,000*	600,000; 1,200,000; 370; 91,000; n/a	20,000; 120,000; 100; 300; 900
		UPM: PLA-based Formi 40 BC custom filament	200	190	2-Butanone; acetone; formaldehyde; acetaldehyde; hexanal	58; 55; 32; 20; 12	60,000; 1,200,000; 370; 46,000*; 42,000*	600,000; 1,200,000; 370; 91,000; n/a	20,000; 120,000; 100; 300; 900
		Custom 15 % PLA-based BC custom filament	200	230	Acetone; 2-butanone; formaldehyde; acetaldehyde; hexanal	67; 52; 41; 32; 12	1,200,000; 60,000; 370; 46,000*; 42,000*	1,200,000; 600,000; 370; 91,000; n/a	120,000; 20,000; 100; 300; 900
		Custom 30 % PLA-based BC custom filament	200	220	Acetone; 2-butanone; formaldehyde; acetaldehyde; hexanal	70; 53; 36; 27; 15	1,200,000; 60,000; 370; 46,000*; 42,000*	1,200,000; 600,000; 370; 91,000; n/a	120,000; 20,000; 100; 300; 900
Powder bed fusion	EOS: Formiga P110 and P396	Glass-fiber reinforced PA 2200 powder	~175	100	Acetaldehyde; formaldehyde; propanal	42; 40; 20	46,000*; 370; 48,000	91,000; 370; n/a	300; 100; 650
Multi jet fusion	Hewlett-Packard: Multi Jet Fusion 4200	Glass-fiber reinforced PA 12 powder	~175	73	Acetone; formaldehyde; 2-butanone	41; 18; 14	1,200,000; 370; 60,000	1,200,000; 370; 600,000	120,000; 100; 20,000

* = value given for 15-minute exposure.

Table 6. Average concentrations of the various sampled particle size fractions encountered using thermal 3D printing methods.

Method	Printer	Feedstock	T (°C)	UFP conc. (#/cm³)	PM$_{2.5}$ conc. (µg/m³)	PM$_{10}$/PM$_{15}$ conc. (µg/m³)	Dust conc. (mg/m³)
Material extrusion	ZMorph: ZMorph 2.0 SX	Formfutura: ABSPro Flame Retardant filament	250	8.1×10^4	n/a	10	Below LOD
		Formfutura: EasyWood BC filament	245	5.1×10^3 (4.1×10^5 malfunction)	n/a	10	Below LOD
		Verbatim: PP Transparent filament	230	1.2×10^3	n/a	n/a	n/a
		Recycled (x5) Verbatim: PP Transparent filament	230	6.4×10^2	n/a	n/a	n/a
		Custom, HWP PP filament	235	2.7×10^3	n/a	n/a	n/a
		Custom, recycled (x3) HWP PP filament	235	7.1×10^3	n/a	n/a	n/a
		Formfutura: PLA ReForm filament	205	4.9×10^2	n/a	n/a	n/a
		Recycled (x5) Formfutura: PLA ReForm filament	205	6.0×10 (60)	n/a	n/a	n/a
		Formfutura: Premium PLA Grey filament	205	5.8×10^2	n/a	n/a	n/a
		Recycled (x5) Formfutura: Premium PLA Grey filament	205	8.5×10 (85)	n/a	n/a	n/a
	Creality: Ender-3	3Devo: PLA Transparent custom filament	200	6.3×10^2	2.0	5	n/a
		UPM: PLA-based Formi 20 BC custom filament	200	1.2×10^3	1.2	5	n/a
		UPM: PLA-based Formi 40 BC custom filament	200	1.7×10^3	1.7	5	n/a
		Custom 15 % PLA-based BC filament	200	2.1×10^3	2.2	5	n/a
		Custom 30 % PLA-based BC filament	200	6.1×10^2	1.4	5	n/a
Powder bed fusion	EOS: Formiga P110 and P396	Glass-fiber reinforced PA 2200 powder	~175	1.4×10^4	n/a	20	Below LOD
Multi jet fusion	Hewlett-Packard: Multi Jet Fusion 4200	Glass-fiber reinforced PA 12 powder	~175	2.2×10^2	n/a	20	Below LOD
Powder bed fusion post-processing		Glass-fiber reinforced PA 2200 powder	Room	n/a	n/a	380 (peak)	5.2–9.1
Multi jet fusion post-processing		Glass-fiber reinforced PA 12 powder	Room	n/a	n/a	160 (peak)	1.4–2.4

LOD = limit of detection.

The used UFP particle counter was capable of detecting particles of aerodynamic diameter of 20 nm and above. The lowest limit of detection is a crucial parameter, as a portion of the produced particles may have evaded detection. However, the existing literature suggests that ME 3D printers produce particles mostly around 15–70 nm size range, and thus, only a small portion of UFPs is expected to have passed undetected in this work. Conflicting literature exists, however, as Poikkimäki et al. (2019) used a particle magnifier in their work, and found that UFPs of extremely small size, down to 1 nm, were produced abundantly in ME 3D printing. These particles are too small to be detected by most particle counters, and this fact can explain why most studies suggest that larger UFPs are produced the most in ME 3D printing. The UFP levels measured in this work, however, comply with many previous studies, but the particle counts may be underestimated, nevertheless.

5.1.2 Powder bed and multi jet fusion methods

The chemical and particulate contaminant levels during the operation of large, industrial PBF and MJF machines were investigated in the original publication I. The PBF machines were equipped with local exhaust systems and the 3D printing process took place under an inert, controlled atmosphere, while the MJF machine was only an enclosed system. Both 3D printer types were located in large industrial halls. In addition to the standard measurements, dust and coarse particle concentrations were also sampled during pre- and post-processing stages.

As it turned out, PBF and MJF operations were the only occasions where notable coarse and dust particle formation was recorded. These particles were formed only during the pre- and post-processing stages where the feedstocks were prepared to be used in the 3D printers, and when manufactured products were dusted off from excess feedstock powder. The Finnish OEL of 5 mg/m^3 for organic dust was occasionally exceeded during these manual tasks (FMSAH 2020), despite the work stages lasting for a relatively short period of time (<1 h). The personal total dust exposures ranged between 1.4–9.1 mg/m^3. Meanwhile, 150–400 $\mu g/m^3$ concentration levels of PM_{15} particles were recorded using a real-time monitor nearby. The representative guideline value for PM_{10} particles was therefore exceeded temporarily. In contrast, dust concentrations were below the limit of detection (LOD) during all 3D printing processes, PBF and MJF included, while the

recorded PM_{15} average concentrations were only 20 µg/m^3 in PBF and MJF manufacturing.

The UFP levels were elevated above the background during 3D printing (mean concentrations were 1.4×10^4 and 2.2×10^2 #/cm^3 during PBF and MJF manufacturing, respectively) despite both machine types being enclosed, and the PBF printers were also equipped with in-built exhaust systems. These findings suggest that the printers and/or the ventilation systems were not airtight, but the concentration levels still remained below the UFP reference values (Van Broekhuizen et al. 2012, WHO 2021). The size distributions of UFPs produced by PBF and similar methods are currently unresolved, but given the high processing temperatures, the particles might be of similar in size in comparison to ME 3D printing. Naturally, the used feedstock and process features influence the particle formation and characteristics. Given no data exists, the margin of error of the obtained UFP number counts is hard to estimate.

TVOC concentration was notably elevated (average 780 µg/m^3) during operation of the MJF 3D printer, which was attributed to ink deposition and thermal docomposition as 2-pyrrolidone and triethylene glycol, a common ink component and a PA additive were the most dominant compounds measured at levels of 480 and 190 µg/m^3, respectively. Apparently, aerosols escaped the MJF 3D printer efficiently. However, no elevated TVOC levels could be identified during simultaneous operation of two PBF 3D printers, regardless of the moderate UFP levels. Only four compounds exceeded the background compound levels, and some of them likely originated from the working personnel, rather than the 3D printers. The two plausibly process-originated compounds were cyclododecanone and ethanol, measured at levels of ≤10 µg/m^3. The TVOC levels were obviously below the suggested industrial TVOC guideline value during PBF 3D printing. The guideline was also not reached during MJF 3D printing, but the target value was, indicating that VOC hazards may occur when MJF 3D printers are used.

Carbonyl compounds were measured during PBF manufacturing at a total level of 100 µg/m^3, with acetaldehyde and formaldehyde being found at the highest concentrations (40 µg/m^3). The source of the carbonyls is unclear, given the fact that VOCs were almost nonexistent at the same time. Carbonyls, however, may have contributed to the elevated UFP levels. In contrast, acetone, and formaldehyde were the dominant carbonyls during MJF manufacturing (found at levels of 40 and 20 µg/m^3, respectively), while carbonyls were recorded at the total concentration level of 70 µg/m^3.

The findings by Damanhuri et al. (2019 and 2021) and Zisook et al. (2020) are parallel with the results obtained in this work: inhalable dust was only encountered during powder processing, and the concentrations were very high in those occasions. The concentrations of VOCs were minute, if detected at all. The particle levels recorded by Azzougagh et al. (2021) using metal feedstocks were also at the same order of magnitude as in this work. Hayes et al. (2021) investigated MJF 3D printer emissions, and their findings correspond with the results listed above. The obtained UFP concentrations were at or close to the background level, while minutely elevated PM_{10} and $PM_{2.5}$ particle concentrations were recorded. Furthermore, the dominant VOCs identified by Hayes et al. (2021) perfectly match with those presented in Table 4, although the concentration levels differ.

The MJF 3D printer combined the application of high temperatures, ink-jet spray, and powdered feedstocks in the same process. These factors contributed to the moderate chemical concentrations during 3D printing, and high post-processing dust concentrations. This was a rather exceptional finding, as in most cases in this thesis the exposure hazards are limited to a single manufacturing stage or process. UFPs, however, were encountered at only low levels, although multiple mechanisms for their formation existed. The industrial environment with a presumably powerful ventilation may have eliminated the airborne contaminants fast enough to prevent particle accumulation. This does not explain why UFPs were encountered during the operation of PBF 3D printers, however. The elevated UFP levels during PBF 3D printing may have resulted from the operation of two simultaneous AM machines rather than one, and a higher degree of thermal decomposition which is likely to occur during the PBF manufacturing process.

Finnish OELs or other regulatory values were available only for few identified VOCs. Such were, however, available for all the detected carbonyls, but those were not exceeded, nor were the ones available for VOCs. Acetaldehyde and formaldehyde were present during the manufacturing processes, indicating that chemical exposure hazards exist during operation of PBF and MJF 3D printers. The two VOCs identified at the highest concentrations in MJF manufacturing were both unregulated, and apparently not particularly toxic. Other major VOCs were either not particularly toxic either, or they were encountered at very low concentration levels when compared to the available regulatory values.

In summary, PBF and MJF potentially generate UFPs at elevated concentration levels, and the MJF 3D printer also emitted notable amounts of VOCs as well, even though the 3D printers were operated in large industrial halls. These large machines

inherently produce more emissions than desktop ME 3D printers due to the larger build volumes and relatively fast production speeds, and thus, their placement and operation should be carefully planned to prevent airborne contaminants from reaching high concentration levels. Only certain emission and exposure characteristics regarding the PBF and MJF method emissions can be generalized given the slim existing body of literature. It can be stated that the feedstocks and used process chemicals have the greatest impact on the produced airborne chemical compositions, but the concentration levels can differ greatly depending on the process principles, and the efficiency of the built-in ventilation systems if such was an integral part of the operated AM machine. It was found that a built-in ventilation system effectively prevented chemical substances from entering the surrounding environment, but at the same time elevated UFP levels were recorded. This is an odd finding, given that UFPs are often a by-product of airborne VOC contamination and thermal decomposition of polymers. The particles may have consisted of semi-volatile chemical nuclei rather than volatile ones, and the inert production atmosphere may have influenced the formation and release of chemical contaminants. Both chemical substance and UFP levels were, on the other hand, elevated above the background using the MJF 3D printer when no built-in emission elimination systems or an inert atmosphere existed, and the manufacturing process involved spray deposition of fusing agents.

The process temperatures are mostly tied to the used feedstock and printer properties, and therefore are not suspect to variation. While the process temperature can easily be changed in, e.g., ME 3D printing, the build chamber's temperature in the PBF method should remain stable and slightly below the feedstock's melting point. Therefore, the processing temperatures play a lesser role of a variable in the emission production when PBF or MJF 3D printers are operated. On the other hand, build speed and the surface area of the manufactured products are variables that can influence the emissions to a greater extent, given that a larger processed surface area plausibly leads to greater amounts of produced emissions than a smaller surface area. This follows the facts that a faster build speed can produce emissions at a faster pace, giving ventilation less time to handle the emissions, and that the polymer is only fused at the cross-sections of the product.

5.2 Methods utilizing photocurable plastic feedstocks

The production of chemical and particulate contaminants during the operation of enclosed VP 3D printers and a large, enclosed MJ 3D printer were studied in the original publication I. The simultaneous operation of two consumer VP printers using two different resins were investigated under 3D printing laboratory conditions, while the operation of a dental VP 3D printer using a dental resin was studied under dental laboratory conditions. The MJ 3D printer was operated in an office. The chemical and particulate contaminants produced under laboratory conditions were also studied in the original publication IV using four different enclosed VP 3D printers, and a large, enclosed, and ventilated MM MJ 3D printer. In addition to chemical and particulate matter air concentration measurements, the size distributions of UFPs released during the operation of VP and MJ 3D printers were resolved in the original publication IV as no respective data was available. The obtained chemical substance concentration results are presented in Tables 7–8, while particulate matter concentration results are shown in Table 9. The particulate contaminants were produced at very constant rates and the peak values deviated from the average concentrations only minutely. No time-series data is presented for this reason.

5.2.1 Vat photopolymerization method

The simultaneous use of two generic resins was sampled using two desktop VP 3D printers, while a dental resin was sampled using a dental VP 3D printer in the original publication I. VOCs were initially encountered total levels of 110–130 µg/m^3, while the concentrations of certain compounds (methyl methacrylate, ethyl methacrylate, 2-butenoic acid, and methyl isobutyl ketone) were above all others (60–30 µg/m^3). The obtained TVOC concentrations were somewhat lower in the original publication IV (40–90 µg/m^3) where a single 3D printer was operated at a time, while the top compounds (isopropyl alcohol, tert-butanol, nonanal, methyl isobutyl ketone, 2-hydroxypropyl methacrylate) were found at 5–25 µg/m^3 concentration levels. Nevertheless, acrylates were commonly encountered in VP 3D printer operations which produces an undisputable exposure hazard following their sensitizing potential (Savonius et al. 1993, Fukumoto et al. 2013, Alifui-Segbaya 2018 and 2020). The differences in the obtained concentration levels and the chemical

compositions were minor overall. Acrylates, solvents, and acids dominated the emissions almost without exceptions (nonanal, alpha-pinene, and 2-ethylpiperazine were documented at the highest concentrations in the use of one particular resin), regardless of certain feedstocks being dental grade rather than generic commercial feedstocks. One VP printer also heated its vat up to 35 °C, but it did not impact the obtained TVOC levels. The TVOC levels fell consistently below the proposed Finnish occupational TVOC target value of 300 µg/m^3, as did individual compound levels remain below their corresponding OELs, and MAK, BAT, and LCI-values.

In contrast to the relatively low TVOC levels encountered in 3D printing, the highest single TVOC value (11,000 µg/m^3) obtained in this thesis was recorded during manual post-processing of products manufactured using the VP method. It should be noted that this sample was taken directly from the breathing zone of the process worker, yielding a true exposure level. Methyl isobutyl ketone, a solvation product, was found at the level of 8100 µg/m^3 in the sample, followed by isopropanol at the concentration level of 1650 µg/m^3, and by various other compounds at lower levels, including methyl methacrylate (300 µg/m^3). Likewise to the post-processing stages in PBF and MJF manufacturing, the post-production tasks can result in particularly high (chemical) exposure levels in VP 3D printing. The risk of dermal exposure also exists when products covered in the photopolymer resin are washed.

Carbonyl levels were low or moderate in comparison to thermal 3D printing methods and ranged between 10–150 µg/m^3 when detected. 2-Butanone, acetone, and formaldehyde were typically the dominant carbonyls and their concentration levels ranged between from ca. 10 to up to 140 µg/m^3, but they were usually found at concentration levels of around 15–30 µg/m^3. These values fell below their representative OELs, MAK, BAT, and LCI-values. No consistent differences in the concentration levels were found that could originate from the used 3D printers or feedstock types. In contrast to thermal 3D printing method results, many of the most common compounds encountered in VP 3D printer operations, in both VOC and carbonyl compound classes, had an existing regulatory limit value.

The number concentrations of UFPs were not found to rise above the background levels by a hand-held particle counter when two VP printers were operated simultaneously in a spacious laboratory environment. However, UFPs were found using a desktop particle counter at the level of 10^3 #/cm^3 in a smaller laboratory environment when a single 3D printer was operated, and the obtained TVOC levels were at corresponding orders of magnitude between the two

measurement sets (although slightly higher when two printers were simultaneously operated). This indicates that the particles are formed inside the 3D printing chamber, from where they disperse into the surrounding environment. The dispersion into the larger laboratory environment resulted in undetectable number concentrations in the first study, while UFPs could be detected in a much smaller laboratory. The UFP concentration levels fell consistently below the proposed threshold or limit values of $2–4×10^4$ #/cm^3.

The dominating particle size during the operation of a desktop VP 3D printer was ca. 11 nm. When an industrial VP 3D printer was operated the corresponding particle size was ca. 19 nm. However, the use of dental VP 3D printers yielded dominant particle sizes of ca. 19, 34, and 45 nm. This can explain why the UFP concentration in the university laboratory were below the limit of detection in the original publication I, and why the particles were found in the dental laboratory still. The obtained PM$_{15}$ and PM$_{10}$ mass concentrations were very low (from below 5 µg/m^3 to 30 µg/m^3) throughout the experiments, and therefore, well below their established guideline values.

Following the chemical characterization of airborne chemicals, which is one of the factors behind particle toxicity, it is plausible that the UFPs produced from the condensed VOCs are hazardous. VOC condensation is assumed to be the main mechanism for UFP formation in the absence of other, e.g., thermal decomposition mechanisms. Toxicity of photocurable resins has been studied by Jorge et al. (2003), Fukumoto et al. (2013), and Alifui-Segbaya et al. (2018 and 2020), and their results support this assumption. Exposure control measures are therefore advised to be issued based on these findings.

Table 7. TVOC and individual VOC compound concentrations, and the number of detected compounds encountered using photocuring 3D printing methods, in comparison to their official reference values, and air quality parameters during the measurements. (1/2)

Method	Printer	Feedstock	T (°C)	TVOC (µg/m³)	N of VOCs	Top compounds	Conc. (µg/m³)	Finnish OEL (µg/m³)	MAK/BAT (µg/m³)	LCI (µg/m³)	Air quality parameters
Vat photo-polymerization	Formlabs: Form 2 (two machines)	Formlabs: Grey and Castable Wax	35	110	5	Methyl methacrylate; ethyl methacrylate; isopropanol; acetic acid	62; 22; 16; 7	42,000 (methyl methacrylate); 47,000 (ethyl methacrylate); 500,000 (isopropanol); 13,000 (acetic acid)	18,000 (methyl methacrylate); 8300 (ethyl methacrylate); 500,000 (isopropanol); 25,000 (acetic acid)	750 (methyl methacrylate); 110 (ethyl methacrylate); n/a; 1200 (acetic acid)	CO_2: 510 ppm, T: 21.3 °C, RH: 15 %
	Formlabs: Form 2	Formlabs: Clear	35	41	11	2-Hydroxypropyl methacrylate; methyl methacrylate; ethyl methacrylate; alpha-pinene; nonanal	6; 6; 4; 4; 3	n/a; 42,000 (methyl methacrylate); 47,000 (ethyl methacrylate); n/a; n/a	n/a; 18,000 (methyl methacrylate); 8300 (ethyl methacrylate); n/a; n/a	110 (2-hydroxypropyl methacrylate); 750 (methyl methacrylate); 110 (ethyl methacrylate); 2500 (alpha-pinene); 900 (nonanal)	CO_2: 440 ppm, T: 18.7 °C, RH: 3 %
		Formlabs: Castable Wax	35	46	12	Nonanal; alpha-pinene; 2-ethylpiperazine; n-xylene; 4-methoxy-1-butanol	13; 6; 4; 3; 3	n/a; n/a; n/a; 220,000 (n-xylene); n/a	n/a; n/a; n/a; 440,000 (n-xylene); n/a	900 (nonanal); 2500 (alpha-pinene); n/a; 500 (n-xylene); n/a	CO_2: 460 ppm, T: 21.1 °C, RH: 3 %
	Nexa3D: NXE400	Nexa3D: xGPP-Translucent	Room	45	11	Alpha-pinene; methacrylic acid; benzoic acid; 2-methylbutanoic acid; toluene	8; 5; 5; 4; 3	n/a; 71,000 (methacrylic acid); n/a; n/a; 81,000 (toluene)	n/a; 180,000 (methacrylic acid); n/a; n/a; 190,000 (toluene)	2500 (alpha-pinene); n/a; n/a; n/a; 1900 (toluene)	CO_2: 450 ppm, T: 22.0 °C, RH: 2 %
		Bego: VarseoWax CAD/Cast	Room	130	10	2-Butenoic acid; methyl isobutyl ketone; methyl methacrylate; n-xylene; ethanol	47; 29; 19; 13; 8	n/a; 80,000 (methyl isobutyl ketone); 42,000 (methyl methacrylate); 220,000 (n-xylene); 1,900,000 (ethanol)	n/a; 83,000 (methyl isobutyl ketone); 18,000 (methyl methacrylate); 440,000 (n-xylene); 960,000 (ethanol)	n/a; 1000 (methyl isobutyl ketone); 750 (methyl methacrylate); 500 (n-xylene); n/a	CO_2: 660 ppm, T: 24.4 °C, RH: 43 %
	Bego: Varseo	Bego: VarseoWax Model	Room	55	10	Isopropyl alcohol; tert-butanol; methyl isobutyl ketone; nonanal; alpha-pinene	18; 12; 7; 6; 5	500,000 (isopropyl alcohol); 150,000 (tert-butanol); 80,000 (methyl isobutyl ketone); n/a; n/a	500,000 (isopropyl alcohol); 62,000 (tert-butanol); 83,000 (methyl isobutyl ketone); n/a; n/a	n/a; 620 (tert-butanol); 1000 (methyl isobutyl ketone); 900 (nonanal); 2500 (alpha-pinene)	CO_2: 600 ppm, T: 21.2 °C, RH: 12 %
		Bego: VarseoWax Tray	Room	87	15	Tert-butanol; isopropyl alcohol; 1,3-dioxolane; methyl isobutyl ketone; nonanal	17; 15; 7; 6; 6	150,000 (tert-butanol); 500,000 (isopropyl alcohol); 310,00 (1,3-dioxolane); 80,000 (methyl isobutyl ketone); n/a	62,000 (tert-butanol); 500,000 (isopropyl alcohol); 310,000 (1,3-dioxolane); 83,000 (methyl isobutyl ketone); n/a	620 (tert-butanol); n/a; n/a 1000 (methyl isobutyl ketone); 900 (nonanal)	CO_2: 540 ppm, T: 20.7 °C, RH: 7 %

Table 7. TVOC and individual VOC compound concentrations, and the number of detected compounds encountered using photocuring 3D printing methods, in comparison to their official reference values, and air quality parameters during the measurements. (2/2)

Method	Printer	Feedstock	T (°C)	TVOC (µg/m^3)	N of VOCs	Top compounds	Conc. (µg/m^3)	Finnish OEL (µg/m^3)	MAK/BAT (µg/m^3)	LCI (µg/m^3)	Air quality parameters
Vat photo-polymerization	Ivoclar Vivadent: PrograPrint PR5	Ivoclar Vivadent: ProArtPrint Model	Room	75	18	Methyl isobutyl ketone; isopropyl alcohol; tert-butanol; nonanal; 2-hydroxypropyl methacrylate	24; 15; 12; 5; 3	80,000 (methyl isobutyl ketone); 500,000 (isopropyl alcohol); 150,000 (tert-butanol); n/a; n/a	83,000 (methyl isobutyl ketone); 500,000 (isopropyl alcohol); 62,000 (tert-butanol); n/a; n/a	1000 (methyl isobutyl ketone); n/a; 620 (tert-butanol); 900 (nonanal); 110 (2-hydroxypropyl methacrylate)	CO_2: 560 ppm, T: 21.7 °C, RH: 11 %
		Ivoclar Vivadent: ProArtPrint Splint	Room	66	11	Isopropyl alcohol; methyl isobutyl ketone; 2-ethoxypropane; nonanal; acetic acid	22; 15; 8; 5; 4	500,000 (isopropyl alcohol); 80,000 (methyl isobutyl ketone); n/a; n/a; 13,000 (acetic acid)	500,000 (isopropyl alcohol); 83,000 (methyl isobutyl ketone); n/a; n/a; 25,000 (acetic acid)	n/a; 1000 (methyl isobutyl ketone); n/a; 900 (nonanal); 1200 (acetic acid)	CO_2: 550 ppm, T: 20.7 °C, RH: 10 %
Material jetting	3D Systems: Projet MJP 2500	3D Systems: VisiJet M2R-CL	Room	1710	23	Isobornyl acrylate; 2-furanopropanoic acid; allyl acrylate; n-xylene; 2,3-dimethyl-2,4-hexadiene	1200; 100; 63; 57; 37	n/a; n/a; n/a; 220,000 (n-xylene); n/a	n/a; n/a; n/a; 440,000 (n-xylene); n/a	110 (isobornyl acrylate); n/a; 110 (allyl acrylate); 500 (n-xylene); n/a	CO_2: 560 ppm, T: 25.5 °C, RH: 19 %
	Stratasys: J735	Stratasys: VeroBlackPlus	Room	70	11	Isobornyl acrylate; propylene glycol; benzoic acid; nonanal; 2-ethylhexanol	17; 11; 7; 5; 4	n/a; n/a; n/a; n/a; 5400 (2-ethylhexanol)	n/a; n/a; n/a; n/a; 54,000 (2-ethylhexanol)	110 (isobornyl acrylate); 2100 (propylene glycol); n/a; 900 (nonanal); 300 (2-ethylhexanol)	CO_2: 460 ppm, T: 21.6 °C, RH: 2 %
	Stratasys: J735	Stratasys: VeroCyan-V, VeroMagenta-V, VeroYellow-V, VeroPureWhite and VeroClear	Room	70	11	Isobornyl acrylate; methyl methacrylate; isopropyl alcohol; propylene glycol; 4-acryloylmorpholine	38; 5; 4; 4; 4	n/a; 42,000 (methyl methacrylate); 500,000 (isopropyl alcohol); n/a; n/a	n/a; 18,000 (methyl methacrylate); 500,000 (isopropyl alcohol); n/a; n/a	110 (isobornyl acrylate); 750 (methyl methacrylate); n/a; 2100 (propylene glycol); n/a	CO_2: 530 ppm, T: 21.3 °C, RH: 1 %
Vat photo-polymerization post-processing (personal)	n/a	Bego: VarseoWax CAD/Cast	Room	11060	20	Methyl isobutyl ketone; isopropanol; tetrahydro-2-furanylmethyl pivalate; methyl methacrylate; ethanol	8100; 1700; 440; 290; 140	80,000 (methyl isobutyl ketone); 500,000 (isopropyl alcohol); n/a; 42,000 (methyl methacrylate); 1,900,000 (ethanol)	83,000 (methyl isobutyl ketone); 440,000 (n-xylene); n/a; 86,000 (styrene); n/a	1000 (methyl isobutyl ketone); n/a; n/a; 750 (methyl methacrylate); n/a	n/a
Material jetting post-processing	n/a	3D Systems: VisiJet M2R-CL	Room	1060	10	Isobornyl acrylate; n-xylene; 2-furanpropanoic acid; styrene; 2-(1-Cyclopent-1-enyl-1-methylethyl)-cyclopentanone	620; 67; 64; 33; 27	n/a; 220,000 (n-xylene); n/a; 86,000 (styrene); n/a	-	110 (isobornyl acrylate); 500 (n-xylene); n/a; 250 (styrene); n/a	n/a

Table 8. Cumulative and individual concentrations of the analyzed carbonyl compounds encountered using photocuring 3D printing methods, in comparison to their official reference values.

Method	Printer	Feedstock	T (°C)	Total carbonyls (µg/m³)	Top carbonyls	Conc. (µg/m³)	Finnish OEL (µg/m³)	MAK/BAT (µg/m³)	LCI (µg/m³)
Vat photo-polymerization	Formlabs: Form 2 (two simultaneous prints)	Formlabs: Grey and Castable Wax resins	35	42	2-Butanone; acetone; formaldehyde	22; 17; 3	60,000; 1,200,000; 370	600,000; 1,200,000; 370	20,000; 120,000; 100
	Formlabs: Form 2	Formlabs: Clear resin	35	21	2-Butanone; hexanal; butanal; acetone; acetaldehyde	6; 4; 4; 3; 2	60,000; 42,000*; 74,000; 1,200,000; 46,000*	600,000; n/a; n/a; 1,200,000; 370	20,000; 900; 650; 120,000; 300
		Formlabs: Castable Wax resin	35	10	Butanal; acetone	3; 2	74,000; 1,200,000	n/a; 1,200,000	650; 120,000
	Bego: Varseo	Bego: VarseoWax CAD/Cast resin	Room	150	Acetone; formaldehyde	140; 12	1,200,000; 370	1,200,000; 370	120,000; 100
		Bego: VarseoWax Model resin	Room	98	2-Butanone; acetone; acetaldehyde; formaldehyde; hexanal	35; 25; 14; 12; 5	60,000; 1,200,000; 46,000*; 370; 42,000*	600,000; 1,200,000; 91,000; 370; n/a	20,000; 120,000; 300; 100; 900
		Bego: VarseoWax Tray resin	Room	54	Acetone; 2-butanone; formaldehyde; acetaldehyde; butanal	26; 15; 4; 4; 2	1,200,000; 60,000; 370; 46,000*; 74,000	1,200,000; 600,000; 370; 91,000; n/a	120,000; 20,000; 100; 300; 650
	Ivoclar Vivadent: PrograPrint PR5	Ivoclar Vivadent: ProArtPrint Model resin	Room	82	Acetone; formaldehyde; acetaldehyde; 2-butanone; hexanal	37; 11; 11; 11; 5	1,200,000; 370; 46,000*; 60,000; 42,000*	1,200,000; 370; 91,000; 600,000; n/a	120,000; 100; 300; 20,000; 900
		Ivoclar Vivadent: ProArtPrint Splint resin	Room	53	Acetone; formaldehyde; 2-butanone; acetaldehyde; hexanal	28; 8; 7; 3; 3	1,200,000; 370; 60,000; 46,000*; 42,000*	1,200,000; 370; 600,000; 91,000; n/a	120,000; 100; 20,000; 300; 900
	Nexa3D: NXE400	Nexa3D: xGPP-Translucent resin	Room	29	Acetone; 2-butanone; butanal; hexanal	12; 10; 3; 2	1,200,000; 60,000; 74,000; 42,000*	1,200,000; 600,000; n/a; n/a	120,000; 20,000; 650; 900
	3D Systems: Projet MJP 2500	3D Systems: Visijet M2R-CL ink resin	Room	0	n/a	n/a	n/a	n/a	n/a
Material jetting	Stratasys: J735	Stratasys: VeroBlackPlus ink resin	Room	24	Formaldehyde; hexanal; butanal; acetaldehyde; acetone	11; 4; 3; 2; 2	370; 42,000*; 74,000; 46,000*; 1,200,000	370; n/a; n/a; 91,000; 1,200,000	100; 900; 650; 300; 120,000
		Stratasys: VeroCyan-V, VeroMagenta-V, VeroYellow-V, VeroPureWhite and VeroClear ink resins	Room	43	Acetone; formaldehyde; benzaldehyde; hexanal; acetaldehyde	14; 12; 5; 4; 3	1,200,000; 370; 4400; 42,000*; 46,000*	1,200,000; 370; n/a; n/a; 91,000	120,000; 100; n/a; 900; 300

* = value given for 15- minute exposure.

Table 9. Average concentrations of the various sampled particle size fractions encountered using photocuring 3D printing methods.

Method	Printer	Feedstock	T (°C)	UFP conc. (#/cm³)	PM$_{10}$/PM$_{15}$ conc. (µg/m³)	Mean particle size (nm)
Vat photo-polymerization	Formlabs: Form 2 (two simultaneous prints)	Formlabs: Grey and Castable Wax resins	35	Below LOD	<5	n/a
	Formlabs: Form 2	Formlabs: Clear resin	35	$1.27×10^3$	<5	10.8
		Formlabs: Castable Wax resin	35	$1.40×10^3$	<5	10.8
	Bego: Varseo	Bego: VarseoWax CAD/Cast resin	Room	$3.60×10^3$	30	n/a
		Bego: VarseoWax Model resin	Room	$2.93×10^3$	<5	34
		Bego: VarseoWax Tray resin	Room	$3.62×10^3$	<5	45.3
	Ivoclar Vivadent: PrograPrint PR5	Ivoclar Vivadent: ProArtPrint Model resin	Room	$1.99×10^3$	<5	19.1
		Ivoclar Vivadent: ProArtPrint Splint resin	Room	$1.21×10^3$	<5	34
	Nexa3D: NXE400	Nexa3D: xGPP-Translucent resin	Room	$2.23×10^3$	<5	19.1
	3D Systems: ProJet MJP 2500	3D Systems: VisJet M2R-CL ink resin	Room	Below LOD	<5	n/a
Material jetting	Stratasys: J735	Stratasys: VeroBlackPlus ink resin	Room	$1.90×10^2$ ($6.05×10^2$ ventilation duct)	<5	80.6
		Stratasys: VeroCyan-V, VeroMagenta-V, VeroYellow-V, VeroPureWhite and VeroClear ink resins	Room	$2.50×10^2$ ($6.60×10^2$ ventilation duct)	<5	45.3

LOD = limit of detection.

5.2.2 Material jetting method

An industrial MJ 3D printer was operated in an office environment in the original publication I. The printer was enclosed, but not ventilated. This was clearly reflected in the results as high VOC emissions and elevated UFP levels. A larger and enclosed, high-end industrial MM MJ 3D printer equipped with local exhaust system emitted only minute amounts of VOCs and UFPs into its environment, as found in the original publication IV.

On one occasion (MJ 3D printing under office conditions) carbonyls were not detected at all, meanwhile the recorded TVOC level was the highest of all the 3D print jobs. This may have been a result of faulty sample collection, extraction, or analysis, as VOCs and carbonyls are expected to be present in the air concurrently. TVOC level produced by the non-ventilated MJ printer was as high as 1700 $\mu g/m^3$. The top compounds were acrylates and acids, with isobornyl acrylate being found at the highest concentration (1200 $\mu g/m^3$), followed with 2-furanopropanoic acid (100 $\mu g/m^3$) and allyl acrylate (60 $\mu g/m^3$). The concentration of isobornyl acrylate exceeded its LCI value of 110 $\mu g/m^3$ 10-fold, which is an exceptional finding. Other VOCs were otherwise below their corresponding OELs or respective regulatory values. Isobornyl acrylate was also found in the room air when the ventilated MJ 3D printer was operated, but at the level of 40 $\mu g/m^3$ or below.

Carbonyl compounds were detected at low levels when the ventilated MJ 3D printer was operated. Cumulative carbonyl concentration was only 25–45 $\mu g/m^3$, with acetone and formaldehyde being found at the highest concentrations (≤ 15 $\mu g/m^3$). These are far lower concentrations than their representative OELs or guideline values. The MJ 3D printing method, therefore, produced low amounts of carbonyls in total when compared to the other studied 3D printing methods.

Aerosolization of the ink-jet spray is the likely mechanism for emission formation, given that no thermal decomposition mechanisms exist, and the inks are stored in closed cartridges rather than open vats. It is somewhat unexpected that PM_{10} concentrations were very low regardless, since aerosolized ink particles could be expected to be formed at beyond UFP size range. Nevertheless, the obtained mean PM_{10} concentrations were only <5 $\mu g/m^3$ in all MJ 3D printing cases, and no elevated UFP levels could be detected during the operation of a MJ printer under office-like conditions. This is an odd finding, given the high TVOC concentration which should have made it possible for UFPs to form. The used particle counter had

a minimum particle diameter detection limit of 20 nm, which may explain this finding. However, UFPs were encountered at the low levels of 2×10^2 #/cm^3 when the ventilated MJ 3D printer was operated in a laboratory environment and a particle counter with the lowest limit of detection of 7 nm was used. UFPs were at the same time found mostly at 45–80 nm size range. Inconsistency exists here, as both used particle counters should have been able to detect particles of this size. However, two different MJ 3D printers were used in the tests, and the factors influencing UFP formation may have differed greatly. All the particle concentrations were, in conclusion, low and below their corresponding reference values.

VOCs and UFPs were also sampled from the exhaust ventilation system of the ventilated, high-end MJ 3D printer. TVOC levels were substantially higher inside the vent (2200–3000 µg/m^3) than in the 3D printing room. More individual compounds were also identified from inside the ventilation system (n = 27 in contrast to n = 11 from the room air). The compounds detected at the highest concentration levels were similar to what was measured from the room air: isobornyl acrylate (1600–2000 µg/m^3), propylene glycol (320–330 µg/m^3), in addition to 4-acrylomorpholine, isopropanol, and various others. The in-built emission elimination system reduced the TVOC level by 97 % (comparison of the TVOC levels obtained from the ventilation system and laboratory air). UFPs, on the other hand, were recorded at only slightly higher levels (6×10^2 #/cm^3) from the ventilation duct.

Ultrasound post-processing of MJ manufactured products did produce VOC emissions, perhaps through spontaneous evaporation from the open ultrasound vat with the assistance of produced heat. Some of the compounds likely originated from the earlier 3D printing process as the VOC sampling was conducted shortly after 3D printing, but the resin-contaminated water in the ultrasound vat is a plausible source for VOCs as well.

Pressurized deposition of photocurable inks was found in this, and similarly in the MJF 3D printing case, to produce notably elevated TVOC levels when no emission elimination systems existed. Such a system was found to reduce the VOC levels in the room air significantly. Furthermore, UFPs produced during MJ 3D printing processes may produce similar exposure hazards as those produced in VP 3D printing, following the chemical characterization of airborne chemicals.

Only certain generalizations can be drawn, given the slim body of existing literature. The hazards related to chemical and particulate contaminants are like those encountered in VP 3D printer operations, following the characterization of emitted chemical substances. The emissions are likely produced during the ink

deposition, as no other processes exist where notable VOC or UFP formation is expected to occur. The emissions can escape an enclosed MJ 3D printer and cause elevated VOC exposure levels, but UFPs or larger particles were found to be formed in only small amounts, suggesting that chemical exposures are the main concern in MJ 3D printer operations.

5.3   Post-production material outgassing

In addition to the documented outgassing from products manufactured using thermal 3D printing techniques, photopolymer resin products also emit chemical substances after manufacturing. The emitted chemicals contribute to post-production exposure to chemicals, especially if freshly manufactured products are stored in plenty, while consumers can also be exposed to them. The hazards are further emphasized on behalf of wearable and medical products which are in contact with biological tissues, and e.g., dental devices (Petrofsky et al. 2014, Lago et al. 2015, Stansbury & Idacavage 2016).

Material outgassing was studied in the original publication IV using cubes manufactured via VP and MJ methods. The cubes manufactured using the VP method were post-processed accordingly: the cubes were first cleansed with a solvent (isopropanol or ethanol) and then photocured following manufacturer instructions. The cubes manufactured using a MJ printer were only rinsed with water to remove dissolvable support structures. The followed measurement protocol was not standardized, as no such a method exists for the evaluation of outgassed chemicals from consumer products and therefore these measurements serve as an independent set of data.

There were notable differences in the total outgassing rates between the test cubes. The cubes manufactured using one manufacturer's resins (n = 2) accepted to be used for dental applications emitted VOCs at the rate of 330-690 µg/m^2/h at 20 °C, and at up to 1100 µg/m^2/h at 37 °C after 24 hours of production. In comparison, cubes 3D printed using another manufacturer's corresponding dental resins (n = 2) emitted VOCs at the rate of 3000–3500 µg/m^2/h at 20 °C, and at up to 8700 µg/m^2/h rate at 37 °C. These rates were reduced to 40–50 and 110–320 µg/m^2/h (20–37 °C), respectively, after three months of storage, which translates into a reduction of 93–97 %. Cubes manufactured using non-dental VP resins (n = 3) unsurprisingly outgassed higher amounts of VOCs. The emissions from these resins initially ranged

from 4100–7200 µg/m^2/h (20 °C) to 10100–13800 µg/m^2/h (37 °C). The outgassing rates were diminished to 110–900 µg/m^2/h after three months (20–37 °C), which also equals 93–97 % reduction in the outgassing rate.

The used solvents were found to be infiltrated into the cube matrixes, which is seen as the high outgassing rates of the solvents in comparison to the other emitted compounds. A major difference between the processing of the dental resin cubes (n = 4) was that the cubes were post-processed with ethanol (n = 2), rather than isopropanol (n = 2), emitted the least amounts of VOCs. Ethanol also contributed to lower percentage of the total outgassed VOCs: the portion of ethanol ranged from 15 to 41 % of total VOCs after 24 hours of production, down to below the limit of accurate quantification (4–32 % when quantified) after three months of storage. In contrast, isopropanol contributed to 39–92 % of total emitted VOCs when it was used as the cleaning solvent after 24 hours of production, and 23–83 % after three months. It should be noted that the quantification of these solvents is not accurate when the applied VOC analysis method is used, and the solvent concentrations are most likely underestimated, and the emission rate of ethanol is most likely even more underestimated than that of isopropanol's due to ethanol's smaller molecular mass. The portions of isopropanol were quite similar, 58–76 % of total VOCs after 24 hours, and 15-38 % after three months in the case of cubes manufactured using non-dental resins. Other compounds with the highest outgassing rates (up to 900 µg/m^2/h at 20 °C and 1650 µg/m^2/h at 37 °C) were diverse, but most of the identified chemicals were oxygenated hydrocarbons, e.g., acids, esters, ketones, acrylates, and aldehydes. 4–10 individual compounds were identified to be emitted from the dental resin cubes, while 11–12 compounds were documented to be outgassed by the non-dental cubes.

The cubes manufactured using the MJ method (n = 2) unexpectedly emitted similar levels of VOCs in total (from the initial 4400–5400 µg/m^2/h at 20 °C, and 7200–9400 µg/m^2/h at 37 °C down to 60–200 µg/m^2/h after three months at 20–37 °C, which equals a 97–99 % reduction after storage) as most cubes manufactured using the VP method did. However, the most abundantly emitted compound was propylene glycol (which initially contributed for 75–86 % of total VOCs, down to 19–34 % after three months) instead of solvents, following the fact that the cubes were only rinsed with water and not cleansed using a solvent. Propylene glycol was also found to be a major emission product in the MJ 3D printing process. The other main outgassed products were mostly alcohols, aldehydes, and ketones, while a total of 10–13 individual compounds were documented to be outgassed from the cubes.

There is no data available on the emission rates of VOCs from ME products albeit outgassing has been recognized on their behalf, although Stefaniak et al. (2017b) briefly tested outgassing emissions from stock filaments. No data exists on VOC outgassing from VP or MJ products, while little research literature exists on the emissions from consumer products. Even et al. (2020), for example, documented outgassing of compounds associated to the used polymer blend from consumer products and found that the emission rates are substantially reduced within days of production, which is a consistent finding with this work. Measurement inaccuracies aside, the non-health based, voluntary Finnish construction material emission classification and the health based European LCI values can be used as references in the absence of dedicated consumer product emission regulation. The strictest emission classification limit in the Finnish construction material emission system is set at ≤200 $\mu g/m^2/h$ after 28 days of production. This classification, however, is only used to evaluate the total emissions from a material and it disregards the chemical composition of the emission profile and therefore, toxicological risks. This threshold was achieved by two dental resins at both 20 and 37 °C after two weeks of storage. Surprisingly, this threshold was still exceeded by most resins after three months, especially at 37 °C; the outgassing rates were below the limit only in the cases of two dental, and one MJ resins, meaning that 6 out of the 9 resin cubes still outgassed excess amounts of VOCs. However, 7 out of the 9 cubes emitted VOCs at below 200 $\mu g/m^2/h$ at 20 °C which represents normal room conditions.

LCI values were found for some outgassed compounds, albeit no applicable value was found for the most of them. The given LCI values ranged mostly between 490 $\mu g/m^3$ (acetophenone) and 2100 $\mu g/m^3$ (2-ethylhexanol). However, a general value of 110 $\mu g/m^3$ was given for most acrylates, and additional three strict LCI concentrations were found: 25 $\mu g/m^3$ for dimethyl glutarate (found to be emitted from a dental resin), 20 $\mu g/m^3$ for dimethyl succinate (found to be emitted from two non-dental resins and one dental resin), and 10 $\mu g/m^3$ for hexamethylene diacrylate (found to be emitted from all three non-dental VP resins). These three compounds were documented to be emitted at rates of up to 400, 900, and 310 $\mu g/m^2/h$ at 20 °C, and at 990, 1650, and 620 $\mu g/m^2/h$ at 37 °C, respectively, after 24 hours of manufacturing. Dimethyl glutarate and succinate are both associated with occupational asthma, irritation, and CNS effects (Rosenman et al. 2003, Heinzow et al. 2009), while multifunctional acrylates like hexamethylene diacrylate have been identified as potent sensitizers (Andrews & Clary 1986, Alifui-Segbaya et al. 2018, Van Amerongen et al. 2019).

(In)direct dermal and mucous membrane exposure to the outgassed or secreted compounds is imminent if the products are worn or used in contact with biological tissues. Exposure to resin remnants have been documented to induce biological effects, including immunostimulatory effects, e.g., dermatoses and sensitization, as well as cytotoxic effects in studies using zebrafish or cell cultures, and in epidemiological studies. (Fukumoto et al. 2013; Petrofsky et al. 2014; Creytens et al. 2017; Nouman et al. 2017; Alifui-Segbaya et al. 2018; Heratizadeh et al. 2018.) Secondary inhalation exposure to the outgassed products is plausible as well, especially soon after manufacturing and product finishing, which produces similar hazards as regular inhalation exposure to volatile substances. The outgassing amplitude can be reduced by proper post-curing, and as suggested by Stansbury & Idacavage (2016). The products manufactured using photocurable resins should be post-processed adequately to ensure they are safe to use. This, in addition to proper storage before use, is recommended to reduce the inhalation and touch exposure hazards related to AM products manufactured using photocurable resins.

6 Concluding remarks

Certain conclusions can be drawn from results obtained in this thesis. The emissions produced by thermal 3D printers were associated with thermal decomposition, while non-thermal 3D printer emissions are associated with spontaneous evaporation of the feedstock or its aerosolization during feedstock deposition. Certain methods, e.g., the MJF method, can produce chemical species that originate from multiple formation pathways. The used feedstock and process chemicals have a major influence on the composition of airborne chemical mixtures and the potential exposure levels.

Both chemical and UFP concentrations were elevated during operation of almost all used 3D printer types and feedstocks. The VP printers did not produce excessive amounts of UFPs, and the PBF printer did not produce notable VOC emissions as documented in the original publication I. Coarse particle formations were limited to pre- and post-processing stages of PBF and MJF methods where powdered feedstocks were handled. Fine and ultrafine fractions were produced at quite constant rates during 3D printing, and only little concentration fluctuations were recorded by the real-time particle counters. The only situation where significantly elevated UFP peaks were recorded was the malfunction of a desktop ME 3D printer. While only necessary pre- and post-processing tasks related to the five used methods were studied, it is plausible that other means of product processing, like vapor polishing or spray coating results in high potential chemical exposures as the pre- and post-processing tasks were found to produce the highest potential individual dust and VOC exposure levels recorded in this thesis. The studied environmentally sustainable feedstocks were identified as similar emission sources as generic feedstocks, and therefore, they are not expected to be more hazardous to use as the existing generic feedstocks. A filament extruder produced emission with very similar compositions in comparison to desktop ME 3D printers, but at slightly lower concentration levels following its lower processing temperatures.

The documented chemical concentrations were consistently below their established Finnish OELs or the available MAK or BAT values. However, LCI values of certain compounds (furfural and certain acrylates) were reached. These findings suggest that the potential exposure levels rarely reach hazardous levels during the correct operation of a single 3D printer of any type. However, many compounds did

not have established limit or guideline values and thus, exposure to them is unregulated and may lack toxicological knowledge. Certain compounds were associated with cancer risk, or identified as potent sensitizers, meaning that exposures should be controlled despite the exposure levels were low in comparison to established OELs or other reference values. All other particle fractions apart from UFPs were extremely low during the operation of any 3D printer using any feedstock type. However, high (above the Finnish OEL) levels of dust were generated during PBF and MJF pre- and post-processes despite them lasting for relatively short periods of time. The documented UFP, $PM_{2.5}$, and PM_{10} concentrations fell consistently below their corresponding reference values. In summary it can be stated that certain pre- and post-processing tasks produce either potentially higher chemical or dust exposure hazards than actual 3D printing processes. These manual process stages are to be performed cautiously.

Chemical outgassing and blooming can produce a chemical exposure hazard to an end-user of a 3D printed product. This is an often a neglected matter as the post-production emissions from consumer products are not regulated properly. Appropriate post-processing, including UV curing, and a sufficient storage period before use can reduce the outgassing substantially and reduce the hazards.

Space and environmental characteristics have a substantial impact on the concentration levels of the contaminants emitted by 3D printers, and therefore on the potential exposures. However, the wide array of operational environments, but the uniform sampling procedure followed in this thesis suggests that exposures to chemicals and particles do always occur at a close proximity of the 3D printers if no emission elimination systems are used. However, the emissions are effectively diluted into a larger space and the potential exposure levels are lower in spacious, well-ventilated environments in comparison to smaller, inefficiently ventilated spaces. Furthermore, 3D printer specifications and the used feedstocks have an influence on the produced contaminant compositions and their levels, in addition to active emission elimination systems. The degree of parameter tuning freedom, however, varies between the 3D printer types. Lower processing temperatures are often associated with lesser amounts of produced contaminants, while the body of evidence on the effect of feedstock deposition speed is mixed. Nevertheless, many variables exist in the production of contaminants in 3D printing, some of which can be controlled by the process operator. Precautionary measures are advised to be always applied when 3D printers are operated in the absence of solid epidemiological evidence on the health hazards related to 3D printing work.

Bibliography

Alberts E, Ballentine M, Barnes E & Kennedy A. 2021. Impact of metal additives on particle emission profiles from a fused filament fabrication 3D printer. *Atmospheric Environment 244(1):117956.*

Afshar-Mohajer N, Wu C-Y, Ladun T & Huang Y. 2015. Characterization of particulate matter and total VOC emissions from a binder jetting 3D printer. *Building and Environment 93(2):293–301.*

Alifui-Segbaya F, Bowman J, White AR, Varma S, Lieschke GJ & George R. 2018. Toxicological assessment of additively manufactured methacrylates for medical devices in dentistry. *Acta Biomaterialia 78:64–77.*

Alifui-Segbaya F, Bowman J, White AR, George R, Fidan I & Love RM. 2020. Chemical characterization of additively manufactured methacrylates for dental devices. *Additive Manufacturing 31:100944.*

Andrews LS & Clary JJ. 1986. Review of the toxicity of multifunctional acrylates. *Journal of Toxicology and Environmental Health 19(2):149–164.*

Azimi P, Zhao D, Pouzet C, Crain NE & Stephens B. 2016. Emissions of ultrafine particles and volatile organic compounds from commercially available desktop 3D printers with multiple filaments. *Environmental Science and Technology 50(3):1260–1268.*

Azimi P, Fazil T & Stephens B. 2017. Predicting concentrations of ultrafine particles and volatile organic compounds resulting from desktop 3D printer operation and the impact of potential control strategies. *Journal of Industrial Ecology 21(S1):107–119.*

Azzougagh MN, Keller F-X, Cabrol E, Cici M & Pourchez J. 2021. Occupational exposure during metal additive manufacturing: A case study of laser powder bed fusion of aluminum alloy. *Journal of Occupational and Environmental Hygiene 18(6):223–236.*

Bakand S & Hayes A. 2016. Toxicological considerations, toxicity assessment, and risk management of inhaled nanoparticles. *International Journal of Molecular Sciences 17(6):929.*

Bharti N & Singh S. 2017. Three-dimensional (3D) printers in libraries: Perspective and preliminary safety analysis. *Journal of Chemical Education 94(7):879–885.*

Bravi L, Murmura F & Santos G. 2019. Additive manufacturing: Possible problems with indoor air quality. *Procedia Manufacturing 41:952–959.*

Brown JS, Gordon T, Price O & Asgharian B. 2013. Thoracic and respirable particle definitions for human health risk assessment. *Particle and Fibre Toxicology 10:12.*

Byrley P, Geer Wallace MA, Boyes WK & Rogers K. 2020. Particle and volatile organic compound emissions from a 3D printer filament extruder. *Science of the Total Environment 736:139604.*

Cabanes A, Valdés FJ & Fullana A. 2020. A review on VOCs from recycled plastics. *Sustainable Materials and Technologies 25:e00179.*

Calignano F, Manfredi D, Ambrosio E P et al. 2017. Overview of additive manufacturing technologies. *Proceedings of IEEE 105(4):593–612.*

Carvalho TC, Peters JI & Williams RO. 2011. Influence of particle size on regional lung deposition – What evidence is there? *International Journal of Pharmaceutics 406(1–2):1–10.*

Chan FL, House R, Kudla I, Lipszyc JC, Rajaram N and Tarlo SM. 2018. Health survey of employees regularly using 3D printers. *Occupational Medicine 68(3): 211–214.*

Chan FL, Hon C-Y, Tarlo SM, Rajaram N & House R. 2020. Emissions and health risks from the use of 3D printers in an occupational setting. *Journal of Toxicology and Environmental Health Part A 83(7):279–287.*

Chang T-Y, Lee L, Wang J-D & Shie R-H. 2004. Occupational risk assessment on allergic contact dermatitis in a resin model making process. *Journal of Occupational Health 46(2):148–152.*

Christensen MS, Vestergaard JM, d'Amore F et al. 2018. Styrene exposure and risk of lymphohematopoietic malignancies in 73,036 reinforced plastics workers. *Epidemiology 29(3):300–310.*

Creytens K, Gilissen L, Huygens S & Goossens A. 2017. A new application for epoxy resin resulting in occupational allergic contact dermatitis: the three-dimensional printing industry. *Contact Dermatitis 77(5):349–351.*

Damanhuri AAM, Abdullah A, Azian H et al. 2019. Indoor air concentration from selective laser sintering 3D printer using virgin polyamide nylon (PA12) powder: A pilot study. *International Journal of Integrated Engineering 11(5):140–149.*

Damanhuri AAM, Hariri A, Ghani SA, Mustafa M SS, Herawan SG & Paiman NA. 2021. The effects of virgin and recycled PA12 powders in SLS process on occupational exposures. *International Journal of Environmental Science and Development 12(11):339–345.*

Darbre PD. 2020. Chemical components of plastics as endocrine disruptors: Overview and commentary. *Birth Defects Research 112(17):1300–1307.*

Davis AY, Zhang Q, Wong JPS, Weber RJ & Black MS. 2019. Characterization of volatile organic compound emissions from consumer level material extrusion 3D printers. *Building and Environment 160:106209.*

Dematteo R, Keith MM, Brophy JT et al. 2012. Chemical exposures of women workers in the plastics industry with particular reference to breast cancer and reproductive hazards. *New Solutions 22(4):427–448.*

Deng Y, Cao S-J, Chen A & Guo Y. 2016. The impact of manufacturing parameters on submicron particle emissions from a desktop 3D printer in the perspective of emission reduction. *Building and Environment 104:311–319.*

Destaillats H, Maddalena RL, Singer BC, Hodgson AT & McKone TE. 2008. Indoor pollutants emitted by office equipment: A review of reported data and information needs. *Atmospheric Environment 42(7):1371–1388.*

Dev Singh D, Mahender T & Reddy AR. 2021. Powder bed fusion process: A brief review. *Materials Today Proceedings 46(1):350–355.*

DFG. Deutsche Forschungsgemeinschaft. Permanent Senate Commission for the Investigation of Health Hazards of Chemical Compounds in the Work Area. 2021. Report 57. List of MAK and BAT Values 2021. *Accessed April 27th 2022 from mbwl_2021_eng.pdf (publisso.de).*

Dickson AN, Abourayana HM & Dowling DP. 2020. 3D printing of fibre-reinforced thermoplastic composites using fused filament fabrication – A review. *Polymers 12(10):2188.*

Ding S & Ng BF. 2021. Particle emission levels in the user operating environment of powder, ink and filament-based 3D printers. *Rapid Prototyping Journal 27(6):1124–1132.*

Dobrzyńska E, Kondej D, Kowalska J & Szewczyńska M. 2021. State of the art in additive manufacturing and its possible chemical and particle hazards – Review. *Indoor Air 31(6):1733–1758.*

Du Preez S, Johnson AR, LeBouf RF, Linde SJL, Stefaniak AB & du Plessis J. 2018. Exposures during industrial 3-D printing and post-processing tasks. *Rapid Prototyping Journal 24(5):865–871.*

EC. European Commission. 2021. EU-LCI values. *Accessed May 27th 2022 from* *https://ec.europa.eu/growth/sectors/construction/eu-lci-subgroup/eu-lci-values_en.*

European Union. 2008. Directive 2008/50/EC of the European parliament and the council on ambient air quality for Europe. *Official Journal of the European Union 152:169–212.*

Fadeyi MO. 2015. Ozone in indoor environments: Research progress in the past 15 years. *Sustainable Cities and Society 18:78–94.*

Farcas MT, Stefaniak AB, Knepp AK et al. 2019. Acrylonitrile butadiene styrene (ABS) and polycarbonate (PC) filaments three-dimensional (3-D) printer emissions-induced cell toxicity. *Toxicology Letters 317:1–12.*

Floyd EL, Wang J & Regens JL. 2017. Fume emissions from a low-cost 3-D printer with various filaments. *Journal of Occupational and Environmental Hygiene 14(7):523–533.*

FMSAH. Finnish Ministry of Social Affairs and Health. 2020. Concentrations known to be harmful. Accessed April 26th 2022 from https://julkaisut.valtioneuvosto.fi/handle/10024/162457.

Fukumoto I, Tamura A, Matsumura M, Miura H & Yui N. 2013. Sensitization potential of dental resins: 2-Hydroxyethyl methacrylate and its water-soluble oligomers have immunostimulatory effects. *PLoS ONE 8(11):e82540.*

Gonzalez RS, Domenek S, Plessis C & Ducruet V. 2017. Quantitative determination of volatile organic compounds formed during polylactide processing by MHS-SPME. *Polymer Degradation and Stability 136:80–88.*

Gu J, Wensing M, Uhde E & Salthammer T. 2019a. Characterization of particulate and gaseous pollutants emitted during operation of a desktop 3D printer. *Environment International 123:476–485.*

Guillemot M, Oury B & Melin S. 2017. Identifying thermal breakdown products of thermoplastics. *Journal of Occupational and Environmental Hygiene 14(7):551–561.*

Gülcan O, Günaydin K & Tamer A. 2021. The state of the art of material jetting – A critical review. *Polymers 13(16):2829.*

Gümperlein I, Fischer E, Dietrich-Gümperlein G et al. 2018. Acute health effects of desktop 3D printing (fused deposition modeling) using acrylonitrile butadiene styrene and polylactic acid materials: An experimental exposure study in human volunteers. *Indoor Air 28(4):611–623.*

Hayes AC, Osio-Nasgaard J, Miller S, Whiting GL & Vance ME. 2021. Air pollutant emissions from multi jet fusion, material-jetting, and digital light synthesis commercial 3D printers in a service bureau. *Building and Environment 202:108008.*

Heinzow B, Santen M, Reinfeldt C & Sagunski H. 2009. Dibasic esters as new and relevant indoor air contaminants. *Umweltmedizin in Forschung und Praxis 14(4):195–201.*

Heratizadeh A, Werfel T, Schubert S & Geier J. 2018. Contact sensitization in dental technicians with occupational contact dermatitis. Data of the information network of departments of dermatology (IVDK) 2001–2015. *Contact Dermatitis 78(4):266–73.*

House R, Rajaram N & Tarlo SM. 2017. Case report of asthma associated with 3D printing. *Occupational Medicine 67(8):652–654.*

Hubs B.V. 2021. Additive manufacturing trend report 2021. *Available upon request from* https://www.hubs.com/get/trends/. *Read on January 28th 2022.*

Höllebacher E, Rieder-Gradinger C, Stratev D & Srebotnik E. 2015. A large-scale test set-up for measuring VOC emissions from wood products under laboratory conditions in simulated real rooms. *Holzforschung 69(4):457–462.*

Jasiuk I, Abueidda DW, Pang S, Su FY & McKittrick J. 2018. An overview on additive manufacturing of polymers. *The Journal of Minerals, Metals & Materials Society 70:275–283.*

Jeon H, Park J, Kim S, Park K & Yoon C. 2020. Effect of nozzle temperature on the emission rate of ultrafine particles during 3D printing. *Indoor Air 30(2):306–314.*

Johannes J, Rezayat T, Wallace WD & Lynch JP. 2016. Chronic hypersensitivity pneumonitis associated with inhaled exposure to nylon powder for 3-D printing: A variant of nylon flock worker's lung disease? *American Journal of Respiratory and Clinical Care Medicine 193:A7071.*

Jorge JH, Giampaolo ET, Teresinha AL & Vergani CE. 2003. Cytotoxicity of denture base acrylic resins: a literature review. *Journal of Prosthetic Dentistry 90(2):190–193.*

Karakurt I & Lin L. 2020. 3D printing technologies: Techniques, materials, and post-processing. *Current Opinion in Chemical Engineering 28:134–143.*

Kasanen J-P, Pasanen A-L, Pasanen P, Liesivuori J, Kosma V-M, Alarie Y. 1999. Evaluation of sensory irritation of 3-carene and turpentine, and acceptable levels of monoterpenes in occupational and indoor environment. *Journal of Toxicology and Environmental Health A 57(2):89–114.*

Kim S, Kim J-A, Kim H-J & Kim SD. 2006. Determination of formaldehyde and TVOC emission factor from wood-based composites by small chamber method. *Polymer Testing 25(5):605–614.*

Kim Y-W, Kim MJ, Chung BY et al. 2013. Safety evaluation and risk assessment of d-limonene. *Journal of Toxicology and Environmental Health B 16(1):17–38.*

Kim Y, Yoon C, Ham S et al. 2015. Emissions of nanoparticles and gaseous material from 3D printer operation. *Environmental Science and Technology 49(20):12044–12053.*

Kim S, Chung E, Kim S & Kwon J. 2020a. Assessment of emitted volatile organic compounds, metals and characteristic of particle in commercial 3D printing service workplace. *Journal of Korean Society of Occupational and Environmental Hygiene 30(2):153–162.*

Kim T, Song B, Cho KS, Lee I-S. 2020b. Therapeutic potential of volatile terpenes and terpenoids from forests for inflammatory diseases. *International Journal of Molecular Sciences 21(6):2187.*

Kostić M, Stanojević J, Tačić A et al. 2020. Determination of residual monomer content in dental acrylic polymers and effect after tissues implantation. *Biotechnology & Biotechnological Equipment 24(1):254–263.*

Krechmer JE, Phillips B, Chaloux N et al. 2021. Chemical emissions from cured and uncured 3D-printed ventilator patient circuit medical parts. *ACS Omega 6(45):30726–30733.*

Kumbhar NN & Mulay AV. 2018. Post processing methods used to improve surface finish of products which are manufactured by additive manufacturing technologies: A review. *Journal of the Institution of Engineers (India): Series C 99:481–487.*

Kwon O, Yoon C, Ham S et al. 2017. Characterization and control of nanoparticle emission during 3D printing. *Environmental Science & Technology 51(18):10357–10369.*

Lago M, Rodriguez A, Sendón R, Bustos J, Nieto M & Paseiro P. 2015. Photoinitiators: A food safety review. *Food Additives & Contaminants. Part A: Chemistry, Analysis, Control, Exposure & Risk Assessment 32(5):779–798.*

Lee JS, Kwak HS, Choi BS & Park SY. 2013. A case of occupational asthma in a plastic injection process worker. *Annals of Occupational and Environmental Medicine 25(1):25.*

Lee BJ, Kim B & Lee K. 2014. Air pollution exposure and cardiovascular disease. *Toxicological Research 30(2):71–75.*

Leso V, Ercolano ML, Mazzotta I, Romano M, Cannavacciuolo F & Iavicoli I. 2021. Three-dimensional (3D) printing: Implications for risk assessment and management in occupational setting. *Annals of Work Exposures and Health 65(6):617–634.*

Ligon SC, Liska R, Stampfl J, Gurr M & Müllhaupt R. 2017. Polymers for 3D printing and customized additive manufacturing. *Chemical Reviews 117(15):10212–10290.*

Lithner D, Larsson Å & Dave G. 2011. Environmental and health hazard ranking and assessment of plastic polymers based on chemical composition. *Science of the Total Environment 409(18):3309–3324.*

Ljunggren SA, Karlsson H, Ståhlblom B et al. 2019. Biomonitoring of metal exposure during additive manufacturing (3D printing). *Safety and Health at Work 10:518–526.*

Manoukian A, Buiron D, Temime-Roussel B, Wortham H & Quivet E. 2015. Measurements of VOC/SVOC emission factors from burning incenses in an environmental test chamber: influence of temperature, relative humidity, and air exchange rate. *Environmental Science and Pollution Research 23(7):6300–6311.*

Mendes L, Kangas A, Kukko K et al. 2017. Characterization of Emissions from a Desktop 3D Printer. *Journal of Industrial Ecology 14:94–106.*

Mikula K, Skrzypczak D, Izydorczyk G et al. 2020. 3D printing filament as a second life of waste plastics – A review. *Environmental Science and Pollution Research 28:12321–12333.*

Min K, Li Y, Wang D et al. 2021. 3D printing-induced fine particle and volatile organic compound emission: An emerging health risk. *Environmental Science and Technology Letters 8:616–625.*

Minamoto K, Nagano M, Inaoka T & Futatsuka M. 2002. Occupational dermatoses among fiberglass-reinforced plastics factory workers. *Contact Dermatitis 46(6):339–347.*

Mylläri V, Hartikainen S, Poliakova V et al. 2016. Detergent impurity effect on recycled HDPE: Properties after repetitive processing. *Journal of Applied Polymer Science 133:43766.*

Nett RJ, Cox-Ganser JM, Hubbs AF et al. 2017. Non-malignant respiratory disease among workers in industries using styrene - A review of the evidence. *American Journal of Industrial Medicine 60:163–180.*

Ngo TD, Kashani A, Imbalzano G, Nguyen K & Hui D. 2018. Additive manufacturing (3D printing): A review of materials, methods, applications and challenges. *Composites Part B: Engineering 143:172–196.*

Nouman M, Saunier J, Jubeli E & Yagoubi N. 2017. Additive blooming in polymer materials: Consequences in the pharmaceutical and medical field. *Polymer Degradation and Stability 143:239–252.*

Nurkiewicz TA, Porter DW, Barger M et al. 2006. Systemic microvascular dysfunction and inflammation after pulmonary particulate matter exposure. *Environmental Health Perspectives 114(3):412–419.*

Oberdörster G. 1988. Lung clearance of inhaled insoluble and soluble particles. *Journal of Aerosol Medicine 1(4):289–330.*

Oberdörster G. 2001. Pulmonary effects of inhaled ultrafine particles. *International Archives of Occupational and Environmental Health 74(1):1–8.*

Ohlwein S, Kappeler R, Kutlar M, Künzli N & Hoffmann B. 2019. Health effects of ultrafine particles: a systematic literature review update of epidemiological evidence. *International Journal of Public Health 64(4):547–559.*

Oskui SM, Diamante G, Liao C et al. 2016. Assessing and reducing the toxicity of 3D-printed parts. *Environmental Science and Technology Letters 3:1–6.*

Pagac M, Hajnys J, Ma Q-P et al. 2021. A review of vat photopolymerization technology: Materials, applications, challenges, and future trends of 3D printing. *Polymers 13(4):598.*

Peters A, Veronesi B, Calderón-Garcidueñas L et al. 2006. Translocation and potential neurological effects of fine and ultrafine particles a critical update. *Particle and Fibre Toxicology 3:13.*

Petretta M, Desando G, Grigolo B & Roseti L. 2019. 3D printing of musculoskeletal tissues: Impact on safety and health at work. *Journal of Toxicology and Environmental Health Part A: 82(16):891–912.*

Petrofsky JS, Browne M, Jamshidi M, Libo-on A & Lee H. 2014. Can prosthetic limbs made too quickly cause kidney damage?: A pilot study. *Physical Therapy Rehabilitation Science 3:119–24.*

Piedra-Cascón W, Krishnamurthy VR, Att W & Revilla-León M. 2021. 3D printing parameters, support structures, slicing, and post-processing procedures of vat photopolymerization additive manufacturing technologies: A narrative review. *Journal of Dentistry 109:103630.*

Pohleven J, Burnard MD, Kutnar A. 2019. Volatile organic compounds emitted from untreated and thermally modified wood – A review. *Wood and Fiber Science 51(3):1–24.*

Poikkimäki M, Koljonen V, Leskinen N et al. 2019. Nanocluster aerosol emissions of a 3D printer. *Environmental Science & Technology 53(23):13618–13628.*

Pope CA & Dockery DW. 2006. Health Effects of Fine Particulate Air Pollution: Lines that Connect. *Journal of Air and Waste Management Association 56(6):709-742.*

Rao C, Gu F, Zhao P, Sharmin N, Gu H & Fu J. 2017. Capturing $PM_{2.5}$ emissions from 3D printing via nanofiber-based air filter. *Scientific Reports 7:10366.*

Rosenman KD, Reilly MJ, Schill DP et al. 2003. Cleaning products and work-related asthma. *Journal of Occupational and Environmental Medicine 45(5):556–563.*

Roth GA, Geraci CL, Stefaniak A, Murashov V & Howard J. 2019. Potential occupational hazards of additive manufacturing. *Journal of Occupational and Environmental Hygiene 16(5):321–328.*

Rumchev K, Brown H & Spickett J. 2007. Volatile organic compounds: Do they present a risk to our health? *Reviews in Environmental Health 22(1):39–56.*

Ryan T & Hubbard D. 2016. 3D Printing hazards: Literature review & preliminary hazard assessment. *Professional Safety 61(6):56–62.*

Sarigiannis DA, Karakitsios SP, Gotti A, Liakos IL & Katsoyiannis A. 2011. Exposure to major volatile organic compounds and carbonyls in European indoor environments and associated health risk. *Environment International 37(4):743–765.*

Sarwar G, Olson DA, Corsi RL, Weschler CJ. 2004. Indoor fine particles: The role of terpene emissions from consumer products. *Journal of the Air Waste Management Association 54(3):367–377.*

Savonius B, Keskinen H, Tuppurainen M & Kanerva L. 1993. Occupational respiratory disease caused by acrylates. *Clinical and Experimental Allergy 23(5) 416–424.*

Secondo LE, Adawi HI, Cuddehe J et al. 2020. Comparative analysis of ventilation efficiency on ultrafine particle removal in university MakerSpaces. *Atmospheric Environment 244:117321.*

Shahnaz B, Hayes A & Dechsakulthorn F. 2012. Nanoparticles: a review of particle toxicology following inhalation exposure. *Inhalation Toxicology 24(2):125-135.*

Short DB, Sirinterlicki A, Badger P & Artieri B. 2015. Environmental, health, and safety issues in rapid prototyping. *Rapid Prototyping Journal 21(1):105–110.*

Singh R, Gupta A, Tripathi O et al. 2021. Powder bed fusion process in additive manufacturing: An overview. *Materials Today Proceedings 26(2):3058–3070.*

Stabile L, Scungio M, Buonanno G, Arpino F & Ficco G. 2016. Airborne particle emissions of a commercial 3D printer: The effect of filament material and printing temperature. *Indoor Air 27(2):398–408.*

Stansbury JW & Idacavage MJ. 2016. 3D printing with polymers: challenges among expanding options and opportunities. *Dental Materials 32:54–64.*

Stefaniak AB, LeBouf RF, Duling MG, Yi J, Abukadba AB, McBride CR & Nurkiewicz TR. 2017a. Inhalation exposure to three-dimensional printer emissions stimulates acute hypertension and microvascular dysfunction. *Toxicology and Applied Pharmacology 355:1–5.*

Stefaniak AB, LeBouf RF, Yi J et al. 2017b. Characterization of chemical contaminants generated by a desktop fused deposition modeling 3-dimensional printer. *Journal of Occupational and Environmental Hygiene 14(7):540–550.*

Stefaniak AB, Johnson AR, Du Preez S et al. 2019a. Evaluation of emissions and exposures at workplaces using desktop 3-dimensional printer. *Journal of Chemical Health & Safety 26(2):19–30.*

Stefaniak AB, Bowers LN, Knepp AK et al. 2019b. Particle and vapor emissions from vat polymerization desktop-scale 3-dimensional printers. *Journal of Occupational and Environmental Hygiene 16(8):519–531.*

Stefaniak AB, Du Preez S & du Plessis JL. 2021. Additive manufacturing for occupational hygiene: A comprehensive review of processes, emissions & exposures. *Journal of Toxicology and Environmental Health, Part B 24(5):173–222.*

Steinle P. 2016. Characterization of emissions from a desktop 3D printer and indoor air measurements in office settings. *Journal of Occupational and Environmental Hygiene 13(2):121–132.*

Stephens B, Azimi P, El Orch Z & Ramos T. 2013. Ultrafine particle emissions from desktop 3D printers. *Atmospheric Environment 79:334–339.*

Tan LJ, Zhu W & Zhou K. 2020. Recent progress on polymer materials for additive manufacturing. *Advanced Functional Materials 30(43):2003062.*

Tosti A, Guerra L, Vincenzi C & Peluso AM. 1993. Occupational skin hazards from synthetic plastics. *Toxicology and Industrial Health 9(3):493–502.*

Tuomi T & Vainiotalo S. 2014. The guideline and target values for total volatile organic compound concentrations in industrial indoor environments in Finland. *Indoor and Built Environment 25(2):434–434.*

Tyagi S, Yadav A & Deshmukh S. 2021. Review on mechanical characterization of 3D printed parts created using material jetting process. *Materials Today: Proceedings 51(1):1012–1016.*

Unwin J, Coldwell MR, Keen C & McAlinden JJ. 2013. Airborne emissions of carcinogens and respiratory sensitizers during thermal processing of plastics. *Annals of Occupational Hygiene 57(3):399–406.*

Vaezi M, Chianrabutra S, Mellor B & Yang S. 2013. Multiple material additive manufacturing – Part 1: A review. *Virtual and Physical Prototyping 8(1):19–50.*

Vallabani NVS, Alijagic A, Persson A, Odnevall I, Särndahl E, Karlsson HL. 2022. Toxicity evaluation of particles formed during 3D-printing: Cytotoxicity, genotoxic, and inflammatory response in lung and macrophage models. *Toxicology 467:153100.*

Van Amerongen CC, Dahlin J, Isaksson M & Schuttelaar MLA. 2019. Allergic contact dermatitis caused by 1,6-hexanediol diacrylate in a hospital wristband. *Contact Dermatitis 81(6):446–449.*

Van Broekhuizen P, Van Veelen W, Streekstra W-H, Schulte P, Reijnders L. 2012. Exposure limits for nanoparticles: Report of an international workshop on nano reference values. *Annals of Occupational Hygiene 56(5):515–524.*

Van Kampen V, Merget R & Baur X. 2000. Occupational airway sensitizers: An overview on the respective literature. *American Journal of Industrial Medicine 38(2):164–218.*

Vance ME, Pegues V, Van Montfrans S, Leng W & Marr LC. 2017. Aerosol emissions from fuse-deposition modeling 3D printers in a chamber and real indoor environments. *Environmental Science and Technology 51(17):9516–9523.*

Wang X, Vallabani NVS, Giboin A et al. 2021. Bioaccessibility and reactivity of alloy powders used in additive manufacturing in powder bed fusion additive manufacturing. *Materialia 19:101196.*

Vermeulen R, Kromhout H & Smit HA. 2002. Respiratory symptoms and occupation: A cross-sectional study of the general population. *Environmental Health 1:5.*

WHO. World Health Organization. 1995. Dry cleaning, some chlorinated solvents and other industrial chemicals. IARC Monographs on the Evaluation of Carcinogenic Risk to Humans Vol. 63. World Health Organization, Geneve, Switzerland.

WHO. World Health Organization. 1999. Hazard prevention and control in the work environment: Airborne dust. Occupational and environmental health series. Department of protection of the human environment, Geneve, Switzerland.

WHO. World Health Organization. 2006. International Agency for Research on Cancer. IARC monographs on the evaluation of carcinogenic risks to humans. Volume 88. Formaldehyde, 2-Butoxyethanol and 1-*tert*-Butoxypropan-2-ol. World Health Organization, Lyon, France.

WHO. World Health Organization. 2021. WHO global air quality guidelines. Particulate matter ($PM_{2.5}$ and PM_{10}), ozone, nitrogen dioxide, sulfur dioxide and carbon monoxide. World Health Organization, Geneve, Switzerland.

Win-Shwe T-T, Fujimaki H, Arashidani K & Kunugita N. 2013. Indoor Volatile Organic Compounds and Chemical Sensitivity Reactions. *Clinical and Developmental Immunology 2013:623812.*

Wojtyła S, Klama P & Baran T. 2017. Is 3D printing safe? Analysis of the thermal treatment of thermoplastics: ABS, PLA, PET, and nylon. *Journal of Occupational and Environmental Hygiene 14(6):80–85.*

Wolkoff P, Clausen PA, Wilkins CK & Nielsen GD. 2000. Formation of strong airway irritants in terpene/ozone mixtures. *Indoor Air 10(2):82–91.*

Wolkoff P, Wilkins CK, Clausen PA & Nielsen GD. 2006. Organic compounds in office environments – sensory irritation, odor, measurements and the role of reactive chemistry. *Indoor Air 16(1):7–19.*

Wolkoff P. 2020. Indoor air chemistry: Terpene reaction products and airway effects. *International Journal of Hygiene and Environmental Health 255:113439*

Wu H, Fahy WP, Kim S et al. 2020. Recent developments in polymer/polymer nanocomposites for additive manufacturing. *Progress in Materials Science 111:100638.*

Yamasita K, Yamamoto N, Mizukoshi A, Noguchi M, Ni Y & Yanagisawa Y. 2012. Compositions of volatile organic compounds emitted from melted virgin and waste plastic pellets. *Journal of the Air & Waste Management Association 59(3):273–278.*

Yang H, Lim JC, Liu Y et al. 2016. Performance evaluation of ProJet multi-material jetting 3D printer. *Virtual and Physical Prototyping 12(1):96–103.*

Yang Y & Li L. 2018. Total volatile organic compound emission evaluation and control for stereolithography additive manufacturing process. *Journal of Cleaner Production 170(1):1268–1278.*

Yi J, LeBouf RF, Duling MG et al. 2016. Emission of particulate matter from a desktop three-dimensional (3D) printer. *Journal of Toxicology and Environmental Health Part A 79(11):453–465.*

Zhang J. 1994. Indoor air chemistry: Formation of organic acids and aldehydes. *Environmental Science & Technology 28:1975–1982.*

Zhang Q, Wong JPS, Davis AY, Black MS & Weber RJ. 2017. Characterization of particle emissions from fused deposition modeling 3D printers. *Aerosol Science and Technology 51(11):1275–1286.*

Zhang Q, Pardo M Rudich Y et al. 2019. Chemical composition and toxicity of particles emitted from a consumer-level 3D printer using various materials. *Environmental Science and Technology 53(20):12054–12061.*

Zhang F, Zhu L, Li Z et al. 2021. The recent development of vat photopolymerization: A review. *Additive Manufacturing Part B 48:102423.*

Zisook RE, Simmons BD, Vater M et al. 2020. Emissions associated with operations of four different additive manufacturing or 3D printing technologies. *Journal of Occupational and Environmental Hygiene 17(10):464–479.*

Zontek TL, Ogle BR, Jankovic JT & Hollenbeck SM. 2017. An exposure assessment of desktop 3D printing. *Journal of Chemical Health & Safety 24(2):15–25.*

Zulu Z & Naidoo RN. 2021. Styrene associated respiratory outcomes among reinforced plastic industry workers. *Archives of Environmental & Occupational Health. Published online September 21st 2021. Available from https://doi.org/10.1080/19338244.2021.1972279.*

Appendices

ARTICLES

ARTICLE I
Väisänen A., Hyttinen M., Ylönen S. & Alonen L. 2019. Occupational exposure to gaseous and particulate contaminants originating from additive manufacturing of liquid, powdered, and filament plastic materials and related post-processes. *Journal of Occupational and Environmental Hygiene 16(3):258–271.*

ARTICLE II
Väisänen A., Alonen L., Ylönen S., Lyijynen I. & Hyttinen M. 2021. The impact of thermal reprocessing of 3D printable polymers on their mechanical performance and airborne pollutant profiles. *Journal of Polymer Research 28:436.*

ARTICLE III
Väisänen A., Alonen L., Ylönen S. & Hyttinen M. 2022. Volatile organic compounds and particulate emissions from the production and use of thermoplastic biocomposite 3D printing filaments. *Journal of Occupational and Environmental Hygiene 19(6):381–393.*

ARTICLE IV
Väisänen A., Alonen L., Ylönen S. & Hyttinen M. 2022. Organic compound and particle emissions of additive manufacturing with photopolymer resins and chemical outgassing of manufactured resin products. *Journal of Toxicology and Environmental Health, Part A 85(5):198–216.*

ARTICLE I

Väisänen A., Hyttinen M., Ylönen S. & Alonen L. 2019. Occupational exposure to gaseous and particulate contaminants originating from additive manufacturing of liquid, powdered, and filament plastic materials and related post-processes. *Journal of Occupational and Environmental Hygiene 16(3):258–271.*

ARTICLE II

Väisänen A., Alonen L., Ylönen S., Lyijynen I. & Hyttinen M. 2021. The impact of thermal reprocessing of 3D printable polymers on their mechanical performance and airborne pollutant profiles. *Journal of Polymer Research 28:436.*

ORIGINAL PAPER

The impact of thermal reprocessing of 3D printable polymers on their mechanical performance and airborne pollutant profiles

Antti Juho Kalevi Väisänen[1,2] ⬚ · Lauri Alonen[2] · Sampsa Ylönen[2] · Isa Lyijynen[3] · Marko Hyttinen[1]

Abstract

The alterations in volatile organic compound (VOC) and ultrafine particulate (UFP) matter emission profiles following thermal reprocessing of multiple materials were examined. Additionally, mechanical performance of the materials was studied. The VOCs were identified by collecting air samples with Tenax® TA tubes and analyzing them with a GC–MS system. UFP concentrations were monitored with a portable ultrafine particle counter. Total VOC emissions of all materials were reduced by 28–68% after 5 thermal cycles (TCs). However, slight accumulation of 1,4-dioxane was observed with poly(lactic acid) materials. UFP emissions were reduced by 45–88% for 3D printing grade materials over 5 TCs but increased by 62% in the case of a waste plastic material over 3 TCs. The mechanical performance of the materials was investigated by measuring their tensile strengths (TSs) and elastic moduli (EM) with an axial-torsion testing system. The reprocessed materials expressed fluctuations in their 3D printing qualities and mechanical performances. The mechanical performances were observed to reduce only slightly after 5 TCs, and the trend was observable only after the data was mass-normalized. The TSs of the samples were reduced by 10–24%, while the EM were reduced by 1–9% after 5 TCs. The TS and EM of one material were increased by 14 and 33%, respectively. In conclusion, recycled polymers are plausible 3D printing feedstock alternatives as they possess acceptable mechanical performance and low emittance according to this study. Furthermore, non-3D printing grade polymers may be applied in a 3D printer with caution.

Keywords Additive manufacturing · Tensile strength · Plastics · Thermal treatment · Volatile organic compounds

Introduction

The environmental impacts of plastics and demands for effective recycling measures have been recent topics of intensive debate. These issues call for new innovative solutions, of which one is the sustainable use of plastic materials. The 3D printing industry is another source – or a potential consumer – of waste plastics. Failed 3D printed objects typically end up in waste disposal as the object is ruined and cannot be used either for its designed purpose or as a feedstock material for a new 3D print job attempt. However, novel and inexpensive 3D printing filament extruders which are capable of producing 3D printable filaments out of plastic scrap materials have been introduced into the consumer markets over the past years. These devices can increase the small-scale recycling of plastics. They can make use of failed 3D prints and household waste plastics (HWPs) in 3D printer feedstock filament production. Additionally, the first 3D printing material producers have entered the recycled feedstocks market.

Thermal degradation of polymers is a phenomenon that occurs when a polymer (plastic) is exposed to sufficiently high temperatures, and physical or chemical stress [1–3]. Polymer chains undergo chain scission and low molecular-weight compounds, including property enhancing additives, are disintegrated from the base polymer bulk. The leftover polymer bulk becomes increasingly shorter, lighter, fragile, [1, 2, 4] and too intractable to apply in a 3D printer [5]. Additionally, polymers can suffer from water-induced hydrolysis and thermo-oxidative degradation when exposed

✉ Antti Juho Kalevi Väisänen
antti.vaisanen@uef.fi

1   Faculty of Science and Forestry, Department of Environmental and Biological Sciences, University of Eastern Finland, Kuopio, Finland

2   School of Engineering and Technology, Savonia University of Applied Sciences, Kuopio, Finland

3   Faculty of Science and Forestry, Department of Applied Physics, University of Eastern Finland, Kuopio, Finland

⚫ Springer

to air, which results in further chemical decomposition [2]. Cross-linking is another common physiochemical occurrence in which additional bonds are formed inside a base polymer bulk. Cross-linking hardens the polymer substantially, resulting in a hard but brittle polymer structure [1, 2, 4, 6, 7]. These alterations in the polymer structure affect the mechanical performance of a recycled material [3, 6]. The main factors which affect the level and the mechanism of degradation during thermal treatment are the processing temperature and the presence of oxygen and other catalysts [1, 2, 5, 6]. Thermal degradation results in reductions in the mass and the density of the polymer. These factors are major determinants of the tensile strength (TS) of a material [2, 8]. Mechanical performance is impaired in tandem with polymer chain transformations, up until a point where the material is no longer reprocessable [5]. Furthermore, the 3D printing parameters, e.g. printing temperature, infill ratio, and pattern, all affect the physical features, and layer-to-layer adhesion of the 3D printed object. These factors, in addition to polymer filament integrity, all have a significant impact on the mechanical properties of the printed object [8–12].

The emissions of material extrusion 3D printing with the most common polymer types have been extensively studied. However, the impact that thermal reprocessing has on the emissions and the mechanical properties of polymers has not been documented as comprehensively. The thermal processing of polymers is a known source of volatile organic compounds (VOCs). These compounds consist of a carbon skeleton and may carry bound functional groups [13–19]. The typical organic compounds emitted in a polymer decomposition process are short, usually 2 to 8 carbon atoms in length, and capable of attaching to airborne particles [2, 7, 20]. In addition, 3D printing has been documented to be an emission source for ultrafine particles (UFPs) which are formed through polymer chain decomposition and the condensation of VOCs [13–16, 18, 19, 21–24]. VOCs and UFPs both have the potency for adversely affecting human health through the promotion of lung diseases and the induction of oxidative stress, irritation, inflammation, sensitization, influences in the central nervous system (CNS) and skin effects. These exposure agents are ultimately recognized as the main health hazards of 3D printing [25–33].

Thermal reprocessing of polymers has been found to result in lower total VOC (TVOC) emissions during subsequent extrusion processes. This is a result of the most readily volatilized compounds disintegrating from a polymer chain during the initial extrusion processes. Less volatile chemical structures persist, and thus the TVOC emissions are reduced during thermal reprocessing [20, 34]. The applied temperature, the presence of oxygen and other reactive compounds and the polymer base are the main factors affecting the formed degradation products. Higher temperatures drive the degradation products towards compounds with larger molecular mass. Oxygen is highly reactive with alkyl compounds, resulting in the production of oxygenated hydrocarbons, e.g., aldehydes and acids. The polymer base ultimately determines the possible off-gassed emission profile [1–3, 20]. The accumulation of certain compounds and impurities, e.g., dioxanes, has been reported along with the overall reduction of the TVOC emissions over repetitive thermal reprocessing [20, 34]. The accumulation and the volatilization of impurities and pollutants is a major health concern regarding HWP filament application. Unknown additives which improve the desired properties of a plastic may have been used in the polymer production. Additionally, residues of food or consumer chemicals may be present in or absorbed into the polymer structure [34]. Thermal processing of such contaminated plastics is a potential source of unpredicted chemical emissions, which may possess harmful characteristics. Exposure to these emissions can lead to adverse health outcomes which are difficult to predict. In addition, the additives used in HWPs are likely to differ from the ones used in 3D printing grade plastics. Henceforth, the 3D printability and the mechanical performance of the products 3D printed with HWP plastics may be unsatisfactory.

Thermal reprocessing of plastics has been recorded to reduce the TS of the material. Elastic modulus (EM) has not been found to follow a similar pattern, as the modulus has been recorded to fluctuate from increasing to decreasing over the course of multiple thermal treatment cycles [5, 34]. The alteration of mechanical properties of reprocessed plastics is of interest in the 3D printing industry, as it could be a consumer of recycled plastics. However, the objects produced from recycled plastics should express adequate mechanical properties and processability to be applicable in real-life situations. Additionally, safety aspects regarding the application of thermally reprocessed materials must be evaluated before such materials are applied by 3D printer operators.

The main goal of this study was to observe how the VOC and UFP profiles of multiple plastic materials alter after repetitive thermal reprocessing. The gathered results are used to estimate the safety aspects of thermally reprocessed plastics when applied in a 3D printer. A secondary objective was to examine the alteration of mechanical performance of 3D printed objects fabricated from thermally reprocessed materials. A joint goal of this study was to find justifications for the application of recycled materials over virgin polymers in the 3D printing industry.

Materials and methods

The VOC and UFP emission concentrations were measured during 3D printing of ASTM D638 type IV tensile test specimens. These pollutants were selected because they have been

identified as the main emission products originating from material extrusion 3D printing [13–19, 21–24]. The tensile test specimens with a calculated volume of 6.22 cm^3 were fabricated by applying 0/90-degree printing angle, 100% infill and feed rates, 0.2 mm layer thickness, and 0.4 mm path width. The pollutant concentrations were measured during printing with virgin and from one to five times thermally reprocessed materials. TS and EM were measured from virgin materials and after one to five thermal reprocessing cycles of every filament type. All the used equipment were factory and/or zero calibrated accordingly before sample collection and material property testing.

Four filament types were used in this study: ReForm rPLA (Formfutura B.V., Nijmegen, Netherlands, made from extrusion waste stream plastic, density 1.24 g/cm^3, subsequently referred to as PLA ReForm), Premium PLA Robotic Grey (Formfutura B.V., density 1.24 g/cm^3, subsequently referred to as PLA Robotic Gray), Natural Transparent PP Filament (Verbatim Corp., Tokyo, Japan, density 0.89 g/cm^3, subsequently referred to as PP Transparent) and PP waste plastic filament produced from water-washed PP bottle caps (density unknown, subsequently referred to as PP HWP). The materials applied in this study represent environmentally friendly and readily available plastic types. PLA was chosen based on its renewable origin and wide application in the 3D printing industry, while PP was chosen because it is an abundant commodity plastic used widely among different industries, including as a packaging material. A SHR3D IT plastic shredder (3devo B.V., Utrecht, Netherlands) and a Composer 450 filament extruder (3devo B.V.) with four temperature-adjustable heating zones were used in filament reproduction. The study was performed by manufacturing three parallel tensile specimens with each filament. The leftover filament bulk was shredded, a new filament was extruded from the produced filament bits, and additional tensile specimens were printed with the reprocessed filament, and so forth. The PP HWP bottle caps were initially shredded and extruded into the form of a filament, whereafter it underwent similar processing procedure. The shredder was cleaned with pressurized air after each shredding process to prevent cross-contamination of the materials.

Eri Keeper glue (Oy Sika Finland Ab, Espoo, Finland) and generic PP packaging tape were, respectively, used to enhance the adhesion of PLA and PP materials to the 3D printing platform. For temperature settings applied during 3D printing and filament production, see the Table 1. A ZMorph 2.0 SX material extrusion 3D printer (ZMorph S.A., Wroclaw, Poland) with a 0.4 mm print head was operated in this study under laboratory conditions. The research area with a volume of 256 m^3 was mechanically ventilated. The space was ventilated after each print job and the clearance of pollutants was verified by the reduction of UFP concentration down to the background level. The space was

ventilated for an additional hour to ensure the absence of pollutants. The duration of each individual printing process was approx. 150 min.

Exposure agent measurements

Blank and background VOC and UFP samples were collected before 3D printing was initiated. The two classes of pollutants were individually measured from two successive print jobs to prevent the VOC sampling from being affected by the emission of isopropyl alcohol released during the UFP sampling.

The VOCs were collected with Tenax® TA adsorption tubes (Markes Inc., Sacramento, CA) containing 200 mg of sorbent, and AirChek 3000 pumps (SKC Inc., Eighty Four, PA) calibrated with a mini-BUCK Calibrator (A. P. BUCK Inc., Orlando, FL). Three consecutive samples were collected over each 3D print job from the beginning, middle and end phases of the print job. The samples were collected from the altitude of the breathing zone (approx. 1.5 m) and a close proximity of the printer (approx. distance 1 m). The collection time for an individual sample was 20 min. The samples were analyzed according to the ISO-16000 standard method. A TD100 thermal desorber (Markes Inc.), a 7890A gas chromatography system with an HP5ms column (50 m length and 200 μm film thickness, Agilent Technologies Inc., Santa Clara, CA) and a 5975C mass spectrometer (Agilent Technologies Inc.) were used for the sample analysis. The results were background and blank corrected. Furthermore, the VOCs released from the adhesives were analyzed and subtracted from the presented VOC results. Four-point standard curves were produced from an HC 48 component 40,353-U standard solution (Supelco Inc., Bellefonte, PA). The mass spectrometer was operated under SCAN mode to allow the identification of all compounds captured in the Tenax® sampling tubes. Every compound which was detected in at least 2 of the 3 consecutive samples were included in the results. This procedure reduced results bloat and disregarded certain compounds which were not formed in abundance during the 3D printing processes. An MSD ChemStation program version F.01.00.1903 (Agilent Technologies Inc.) was used for the compound identification. The limit of detection of an individual compound was the exceeding of the background noise by fivefold. The compound concentrations were calculated as toluene equivalents. For additional details, please see the preliminary study [19].

The UFPs were monitored with a P-Trak Ultrafine Particle Counter 8525 instrument (TSI Inc., Shoreview, MN) over the complete 3D printing jobs. The UFP samples were collected from the same location as the VOC samples. The presented results are corrected by the background UFP concentration. The ISO/ASTM CD 52,932 standard for 3D printing emission rate analysis was not yet published

Table 1 3D Printing and filament production specifications

Filament Type	3D Printing temperatures	Adhesive	Filament production temperatures
PLA Robotic Gray	205 °C nozzle, 60 °C bed	Glue	200/215/195/190 °C
PLA ReForm	205 °C nozzle, 60 °C bed		200/210/190/185 °C
PP Transparent	230 °C nozzle, 85 °C bed	Packaging tape	205/215/190/185 °C
PP HWP	235 °C nozzle, 90 °C bed		220/225/215/195 °C

when the samples were collected, thus the sampling was performed at the vicinity of the 3D printer, similarly to the preliminary study [19].

Material property measurements

The tensile specimens were tested according to the ASTM D638 standard with an Instron 8874 universal axial-torsion testing system (Instron Corp., High Wycombe, UK) by applying 4 mm/min pulling speed under normal room temperature and conditions. Three parallel specimens were used in every test. The TS and EM were derived from the produced stress–strain curve. A MATLAB program version R2016b (Mathworks Corp., Brentwood, CA) was used to analyze the mechanical properties by plotting the relative strain in accordance with the relative stress. EM was derived from the slope of a fitted least squares function in the linear area of the curve. TS was derived from the peak Y-axis value (applied force in Newtons). Dimensions of the specimens were measured with a QuantuMike IP65 caliper (Mitutoyo Corp., Kawasaki, Japan) and weighed with an AC100 scale (Mettler Toledo Inc.).

Results

Exposure agent measurement results

The initial TVOC emissions were relatively low [29] during printing with all tested materials and the measured concentrations decayed further after each successive thermal cycle (TC), as seen in the Fig. 1. The steepest reduction was detected between the virgin and once reprocessed materials. Thereafter the reducing effect was notably lower and most readily detected with the PLA materials. Additionally, the virgin PLA materials were slightly higher VOC emitters than the virgin PP filaments, but the TVOC levels evened out after one TC. The TVOC values were reduced by 62–68% over 5 TCs for the PLA materials and by 28–48% for the PP materials. The full VOC profiles are presented in the Supplementary Tables 1 and 2.

The concentrations of the most prevalent individual VOCs measured during 3D printing with PLA materials were the same for both filaments. The concentrations of the individual compounds followed a similar reducing trend as the TVOC concentrations did, as seen in the Figs. 2 and 3.

Fig. 1 TVOC concentrations and standard deviations measured from 3D printing with virgin and thermally reprocessed filaments
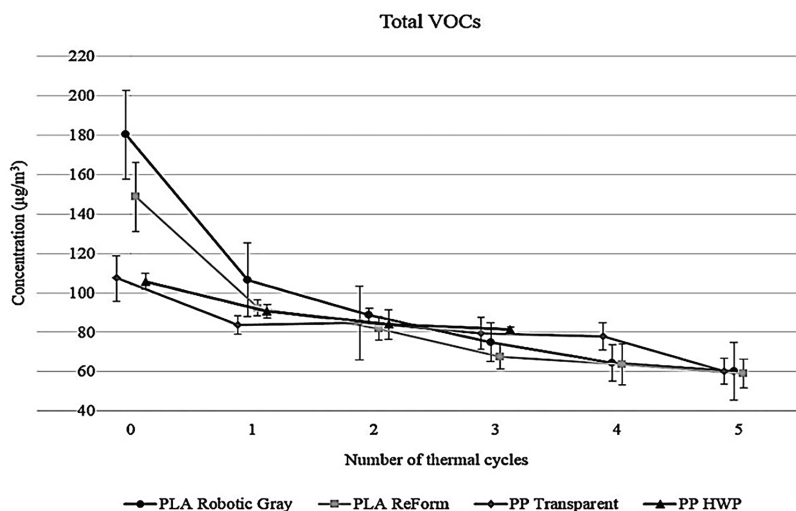
One compound, 1,4-dioxane, portrayed a reverse behavior. It was not detected during printing with the virgin materials but was eventually found at increasing concentrations during printing with all the reprocessed PLA materials. Additionally, the number of individual compounds reduced as the number of TCs increased.

Similar reduction of the VOC emissions was observed during 3D printing with the thermally reprocessed PP filaments as well, but to a lesser extent. The effect was least notable with the PP HWP material. No observable accumulation of any single compound was detected, even though 3D printing with the PP HWP material was expected to raise the highest concerns. The most prevalent VOCs released during printing with the PP filaments are presented in the Figs. 4 and 5. Propylene glycol was the only actual detected outlier compound, but certain compounds could be confined as the

other main emission products and are therefore presented in the figures.

Similarly to the TVOC concentration reduction, lower concentrations of UFPs were emitted during printing with reprocessed filaments with the most materials. The PP HWP material was an exception and a contrary trend was found, as seen in the Fig. 6. This odd behavior can be explained with the polymer grade, as the PP HWP material was a molding grade polymer rather than a 3D printing grade one. Therefore, no 3D printability enhancing additives were present in the material. Overall, the UFP emissions were very low, except during printing with thermally reprocessed PP HWP filament. The measured concentrations were up to 100-fold in comparison to the least UFP emitting PLA material. Still, the concentrations were relatively low in comparison to the proposed occupational lightweight UFP reference value of

Table 2 Material properties of 3D printed specimens

	Polymer grade: PLA							
	PLA Robotic Gray			PLA ReForm			Pooled PLA reference data[9–12,36–38]	
Sample	Tensile Strength (MPa)	Elastic Modulus (GPa)	Mass (g)	Tensile Strength (MPa)	Elastic Modulus (GPa)	Mass (g)	Tensile Strength (MPa)	Elastic Modulus (GPa)
Virgin	54.3±0.7 (53.5–54.7)	1.97±0.08 (1.88–2.04)	7.63±0.03 (7.60–7.66)	47.5±1.1 (46.3–48.3)	1.86±0.05 (1.81–1.91)	7.43±0.07 (7.35–7.49)	49.1±10.3 (28.4–65.5)	3.36±0.52 (2.66–4.26)
TC 1	41.8±1.1 (40.9–43.0)	1.72±0.02 (1.71–1.74)	6.73±0.03 (6.71–6.76)	40.5±0.8* (39.9–41.0)	1.69±0.01* (1.68–1.69)	6.88±0.03 (6.85–6.91)	35.9±0.3	4.03±0.50
TC 2	44.1±2.3* (42.4–45.7)	1.78±0.06* (1.74–1.82)	6.30±0.05 (6.26–6.34)	30.7±0.9 (29.7–31.2)	1.44±0.04 (1.41–1.48)	5.88±0.07 (5.70–5.93)	-	-
TC 3	45.9±1.5 (44.2–47.2)	1.79±0.02 (1.77–1.81)	7.10±0.03 (7.08–7.13)	40.4±1.2 (39.4–41.8)	1.68±0.11 (1.61–1.81)	7.41±0.04 (7.37–7.44)	-	-
TC 4	38.1±0.9 (37.3–39.1)	1.54±0.07 (1.47–1.61)	7.02±0.04 (6.99–7.07)	38.7±1.1 (37.5–39.8)	1.55±0.03 (1.52–1.57)	7.12±0.10 (7.01–7.21)	-	-
TC 5	43.1±0.6 (42.4–43.6)	1.69±0.06 (1.64–1.75)	7.23±0.06 (7.20–7.31)	43.1±1.8 (41.7–45.1)	1.80±0.04 (1.77–1.84)	7.50±0.06 (7.45–7.57)	-	-
	Polymer grade: PP							
	PP Transparent			HWP-PP			Pooled PP reference data[39–42]	
Sample	Tensile Strength (MPa)	Elastic Modulus (GPa)	Mass (g)	Tensile Strength (MPa)	Elastic Modulus (GPa)	Mass (g)	Tensile Strength (MPa)	Elastic Modulus (GPa)
Virgin	14.3±0.5 (13.8–14.9)	0.24±0.00 (0.24)	5.28±0.02 (5.27–5.30)	21.4±2.0 (19.0–22.8)	0.75±0.01 (0.74–0.75)	4.34±0.26 (4.04–4.49)	27.2±6.0 (21.1–35.5)	1.05±0.22 (0.85–1.25)
TC 1	14.4±0.5 (14.0–14.9)	0.28±0.01 (0.27–0.29)	4.62±0.02 (4.60–4.64)	17.8±0.2 (17.6–18.0)	0.72±0.01 (0.72–0.73)	4.34±0.11 (4.26–4.46)	23.6±2.6 (19.9–27.3)	0.89±0.19 (0.75–1.13)
TC 2	14.8±0.2 (14.6–15.0)	0.29±0.02 (0.28–0.31)	4.81±0.05 (4.76–4.84)	19.0±1.0* (18.2–19.7)	0.77±0.01* (0.76–0.78)	3.69±0.13 (3.60–3.81)	-	-
TC 3	13.9±0.4 (13.7–14.3)	0.28±0.01 (0.28–0.29)	4.76±0.04 (4.72–4.79)	13.5±1.2 (12.6–14.8)	0.63±0.01 (0.61–0.64)	3.68±0.07 (3.63–3.76)	-	-
TC 4	14.4±0.1 (14.3–14.5)	0.28±0.02 (0.27–0.30)	4.65±0.03 (4.62–4.67)	-	-	-	-	-
TC 5	14.3±0.2 (14.2–14.5)	0.28±0.01 (0.28–0.29)	4.63±0.03 (4.61–4.66)	-	-	-	-	-

Average value±standard deviation of $n=3$ parallel samples. Range shown in brackets. *=Sample size $n=2$

Fig. 2 Concentrations and standard deviations of the most prevalent compounds detected during 3D printing with PLA Robotic Gray filament. Number of compounds detected during virgin material printing = 23 and after 5 TCs = 13
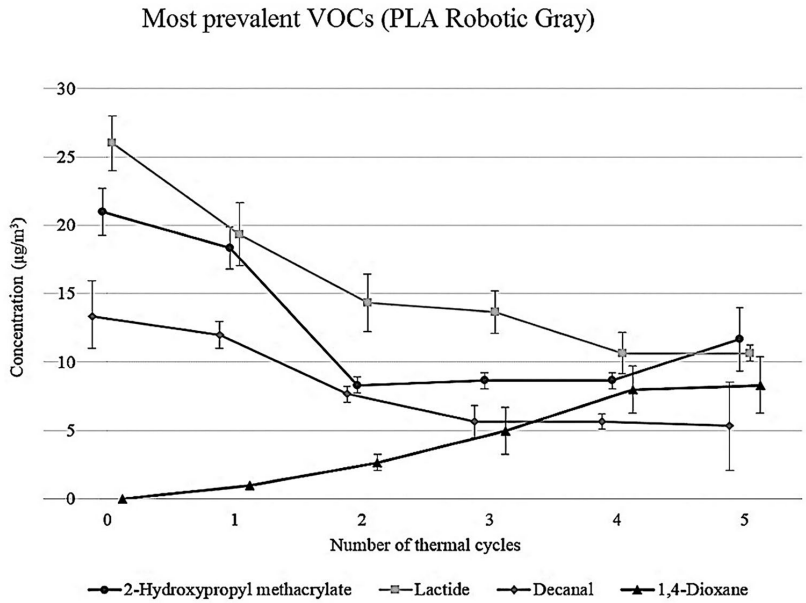

Fig. 3 Concentrations and standard deviations of the most prevalent compounds detected during 3D printing with PLA ReForm filament. Number of compounds detected during virgin material printing = 22 and after 5 TCs = 13
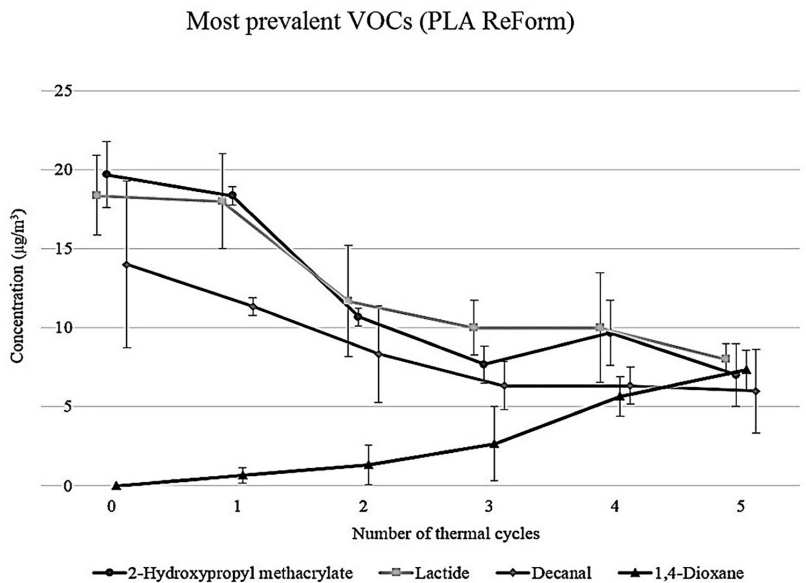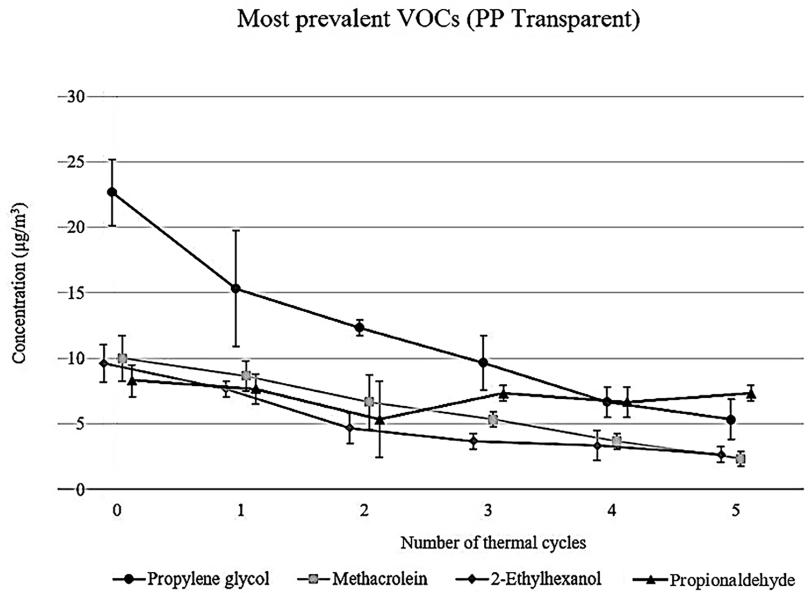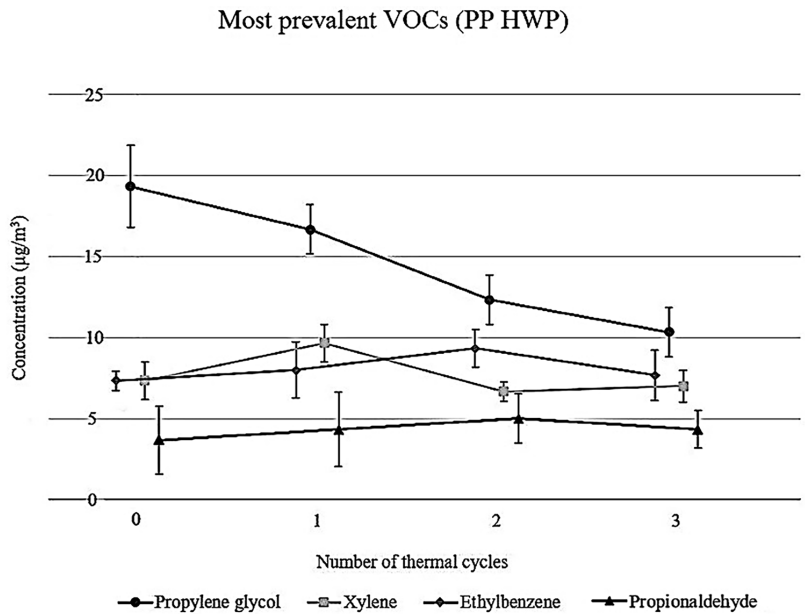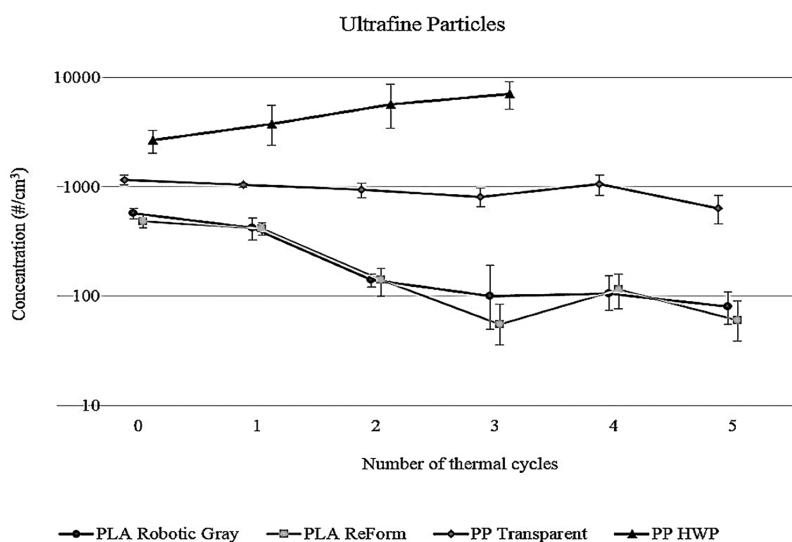
Fig. 4 Concentrations and standard deviations of the most prevalent compounds detected during 3D printing with PP Transparent filament. Number of compounds detected during virgin material printing = 22 and after 5 TCs = 16

Most prevalent VOCs (PP Transparent)

Fig. 5 Concentrations and standard deviations of the most prevalent compounds detected during 3D printing with PP HWP filament. Number of compounds detected during virgin material printing = 27 and after 3 TCs = 20

Most prevalent VOCs (PP HWP)

Fig. 6 UFP concentrations and standard deviations measured from 3D printing with virgin and thermally reprocessed filaments

Ultrafine Particles

Material property measurement results

The material properties of the 3D printed samples are shown in the Table 2. Masses of all PLA samples, which can be used to calculate the densities and to predict mechanical properties, fluctuated inconsistently as the number of TCs increased. The mass of a specimen is a reliable indicator of its tensile strength, and tensile strengths were observed to follow a similar fluctuating pattern. Only slight fluctuation of these parameters was detected with the PP specimens. The masses of the PLA samples were systematically larger than the masses of the PP samples, as expected, which is reflected in the mechanical property results. The filaments produced with the filament extruder had some inconsistency in their thicknesses, which ranged from 1.54 mm to 1.84 mm, but the 3D printed objects expressed no notable dimensional inaccuracy. The densities of the specimens printed with all virgin materials ranged from 96 to 99%, while the density reduced to as low as 74% in the case of the thermally reprocessed PLA ReForm material. Complete tensile specimen data is presented in the Supplementary Tables 4 and 5.

Increase in the number of TCs had no directly observable effect on the alteration of mechanical properties of the studied materials (see the Supplementary Figs. 1 and 2).

40,000 #/cm^3 [35]. The UFP emissions were reduced by 86–88% in the cases of the PLA materials, and by 45% in the case of the PP Transparent material over 5 TCs. The UFP emissions increased by as much as 62% in the case of the PP HWP material over 3 TCs. Full UFP data is presented in the Supplementary Table 3.

Likewise to mass and density, both TS and EM fluctuated inconsistently after thermal reprocessing and the parameters did not express a consistent altering trend. An explicit trend was not observable even after the data was mass-normalized. The mass-normalization of the data was performed to reduce the impact of poor filament quality and the voids on the results, and to promote the impact of thermal degradation on the mechanical performance of the materials. Please see the Supplementary Tables 6 and 7 for normalized mechanical property data. However, the mass, density, TS and EM all followed a similar fluctuation pattern. A simple linear regression analysis of the complete data ($n = 63$) unveiled that the relative mass can accurately be used to predict both the value of TS ($p < 0.01$) and EM ($p < 0.01$). Furthermore, the TS and EM expressed a strong linear correlation (Pearson correlation, $p < 0.01$, $n = 63$, see the Supplementary Figs. 3, 4 and 5).

The virgin PLA sample TS values were comparable to those documented in literature. The average TS of the PLA Robotic Gray samples were reduced by 16% after 5 TCs after the data was normalized in accordance with mass, yielding expected values and negating the impact of 3D printing quality anomalies and voids. The normalization assumes an infill rate of 100% and thus, zero voids. For the average EM, the difference was 9%. For the corresponding PLA ReForm samples the reductions were only 10% and 4%, respectively. However, the measured EM values of the PLA materials were notably low overall, a meager 55–59% of what is documented before. This implicates that the studied PLA materials were drastically more elastic and thus less rigid than those studied before.

A contrary trend was found with the PP Transparent samples. The tensile specimen masses were notably reduced after 5 TCs, while the measured mechanical properties were virtually unchanged. The TS of the material was increased by 14% and EM as greatly as 33% after 5 TCs after the data was normalized. Simultaneously, the PP HWP material expressed 24% reduction in its TS and only 1% reduction in its EM after 3 TCs. The initially measured values were, however, far inferior in comparison to those documented in literature. The initially measured TS values were 53–79% of previously reported values, while the EM values were 23–71% of what has been measured before. Surprisingly, the commercial PP Transparent expressed poor mechanical performance.

Both PLA filaments were effortlessly reprocessed four times. Challenges were encountered during the fifth cycle when the extruded filament became notably sticky. The stickiness resulted in blockages in the feeding and coiling systems of the filament extruder. The filament thickness was also more inconsistent after the 4th cycle, which resulted in several failed prints before an ultimate success. No 3D printable filament could be produced after the fifth cycle. However, by personal monitoring of the filament production an unspecified amount of 3D printable filament could be produced. This was not proven in this study, however. The filament extruder was supposed to be an independent device, and its purpose would be defeated if it required constant monitoring. Henceforth, the fifth thermal cycle was the concluding point in this study.

Printing with both PP Transparent and PP HWP filaments was challenging as the printed objects were subject to considerable warping. 3D print jobs were successful when the printing platform was coated with a generic PP packaging tape. However, the PP Transparent material was easily reprocessed five times as it did not suffer from a notable reduction in its extrudability, unlike the PLA materials did. The PP HWP material on the other hand expressed similar behavior as the PLA materials and could be reprocessed only three times.

Discussion

As found to be consistent with previous studies, the observed 3D printing TVOC emission reduced as the number of TCs increased [34]. Similar trend was found with the UFP emissions, except during 3D printing with the PP HWP material where the effect was contrary. The evaporation and condensation of the most readily volatile compounds during the first cycles was the most likely cause of the highest initially measured concentrations [3, 7]. After the VOC emissions receded, the UFP emissions followed as nucleation capable matter reduced in the air phase [31, 35]. The TVOC emission concentrations of the studied polymer types evened out after one to two TCs, even though the differences between the PLA and PP materials were notable at first. The initially observed TVOC emission differences can be explained with the polymer base structure and the applied 3D printing temperature. The PP materials were printed at a higher temperature, which has a notable impact on 3D printing emissions [13, 22].

The main emitted chemical compounds were the same for both PLA filaments. However, even the most prevalent compounds were found in low concentrations. Additionally, these compounds do not pose a high risk, as they are not linked to acute or severe adverse health effects. However, both filaments expressed the accumulation of 1,4-dioxane, a CNS depressant and a probable human carcinogen, [43] as the number of TCs increased. The source of the compound was unclear, as there is no recorded evidence for the spontaneous formation of the compound during thermal reprocessing of PLA polymer. However, lactide, a common off-gassed compound encountered in thermal processing of PLA [14, 15] shares the same carbon–oxygen backbone with 1,4-dioxane, and the elimination of attached oxygen and carbon atoms could result in the formation of 1,4-dioxane. Another possible source for the compound was an unknown additive or other reactive degradation product that undergoes chemical transformation which ultimately results in the formation of 1,4-dioxane [44].

Another interesting finding was that the most prevalent compounds released during 3D printing with the PP materials were more diverse. Propylene glycol, a compound not linked to serious health risks, was the most prevalent compound and an evident outlier found during 3D printing with both filaments. It must be noted that the applied VOC collection method is best suitable for compounds that are 6 to 16 carbon atoms in length. Henceforth, portions of certain compounds, including propylene glycol, methacrolein, and propionaldehyde, may have passed through the sampling system. Therefore, the true concentrations of these compounds may have been greater than what is presented. In addition to propylene glycol, propionaldehyde was also detected during 3D printing with both PP filaments. However, certain other major compounds released during 3D printing with the PP materials were potentially harmful. 2-ethylhexanol expresses irritation and sensitizing potential, [45] while ethylbenzene and other hydrocarbons, e.g. xylene, possess irritation tendency along with CNS depressive and carcinogenic hazards [46]. Methacrolein is also a particularly hazardous chemical which can cause severe irritation of mucous membranes and the respiratory tract, CNS depression and sensitization [47].

The proposed lightweight UFP reference value of 40,000 #/cm^3 was not exceeded and henceforth the measured concentrations are considered to be relatively safe. However, it is plausible that even the measured concentrations can promote adverse health impacts, e.g., lung and cardiovascular

effects, in prolonged exposure. This is due to the fact that the UFP dose–response relationship is practically linear [32, 33, 35]. The UFP exposure levels appeared to be concerning only when printing with the non-3D printing grade PP polymer, as the levels were low and receded further as the number of TCs increased when the 3D printing grade polymers were applied. As another note, the higher applied 3D printing temperatures of the PP filaments were certainly a major contributor for the higher UFP emissions [21–23]. Furthermore, as seen during 3D printing with the HWP material the UFP levels were increased notably after each TC. Interestingly enough, the increase in UFP emissions was observed simultaneously with decreases in the TVOC levels, while a contrary trend was observed with all other materials. Incomplete burning of the 3D printing material can attribute to the increased UFP emissions through the production and condensation of airborne polycyclic hydrocarbons and semivolatile compounds. These compounds are not detected by the applied chemical sampling method. This assumption can be supported by the further reduction in the filament quality during thermal reprocessing, which was poor to begin with. Irregular material feeding, clogging and slight material burning in the printing nozzle were observed during 3Dprinting. These are factors that drastically increase the UFP emissions. Additionally, it must be noted that the UFP reference value was designed for occupational health protection with a daily 8-h exposure limit in mind, rather than for the preservation of the general populations. In occupational setting the exposure length is limited, and therefore reference value may not be a valid tool for assessing the exposure levels in non-industrial environments.

When certain material property enhancing compounds are disintegrated from the polymer structure the mechanical performance and the physical properties of the materials weaken [1, 2, 4, 5]. These alterations leave the materials less useful for purposes where a 3D printed object is subject to mechanical stress, e.g., bending. However, 3D printed plastic objects are seldom used for particularly demanding purposes, as other methods of both traditional and additive manufacturing offer superior alternatives for purposes where the mechanical properties of an object truly matter. The disintegration of stabilizing agents may also expose the polymer for further chemical transformations where novel decomposition products can be formed [1, 2, 34].

Thermal treatment of polymers has been observed to reduce the molecular mass of the material, followed with decrease of mechanical properties [2, 8]. It was found that the samples 3D printed with the virgin materials expressed the greatest mass in all cases, but the documented trends were not directly found even after the data was mass-normalized. The masses, densities, and mechanical properties were found to fluctuate as the number of TCs increased, and the trend was most distinguishable with the PLA materials.

Mass-normalization of the data negated the fluctuation effect to some extent but not decisively. The measured TS values of the PLA samples were initially only slightly lower than what is documented in literature. However, the measured EM values were greatly lower, almost half of the documented values. The lower EM values implicate that the PLA materials used in this study were notably more elastic than those documented in literature, which is plausible as the materials applied in this study were very likely treated with 3D printability enhancing additives for better extrudability. It must noted, however, that the referenced mechanical property values were pooled from various sources and the specimens tested in them did not completely match those tested in this study, and thus the results are not fully comparable.

The measured mechanical properties and the masses and the densities of the 3D printed samples had a connection between them. An alteration in the specimen mass was followed by a similar alteration in both TS and EM. This observation supports the claim which suggests that the relative mass or density of a material is one of the main determinants of its mechanical properties [2, 8]. Additionally, the fluctuation of the mechanical properties in this study were most likely a result of the reduced 3D printability of the studied materials, which is a known side effect of thermal reprocessing of polymers [38]. While the filament extruder performed adequately in producing 3D printable filament, the thicknesses of the produced filaments were found to be inconsistent. The 3D printed objects will contain mechanical performance altering improperly filled voids if the thickness of the applied filament falls below the standard value of 1.75 mm. This is what was expected to have occurred over the course of this study, as seen from the fluctuating pattern in mechanical properties and relative masses despite all samples being fabricated based on the same model and parameters. This assumption is supported by the mechanical property and mass measurements, as the virgin materials expressed the best mechanical properties, expect for the PP Transparent material. Even the PP HWP material expressed a similar trend which was found among the PLA materials, regardless of it not being a commercially produced 3D printing material to begin with. It can be stated that thermal reprocessing of 3D printing materials has a lesser impact on the mechanical properties of 3D printed objects than on the 3D printing filament integrity and quality. Recycled plastics can be used as 3D printing feedstocks without compromising mechanical performance if the applied filament is of adequate quality.

A simple regression analyses of the relationships between the tensile specimen masses and the measured mechanical properties, and a TS-EM correlation analysis were performed on the whole collected data. All these results were statistically significant ($p < 0.01$), which further supports the claim that thermal reprocessing has little effect on the

measured mechanical properties of PLA or PP plastics. However, thermal recycling has a more notable impact on the reprocessability itself, which was reflected as inconsistencies in the qualities of the filaments and ultimately in 3D printability, printing quality, and mechanical performance.

All PLA filaments maintained acceptable surface quality and adequate mechanical performance thorough the experiment. These materials were also lower VOC and UFP emitters and the listed findings promote PLA materials as a one of the best choices for material extrusion 3D printing. Even though the 3D printed PP objects were slightly poorer than the PLA objects in quality, the print jobs were successful. The recycled filaments filled their purpose for applications where the surface properties or dimensional accuracy of a printed object are not demanding. This suggests that even the recycled HWP materials are a plausible 3D printer feedstock alternative, even without introduction of 3D printability enhancing additives. Adhesion to the printing bed requires assistance, however.

Conclusions

The findings suggest that recycled 3D printing grade polymers are not particularly more hazardous to 3D print than virgin polymers. The concentrations of the most individual compounds decrease along with the TVOC concentration as the magnitude of thermal processing increases, which results in increasingly lower chemical exposure levels. Interestingly however, new compounds may be introduced into the VOC profile over thermal reprocessing and thus, unforeseen potential health hazards can emerge. A practical example is the accumulation of 1,4-dioxane in the studied PLA materials. It must be noted that the measured concentrations were low through the experiment and no acute health complications are expected to emerge from the use of recycled 3D printing filaments. Caution is advised especially when 3D printer filaments produced from non-3D printing grade polymers are applied, as the UFP levels were very high during printing with the PP HWP materials in comparison to the 3D printing grade materials. Nevertheless, basic 3D printing safety precautions, e.g., printing in a well-ventilated space and spending the least possible amount of time in the same space with a 3D printer should be always applied. These maneuvers notably reduce unnecessary exposure to the VOCs and UFPs emitted during a 3D printer operation.

Based on this study recycled plastics are a compelling feedstock alternative for virgin plastic materials for 3D printing. These materials can be applied on a large scale if a supply of such materials is developed. This is, given that the original polymer grade is suitable for an extrusion process. Household waste plastics, on the other hand, can be used for vanity purposes, as the material was found to be of meager quality and processability. Quite surprisingly, such a material was not found to be particularly hazardous. Further research on the factors affecting the mechanical, thermal, and polymer properties and the micro-scale alterations that influence 3D printability of thermally reprocessed polymers is recommended. Additionally, the effects of polymer blending should also be studied further as polymer cross-contamination is inevitable when polymer recycling is performed on a large scale. The understanding of these factors will substantially benefit in the development of more sustainable 3D printing materials.

Declarations

References

1. Pospíšil J, Horák Z, Kruliš Z, Nešpůrek S, Kuroda S-I (1999) Degradation and aging of polymer blends I. Thermo-mechanical and thermal degradation. Polym Degrad Stabil 65(3):405–414. https://doi.org/10.1016/S0141-3910(99)00029-4

2. Kutz M (2018) Handbook of environmental degradation of materials, 3rd edn. Elsevier, Amsterdam, Netherlands

3. Murata K, Hirano Y, Sakata Y, Uddin MA (2002) Basic study on a continuous flow reactor for thermal degradation of polymers. J Anal Appl Pyrolysis 65(1):71–90. https://doi.org/10.1016/j.jaap.2009.08.009

4. Alex A, Ilango NK, Ghosh P (2018) Comparative role of chain scission and solvation in the biodegradation of polylactic acid (PLA). J Phys Chem B 122(41):9516–9526. https://doi.org/10.1021/jp500219j
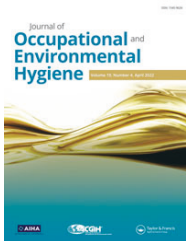
5. Żenkiewicz M, Richert J, Rytlewski P, Moraczewski K, Stepczyńska M, Karasiewicz T (2009) Characterisation of multi-extruded poly(lactic acid). Polym Test 28(4):412–418. https://doi.org/10.1016/j.polymertesting.2009.01.012

6. Garlotta D (2001) A literature review of poly(lactic acid). J Polym Environ 9(2):63–84. https://doi.org/10.1023/A:1020200822435

7. Andersson T, Stålblom B, Wesslén B (2004) Degradation of polyethylene during extrusion. II. Degradation of low-density polyethylene, linear low-density polyethylene, and high-density polyethylene in film extrusion. J Appl Polym Sci 91(3):1525–1537. https://doi.org/10.1002/app.13024

8. Tanikella NG, Wittbrodt B, Pearce JM (2017) Tensile strength of commercial polymer materials for fused filament fabrication 3D printing. Addit Manuf 15:40–47. https://doi.org/10.1016/j.addma.2017.03.005

9. Tymrak BM, Kreiger M, Pearce JM (2014) Mechanical properties of components fabricated with open-source 3-D printers under realistic environmental conditions. Mater Des 58:242–246. https://doi.org/10.1016/j.matdes.2014.02.038

10. Lechter T, Waytashek M (2015) Material property testing of 3D-printed specimen in PLA on an entry-level 3D printer. ASME 2014 International Mechanical Engineering Congress and Exposition Volume 2A: Advanced Manufacturing. Montreal, Quebec, Canada. https://doi.org/10.1115/IMECE2014-39379

11. Lanzotti A, Grasso M, Staiano G, Martorelli M (2015) The impact of process parameters on mechanical properties of parts fabricated in PLA with an open-source 3-D printer. Rapid Prototyp J 21(5):604–617. https://doi.org/10.1108/RPJ-09-2014-0135

12. Wittbrodt B, Pearce JM (2015) The effects of PLA color on material properties of 3-D printed components. Addit Manuf 8:110–116. https://doi.org/10.1016/j.addma.2015.09.006

13. Mendes L, Kangas A, Kukko K et al (2017) Characterization of emissions from a desktop 3D printer. J Indust Ecol 14:94–106. https://doi.org/10.1111/jiec.12569

14. Azimi P, Zhao D, Pouzet C, Crain NE, Stephens B (2016) Emissions of ultrafine particles and volatile organic compounds from commercially available desktop three-dimensional printers with multiple filaments. Environ Sci Technol 50(3):1260–1268. https://doi.org/10.1021/acs.est.5b04983

15. Floyd EL, Wang J, Regens JL (2017) Fume emissions from a low-cost 3-D printer with various filaments. J Occup Environ Hyg 14(7):523–533. https://doi.org/10.1080/15459624.2017.1302587

16. Steinle P (2016) Characterization of emissions from a desktop 3D printer and indoor air measurements in office settings. J Occup Environ Hyg 13(2):121–132. https://doi.org/10.1080/15459624.2015.1091957

17. Stefaniak AB, LeBouf RF, Yi J et al (2017) Characterization of chemical contaminants generated by a desktop fused deposition modeling 3-dimensional printer. J Occup Environ Hyg 14(7):540–550. https://doi.org/10.1080/15459624.2017.1302589

18. Kim Y, Yoon C, Ham S et al (2015) Emissions of nanoparticles and gaseous material from 3D printer operation. Environ Sci Technol 49(20):12044–12053. https://doi.org/10.1021/acs.est.5b02805

19. Väisänen AJK, Alonen L, Ylönen S, Hyttinen M (2019) Occupational exposure to gaseous and particulate contaminants originating from additive manufacturing of liquid, powdered and filament plastic materials and related post-processes. J Occup Environ Hyg 16(3):258–271. https://doi.org/10.1080/15459624.2018.1557784

20. Sogancioglu M, Ahmetli G, Yel E (2017) A comparative study on waste plastic pyrolysis liquid products quantity and energy recovery potential. Energy Procedia 118:221–226. https://doi.org/10.1016/j.egypro.2017.07.020

21. Stephens B, Azimi P, El Orch Z, Ramos T (2013) Ultrafine particle emissions from desktop 3D printers. Atmos Environ 79:334–339. https://doi.org/10.1016/j.atmosenv.2013.06.050

22. Yi J, LeBouf RF, Duling MG et al (2016) Emission of particulate matter from a desktop three-dimensional (3D) printer. J Toxicol Environ Health A 79(11):453–465. https://doi.org/10.1080/15287394.2016.1166467

23. Zhang Q, Wong JPS, Davis AY, Black MS, Weber RJ (2017) Characterization of particle emissions from consumer fused deposition modeling 3D printers. Aer Sci Technol 51(11):1275–1286. https://doi.org/10.1080/02786826.2017.1342029

24. Vance ME, Pegues V, van Montfrans S, Leng W, Marr LC (2017) Aerosol emissions from fuse-deposition modeling 3D printers in a chamber and in real indoor environments. Environ Sci Technol 51(17):9516–9523. https://doi.org/10.1021/acs.est.7b01546

25. House R, Rajaram N, Tarlo SM (2017) Case report of asthma associated with 3D printing. Occup Med 67(8):652–654. https://doi.org/10.1093/occmed/kqx129

26. Chan FL, House R, Kudla I, Lipszyc JC, Rajaram N, Tarlo SM (2018) Health survey of employees regularly using 3D printers. Occup Med 68(3):211–214. https://doi.org/10.1093/occmed/kqy042

27. Unwin J, Coldwell MR, Keen C, McAlinden JJ (2013) Airborne emissions of carcinogens and respiratory sensitizers during thermal processing of plastics. Ann Occup Hyg 57(3):399–406. https://doi.org/10.1093/annhyg/mes078

28. Win-Shwe T-T, Fujimaki H, Arashidani K, Kunugita N (2013) Indoor volatile organic compounds and chemical sensitivity reactions. Clin Dev Immunol 2013;2013:623812. https://doi.org/10.1155/2013/623812

29. Tuomi T, Vainiotalo S (2014) The guideline and target values for total volatile organic compound concentrations in industrial indoor environments in Finland. Ind Built Env 25(2):434–434. https://doi.org/10.1177/1420326X14554270

30. Savonius B, Keskinen H, Tuppurainen M, Kanerva L (1993) Occupational respiratory disease caused by acrylates. Clin Exp Allergy 23(5):416–424. https://doi.org/10.1111/j.1365-2222.1993.tb00348.x

31. Wang Z-M, Wagner J, Wall S (2010) Characterization of laser printer nanoparticle and VOC emissions, formation mechanisms, and strategies to reduce airborne exposures. Aer Sci Technol 45(9):1060–1068. https://doi.org/10.1080/02786826.2011.580799

32. Pope CA, Dockery DW (2006) Health effects of fine particulate air pollution: lines that connect. J Air Waste Manag Assoc 56(6):709–742. https://doi.org/10.1080/10473289.2006.10464485

33. Mossman BT, Borm PJ, Castranova V, Costa DL, Donaldson K, Kleeberger SR (2007) Mechanisms of action of inhaled fibers, particles and nanoparticles in lung and cardiovascular diseases. Part Fibre Toxicol 4:4. https://doi.org/10.1186/1743-8977-4-4

34. Mylläri V, Hartikainen S, Poliakova V et al (2016) Detergent impurity effect on recycled HDPE: Properties after repetitive processing. J Appl Polym Sci 133:43766. https://doi.org/10.1002/app.43766

35. van Broekhuizen P, van Veelen W, Streekstra WH, Schulte P, Reijnders L (2012) Exposure limits for nanoparticles: report of an international workshop on nano reference values. Ann Occup Hyg 56(5):515–524. https://doi.org/10.1093/annhyg/mes043

36. Cicala G, Giordano D, Tosto C, Filippone G, Recca A, Blanco I (2018) Polylactide (PLA) filaments a biobased solution for additive manufacturing: correlating rheology and thermomechanical properties with printing quality. Materials 11(7):1191. https://doi.org/10.3390/ma11071191

37. Raj SA, Muthukumaran E, Jayakrishna K (2018) A case study of 3D printed PLA and its mechanical properties. Mater Today Proc 5(5):11219–11226. https://doi.org/10.1016/j.matpr.2018.01.146

38. Anderson I (2017) Mechanical properties of specimens 3D printed with virgin and recycled polylactic acid. 3D Print Addit Manuf 4(2):110–115. https://doi.org/10.1089/3dp.2016.0054

39. Carneiro OS, Silva AF, Gomes R (2015) Fused deposition modeling with polypropylene. Mater Des 83:768–776. https://doi.org/10.1016/j.matdes.2015.06.053

40. Zander NE, Gillan M, Burckhard Z, Gardea F (2019) Recycled polypropylene blends as novel 3D printing materials. Addit Manuf 25:122–130. https://doi.org/10.1016/j.addma.2018.11.009

41. Milosevic M, Stoof D, Pickering KL (2017) Characterizing the mechanical properties of fused deposition modelling natural fiber recycled propylene composites. J Compos Sci 1(1):7. https://doi.org/10.3390/jcs1010007

42. Kaynak B, Spoerk M, Shirole A, Ziegler W, Sapkota J (2018) Polypropylene/cellulose composites for material extrusion additive manufacturing. J Macromol Mater Eng 303:1800037. https://doi.org/10.1002/mame.201800037

43. International Agency for Research on Cancer (IARC) (1999) IARC monographs on the evaluation of carcinogenic risks to humans. Re-evaluation of some organic chemicals, hydrazine and hydrogen peroxide, WHO, Geneva, Switzerland, vol 71, pp 589–602.

44. U.S. Environmental Protection Agency (2017) Preliminary information on manufacturing, processing, distribution, use and disposal: 1,4-Dioxane. Support document for Docket EPA-HQ-OPPT-2016–0723 (2017). Available at:https://www.epa.gov/sites/production/files/2017-02/documents/14-dioxane.pdf. Accessed 3 Oct 2020

45. Wakayama T, Ito Y, Miyake M, Shibata E, Ohno H, Kamijima M (2019) Comprehensive review of 2-ethyl-1-hexanol as an indoor air pollutant. J Occup Health 61(1):19–35. https://doi.org/10.1002/1348-9585.12017

46. Malachowski MJ, Goldberg AF (1999) Health effects of toxic substances, 2nd Edition. Government Institutes, Rockville, Maryland, USA

47. Larsen ST, Nielsen GD (2000) Effects of methacrolein on the respiratory tract in mice. Toxicol Lett 114(1–3):197–202. https://doi.org/10.1016/S0378-4274(99)00300-8

ARTICLE III

Väisänen A., Alonen L., Ylönen S. & Hyttinen M. 2022. Volatile organic compounds and particulate emissions from the production and use of thermoplastic biocomposite 3D printing filaments. *Journal of Occupational and Environmental Hygiene 19(6):381–393.*

Volatile organic compound and particulate emissions from the production and use of thermoplastic biocomposite 3D printing filaments

Antti Väisänen, Lauri Alonen, Sampsa Ylönen & Marko Hyttinen

View supplementary material

Published online: 11 May 2022.

Submit your article to this journal

Article views: 174

View related articles

View Crossmark data

Taylor & Francis
Taylor & Francis Group

Volatile organic compound and particulate emissions from the production and use of thermoplastic biocomposite 3D printing filaments

Antti Väisänen[a], Lauri Alonen[b], Sampsa Ylönen[b], and Marko Hyttinen[a]

[a]Faculty of Science and Forestry, Department of Environmental and Biological Sciences, University of Eastern Finland, Kuopio, Finland; [b]School of Engineering and Technology, Savonia University of Applied Sciences, Kuopio, Finland

ABSTRACT

Biocomposites (BCs) can be used as substitutes for unsustainable polymers in 3D printing, but their safety demands additional investigation as biological fillers may produce altered emissions during thermal processing. Commercial filament extruders can be used to produce custom feedstocks, but they are another source of airborne contaminants and demand further research. These knowledge gaps are targeted in this study. Volatile organic compound (VOC), carbonyl compound, ultrafine particle (UFP), and fine ($PM_{2.5}$) and coarse (PM_{10}) particle air concentrations were measured in this study as a filament extruder and a 3D printer were operated under an office environment using one PLA and four PLA-based BC feedstocks. Estimates of emission rates (ERs) for total VOCs (TVOC) and UFPs were also calculated. VOCs were analyzed with a GC-MS system, carbonyls were analyzed with an LC-MS/MS system, whereas real-time particle concentrations were monitored with continuously operating instruments. VOC concentrations were low throughout the experiment; TVOC ranged between 34–63 µg/m³ during filament extrusion and 41–56 µg/m³ during 3D printing, which represent calculated TVOC ERs of 2.6–3.6 × 10² and 2.9–3.6 × 10² µg/min. Corresponding cumulative carbonyls ranged between 60–91 and 190–253 µg/m³. Lactide and miscellaneous acids and alcohols were the dominant VOCs, while acetone, 2-butanone, and formaldehyde were the dominant carbonyls. Terpenes contributed for ca. 20–40% of TVOC during BC processing. The average UFP levels produced by the filament extruder were 0.85 × 10²–1.05 × 10³ #/cm³, while the 3D printer generated 6.05 × 10²–2.09 × 10³ #/cm³ particle levels. Corresponding particle ERs were 5.3 × 10⁸–6.6 × 10⁹ and 3.8 × 10⁹–1.3 × 10¹⁰ #/min. $PM_{2.5}$ and PM_{10} particles were produced in the following average quantities; $PM_{2.5}$ levels ranged between 0.2–2.2 µg/m³, while PM_{10} levels were between 5–20 µg/m³ for all materials. The main difference between the pure PLA and BC feedstock emissions was terpenes, present during all BC extrusion processes. BCs are similar emission sources as pure plastics based on our findings, and a filament extruder produces contaminants at comparable or slightly lower levels in comparison to 3D printers.

Introduction

The additive manufacturing (AM) industry is an expanding consumer of energy and plastics which contribute to some of the most important environmental issues of recent times. Sustainable polymers derived from renewable sources and polymer composites reinforced with natural fibers referred to as biocomposites (BCs) gain popularity as environmentally friendly alternatives for petroleum-based pure polymers. The advantages of BCs include lightweight, reduced production costs, environmental friendliness, improved dimensional stability and stiffness (Ford and Despeisse 2016; Peng et al. 2018; Calí et al. 2020; Calvino et al. 2020), and even increased processability without affecting processing parameters (Mazzanti et al. 2019; Vaidya et al. 2019). The AM industry can play a role in energy conservation through a shortened supply chain as localized production and the use of sustainable feedstocks become increasingly commonplace. One way to support sustainability is the

---

wider use of BCs which reduces the demand for unsustainable polymers (Ford and Despeisse 2016; Peng et al. 2018; Calí et al. 2020; Calvino et al. 2020).

Commercially available three-dimensional (3D) printer filament extruders have been introduced to consumer markets over the past few years. These extruders can produce custom 3D printer feedstocks from thermoplastic polymers, and additives or fillers, e.g., wood particles, if desired, but they are another source for polymer thermal degradation products. The emissions from such machines have been documented only once so far by Byrley et al. (2020). Their findings indicate the emissions are similar in composition when compared to those produced by material extrusion (ME) 3D printers, but this was not confirmed by using the produced filaments in a 3D printer. Principally, a thermal extruder can produce a wide range of emissions, mainly chemical species including volatile organic compounds (VOCs), ultrafine particles (UFPs), and to a smaller extent, fine ($PM_{2.5}$) and coarse (PM_{10}) particles (Kim et al. 2015a, Azimi et al. 2016; Stabile et al. 2017; Steinle 2016; Yi et al. 2016; Floyd et al. 2017; Kwon et al. 2017; Mendes et al. 2017; Rao et al. 2017; Stefaniak et al. 2017, 2021; Vance et al. 2017; Byrley et al. 2019, 2020; Du Preez et al. 2018; Davis et al. 2019; Väisänen et al. 2019, 2021a; Jeon et al. 2020). These emissions can induce adverse health impacts in humans after exposure, including respiratory symptoms, depression of the central nervous system, irritation, inflammation or sensitization, and they may exacerbate preexisting health conditions, e.g., asthma (WHO 1995, 2006; Van Kampen et al. 2000; Pope and Dockery 2006; Wolkoff et al. 2006; Mossman et al. 2007; Sarigiannis et al. 2011; Weschler 2011; Shahnaz et al. 2012; Klaasen et al. 2013; Rohr 2013; House et al. 2017; Chan et al. 2018).

Additionally, wooden products and BCs have been documented to emit distinctive chemicals that include various terpenes (Roffael 2006; Kim et al. 2006; Höllbacher et al. 2015; Pohleven et al. 2019). BCs can therefore produce altered emissions in comparison to pure plastics when used as filament extruder or 3D printer feedstocks. To be noted, a wide range of VOCs and certain terpenes are classified as irritants or sensitizers (Kasanen et al. 1999; Van Kampen et al. 2000; Kim et al. 2013; Wolkoff et al. 2006; Mossman et al. 2007; Shahnaz et al. 2012; WHO 2021), while terpenes are identified as precursors for secondary reactive chemical species and UFPs in the air phase in the presence of ozone. (Sarwar et al. 2004; Rohr 2013; Kim et al. 2015b; Wolkoff 2020). Indoor terpenes can potentially impair indoor air quality further on this basis. However, terpenes have widely been applied in consumer products, e.g., fragrances for decades without widespread adverse impacts while being present in both indoor and outdoor environments throughout history (Sarwar et al. 2004; Roffael 2006; Wolkoff 2020), and thus their contribution to indoor air quality must be evaluated carefully. In contrast, volatile terpenes are also associated with various health benefits, e.g., anti-inflammatory potential, further challenging their perception as mere pollutants (Kim et al. 2020).

The evaluation of safe use of alternative, sustainable materials is needed to justify the encouraging shift toward BCs. Therefore, multiple relevant indoor exposure agent parameters are sampled or monitored in this study while (poly)lactic acid (PLA) based BC filaments, and a reference PLA filament are produced with a commercial filament extruder and used as an ME 3D printer feedstock. The main aims of this study are to (1) discover how the introduction of wood (and cellulose) content affects the emission composition of 3D printer feedstocks, (2) to estimate how hazardous the produced emissions are in comparison to a pure plastic, (3) to establish if terpenes or other wood-related compounds are commonly produced during thermal processing of BCs, and (4) to document how the emissions from a filament extruder compare to a 3D printer when equivalent feedstocks are used in both machines. VOCs and particles originated from BC processing, and especially their small-scale production has not previously been investigated thoroughly from a safety perspective and the impacts of the introduction of bio-content on emission compositions are not previously discussed in the AM field. Although BC filaments have occasionally been used in ME printer emission studies as a subsidiary material (Azimi et al. 2016; Stabile et al. 2017; Kwon et al. 2017; Vance et al. 2017; Väisänen et al. 2019; Jeon et al. 2020), they have not been a central material of interest and the postulated terpene emissions have not been previously targeted. This study aims to fill in the remaining data gaps.

Materials and methods

Feedstock production and 3D printing

Wood powder used for custom BC filament production was prepared by grinding dried, mixed sawdust (including ca. 40% birch, 40% spruce, and 20% aspen) with an A10 analytical grinder (IKA-Werke GmbH & Co. KG., Staufen, Germany). The powder was sifted with a 250 μm mesh sieve and the larger particles were disposed of. Transparent PLA granules (3devo B. V., Utrecht, The Netherlands) and the wood powders were mixed and heated in a portable oven at 180 °C

Table 1. Material compositions and filament extruder zone temperatures.

Material	Composition	Temperature settings (°C)
Transparent PLA	100 w-% PLA	180/185/190/180
Formi 20	20 w-% cellulose fibers, 80 w-% PLA	180/185/180/170
Formi 40	40 w-% cellulose fibers, 60 w-% PLA	180/185/180/170
BC 15%	15 w-% wood powder, 85 w-% PLA	195/185/185/185
BC 30%	30 w-% wood powder, 70 w-% PLA	200/195/185/185

w-% = percentage in weight.
BC = custom biocomposite.

for 10 min. Two BC batches were produced, one with 15 and the other with 30 percentage in weight (w-%) wood content. For comparison, commercial BC filaments often contain 15–40 w-% wood or cellulose content. The composite mixes were cut into smaller pieces and shredded with a SHR3D IT plastic shredder (3devo B.V., The Netherlands). A total of five different 3D printable filaments with target thicknesses of 1.75 mm were extruded with a Filament Composer 450 extruder (3devo B.V.) using the BC shreds, the aforementioned PLA granules, and commercially available PLA-based Formi 20 and Formi 40 BC granules (UPM-Kymmene Corp., Helsinki, Finland) containing 20 and 40 w-% cellulose fibers, respectively. The filament extruder consisted of four temperature-adjustable heating zones, a feeder screw, an extruder nozzle, and filament puller and roller systems. The filament extruder heating zone temperatures and the compositions of all feedstocks used in this study are presented in Table 1.

The filament extruder was purged by extruding 250 mL of the transparent PLA granules between each feedstock material. Two-hundred-fifty (250) mL of the feedstock was also initially rejected from the spooling process to prevent filament contamination. Filament production lasted for 100–110 min. The filaments were used in an open Ender-3 ME 3D printer (ShenZhen Creality 3D Technology Co. Ltd, Shenzhen, China) to produce sets of eight $4 \times 4 \times 1$ cm plates over 110–120 min. The same printer specifications were used throughout the experiment; 200°C nozzle and 50°C bed temperatures, 0.2 mm layer thickness, 0/90° raster angle, and 1 mm path width as the printer was equipped with a 1 mm diameter nozzle to prevent fiber blockages. No adhesion enhancers were used on the build plate.

Emission and exposure agent measurements

The exposure and emission measurements were performed in a mechanically ventilated office room with floor area of 38.5 m^2, room height of 2.7 m, a total volume of 104 m^3, and a calculated ventilation rate of 3.6 air exchanges per hour (ACH) resolved by measuring air velocity from nine points at the exhaust vent interface after the measurement campaign using a 3000 md micromanometer (Swema AB, Farsta, Sweden). The ACH was calculated using the following equation:

$$ACH = \frac{CFM \times 60}{A \times h}$$

where *CFM* is the volumetric air flow per minute (m^3/min) calculated using the micromanometer readings and the area of the exhaust vent, while *A* and *h* represent the room dimensions (area and height). Air mixing factors or other contributors to the exhaust rate or infiltration were not identified.

A process operator was always present in the room, while a person responsible for the measurements visited the room twice an hour. Sampling was performed at a stationary point; the altitude of the breathing zone (height of 1.5 m) and one-meter distance from the emission sources. Background samples which were used to correct the results were also collected from this point. The room was ventilated between each set of collected samples and the absence of contaminants was verified by UFP concentration reduction down to background level, followed with ventilation for an additional hour. The ANSI/CAN/UL 2904 standard for 3D printer emission sampling was not followed in this study as the collected data sets were intended to represent real-life exposure circumstances, and because the filament extruder could not confidently be operated in a closed chamber.

VOC exposures were also sampled personally. Three parallel samples were collected from both the stationary point and the breathing zone of the process operator. The process operator ensured no errors were occurring during the extrusion processes while performing other tasks in the room which did not produce airborne contaminants. Sample collection time of 45 min was used to ensure the collection of sufficient amounts of compounds with Tenax TA adsorption tubes and SKC 222 pumps (SKC Inc., Eighty-Four, PA) using a calibrated flow rate of 150 mL/min. Background VOC samples were collected like the actual VOC samples, but before the initiation of thermal processes. The samples were analyzed and the mass concentrations (C_m) of individual compounds were calculated according to the ISO 16000-6:2011 standard using a gas chromatography-mass spectrometry system consisting of a TD100 thermal desorber (Markes International Inc., Sacramento, CA), 7890 A gas chromatograph equipped with an HP-5ms

UI column with 60 m length, 0.25 mm internal diameter and 0.25 μm film thickness, and 5975 C mass spectrometer (all manufactured by Agilent Technologies Inc., Santa Clara, CA) operating on scanning mode. The MSD ChemStation software (version F.01.00.1903, Agilent Technologies Inc.) paired with NIST20 database (National Institute of Standards and Technology, Gaithersburg, MD) was used for VOC identification based on compound retention times and ion fingerprints. Concentrations of individual compounds were calculated as toluene equivalents with the assistance of four-point toluene standard curves constructed with standard HC 48-component 40353-U VOC samples (Supelco Inc., Bellefonte, PA). A limitation of the toluene equivalent method is that the sensitivity of the mass spectrometer may be different for the individual chemical species which can lead to result distortion. The VOCs present in at least two of the three parallel samples were included in the results and their presented concentrations are background-corrected. For further details, please see our previous study (Väisänen et al. 2019).

Carbonyl compound air concentrations were sampled by collecting Sep-Pak 2,4-dinitrophenylhydrazine (DNPH) Silica cartridge samples (Waters Corp., Milford, MA) over the full duration of the thermal processes at a calibrated flow rate of 2 L/min using an N022.AN.18 pump (KNF Neuberger Inc., Trenton, NJ). The samples were selectively quantified using an LCMS-8040 triple quadrupole mass spectrometer (Shimadzu Corp., Kyoto, Japan) containing a Kinetex reversed phase C18 column with 1.7 μm pore size, 100 mm length, and 3 mm internal diameter (Phenomenex Inc., Torrance, CA). Acetonitrile and water were used as the eluents. The compounds were identified and quantified with the assistance of four-point standard curves constructed by running Carbonyl-DNPH Mix 1 certified reference material samples compromised of 13 common carbonyls (Sigma-Aldrich Corp., Saint Louis, MO) among the collected samples. The LabSolution Insight program (Shimadzu Corp.) was used to for compound identification and corresponding C_m calculations. Any carbonyls not included in the reference material evaded the analysis method. Background carbonyl samples were collected for 360 min when no operations were performed in the room. The presented results are background-corrected. For further details, please see our previous study (Väisänen et al. 2022).

Exposure levels to particulate matter were determined with two continuously operating devices; the number concentrations (C_n) of UFPs were measured with a P-Trak 8525 device (particle size range 20–1000 nm, TSI Inc., Shoreview, MN) and C_m of coarse (PM_{10}) and fine ($PM_{2.5}$) particles were measured with an Optical Particle Sizer (OPS) 3330 instrument (16 channels, particle size range 0.3–10 μm, TSI Inc.). The OPS instrument neglects the impact of UFPs on the particle air mass concentrations because of the smallest observable particle size of 0.3 μm, which likely results in underestimated mass concentrations. Ten-second logging intervals were used in both, and the devices were zero-calibrated before each measurement set. Background concentrations were measured for 30 min before any extrusion processes were initiated, and actual sampling lasted for the full duration of an extrusion process. The presented particle concentrations are background-corrected. This study was performed in duplicate to prevent VOC sampling from being influenced by isopropyl alcohol, the working fluid emitted by the P-Trak device.

Emission rates (ERs) for TVOC and UFPs were calculated using the simplistic equation:

$$S = ((C_{out} - C_{in}) \times Q)/60$$

where S is ER per minute, C_{out} represents the average C_n of UFPs or C_m of TVOC in m^3, C_{in} equals the measured background C_n of UFPs or C_m of TVOC, and Q is the volumetric flow rate (m^3/h) of exhaust air. Using background-corrected values for C_{out}, the equation can be further simplified:

$$S = (C_{avg} \times Q)/60$$

where C_{avg} is the average C_n of UFPs or C_m of TVOC after background-correction. These calculations are rough estimates which neglect particle losses, agglomeration, and other factors which can impact the evolution and decay of C_n of UFPs or C_m of TVOC as well as assumes complete mixing of air and constant rates for UFP and TVOC productions.

Indoor air quality (IAQ) parameters including carbon dioxide (CO_2), temperature, and relative humidity (RH) were monitored with a continuously operating IAQ-Calc 7525 device (TSI Inc.) using a 30-sec logging interval. The main purpose of these measurements was quality control, but the readings were also used to discover the plausible CO_2 emissions from the extrusion processes as the introduced wood content may burn in the extruder nozzles more easily than the base polymer. These parameters are not background-corrected in the results.

Table 2. The average air concentrations of the most common VOCs, cumulative other VOCs and TVOC ($\mu g/m^3$), and TVOC emission rates (S_{TVOC}, $\mu g/min$).

Description	1-Nonanol	1-Propanol	Acetic acid	Furfural	Lactide	Hexanal	3-Carene	α-Pinene	D-Limonene	Isoprene	p-Cymene	Other	TVOC	S_{TVOC}
Filament production: PLA	3 (3)	2 (0)	3 (2)	0 (0)	22 (16)	0 (2)	0 (0)	0 (0)	0 (0)	0 (0)	0 (0)	17 (13)	42 (34)	2.6×10^2
Filament production: Formi 20	2 (5)	0 (2)	10 (11)	2 (0)	10 (9)	2 (2)	3 (2)	2 (3)	0 (2)	0 (0)	4 (3)	15 (14)	48 (48)	3.0×10^2
Filament production: Formi 40	3 (3)	2 (3)	5 (5)	3 (6)	13 (13)	0 (3)	6 (3)	5 (5)	3 (5)	3 (2)	4 (2)	11 (18)	56 (62)	3.5×10^2
Filament production: BC 15%	3 (2)	2 (0)	6 (4)	3 (0)	15 (18)	2 (2)	5 (5)	3 (3)	0 (2)	2 (0)	2 (3)	7 (13)	46 (48)	2.9×10^2
Filament production: BC 30%	2 (2)	0 (2)	12 (8)	4 (5)	16 (14)	2 (0)	6 (6)	4 (5)	3 (3)	3 (3)	3 (4)	5 (14)	58 (63)	3.6×10^2
3D printing: PLA	8 (7)	5 (6)	4 (7)	0 (0)	16 (14)	3 (3)	0 (0)	0 (0)	0 (0)	0 (0)	0 (0)	21 (22)	55 (56)	3.4×10^2
3D printing: Formi 20	3 (4)	4 (5)	4 (4)	2 (0)	7 (6)	2 (3)	3 (3)	7 (3)	3 (3)	0 (0)	0 (0)	23 (17)	54 (45)	3.4×10^2
3D printing: Formi 40	3 (4)	4 (4)	5 (4)	0 (2)	9 (7)	3 (3)	2 (2)	4 (2)	6 (6)	2 (2)	2 (2)	13 (4)	50 (41)	3.1×10^2
3D printing: BC 15%	5 (4)	5 (2)	4 (3)	0 (2)	9 (8)	3 (2)	2 (2)	3 (2)	5 (3)	0 (2)	2 (3)	19 (17)	54 (44)	3.4×10^2
3D printing: BC 30%	4 (4)	3 (3)	4 (4)	2 (0)	15 (8)	3 (2)	3 (2)	3 (2)	4 (3)	2 (2)	2 (3)	15 (8)	47 (39)	2.9×10^2

Average concentrations of personal samples shown in parentheses.
All presented values are background-corrected.
S_{TVOC} is calculated using the TVOC values obtained from a stationary point (the values without parentheses).

Results

Production of the custom BC filaments was empirically successful. All the studied materials, including the custom BC shreds were pulled into filaments with ease and 3D printing with the filaments demonstrated no malfunctions, nozzle blockages, or other critical errors and the surface qualities of the 3D printed plates were good.

The indoor air parameters were not markedly affected by the thermal processes. Room temperatures ranged between 21.2–22.8 and 19.8–20.6 °C during filament extrusion and 3D printing processes, respectively. Relative humidity is a plausible confounding factor when chemical emissions are sampled; lower RH levels are associated with diminished emissions (Manoukian et al. 2016), which might have had an impact on the overall VOC levels. Corresponding RH ranges were 17–27% and 27–35%. CO_2 was not found to be produced in noteworthy quantities during the measurements; the highest measured single value was 860 ppm (parts per million) during 3D printing, while a peak filament extrusion concentration was only 660 ppm. Corresponding average CO_2 concentrations ranged at 770–830 and 460–570 ppm during 3D printing and filament extrusion processes. These values exceed the background levels only marginally. Detailed air quality parameter results are presented in Supplementary Table 1.

VOCs and carbonyls

The main VOC results are presented in Table 2 and all the detected compounds are listed in Supplementary Tables 2 and 3. The background concentrations for VOCs and carbonyls are presented in Supplementary Table 4. The same compounds were detected during filament extrusion and 3D printing processes, and the total VOC (TVOC) concentration ranges were 34–63 $\mu g/m^3$ during filament extrusion and 41–56 $\mu g/m^3$ during 3D printing. Lactide, commonly encountered in thermal processing of PLA, was the most abundantly detected compound (peak concentrations were 24 and 16 $\mu g/m^3$ during filament extrusion and 3D printing, respectively), followed by various alcohols, acids, and aldehydes. The following terpenes were found in low concentrations: 3-carene, α-pinene, d-limonene, and p-cymene. Isoprene, the base unit of terpenes, was also detected. Cumulative terpene concentrations, including isoprene, ranged between 9 and 22 $\mu g/m^3$, while the peak concentration of any single compound (3-carene and α-pinene) was only 8 $\mu g/m^3$. The personal and stationary VOC results are indistinguishable as the operated machines were open and did not have any emission control mechanisms which resulted in free diffusion of the gaseous contaminants in the air. The concentrations of non-terpene VOCs were lower when wood or cellulose was present in the feedstock, but terpenes were

Table 3. The measured carbonyl compound air concentrations ($\mu g/m^3$).

Description	Formaldehyde	Acetaldehyde	Acetone	2-Butanone	Hexanal	Other	Total
Filament production: PLA	6	6	25	20	2	1	60
Filament production: Formi 20	7	5	47	16	2	1	78
Filament production: Formi 40	7	3	40	18	1	1	70
Filament production: BC 15%	6	5	42	15	1	2	71
Filament production: BC 30%	8	3	54	24	1	1	91
3D printing: PLA	40	27	83	70	16	17	253
3D printing: Formi 20	37	24	69	73	13	14	230
3D printing: Formi 40	32	20	55	58	12	13	190
3D printing: BC 15%	41	32	67	52	18	19	229
3D printing: BC 30%	36	27	70	53	15	15	216

All presented values are background-corrected and obtained from a stationary point.

Table 4. The measured particle air concentrations and UFP emission rates (SUFP).

Description	UFP C_n (#/cm^3)				S_{UFP} (#/min)	PM$_{2.5}$ C_m ($\mu g/m^3$)				PM$_{10}$ C_m ($\mu g/m^3$)			
	Min	Max	Average	SD		Min	Max	Average	SD	Min	Max	Average	SD
Filament production: PLA	0.15×10^2	2.30×10^2	0.85×10^2	0.45×10^2	5.3×10^8	0.1	2.8	0.5	0.4	5	85	10	15
Filament production: Formi 20	1.35×10^2	2.00×10^2	1.65×10^2	0.20×10^2	1.0×10^9	0.1	1.0	0.4	0.2	<5	75	10	10
Filament production: Formi 40	0.65×10^2	1.85×10^2	1.30×10^2	0.40×10^2	8.1×10^8	0.1	0.5	0.2	0.1	<5	60	5	10
Filament production: BC 15%	5.60×10^2	7.65×10^2	6.55×10^2	0.50×10^2	4.1×10^9	0.2	0.5	0.3	0.1	<5	60	20	10
Filament production: BC 30%	8.00×10^2	1.25×10^3	1.05×10^3	1.00×10^2	6.6×10^9	0.3	2.1	0.6	0.3	<5	60	10	10
3D printing: PLA	0.20×10^2	1.41×10^3	6.25×10^2	3.30×10^2	3.9×10^9	1.2	2.9	2.0	0.3	<5	10	5	<5
3D printing: Formi 20	0.15×10^2	2.89×10^3	1.20×10^3	8.90×10^2	7.5×10^9	0.1	2.5	1.2	0.6	<5	10	5	<5
3D printing: Formi 40	1.00×10^3	2.78×10^3	1.74×10^3	4.30×10^2	1.1×10^{10}	1.0	2.6	1.7	0.3	<5	20	5	<5
3D printing: BC 15%	0.20×10^2	3.42×10^3	2.09×10^3	8.10×10^2	1.3×10^{10}	1.4	3.1	2.2	0.3	<5	5	5	<5
3D printing: BC 30%	3.50×10^2	7.60×10^2	6.05×10^2	0.75×10^2	3.8×10^9	0.2	3.1	1.4	0.7	<5	10	5	<5

All presented values are background-corrected and obtained from a stationary point.

introduced as new emission products. Hence, the TVOC levels were equal between the different feedstocks, but their VOC profiles were different. Terpenes contributed for 17–39% of TVOC during filament extrusion and 21–36% during 3D printing. The increase in wood content was associated with higher terpene portions of TVOC roughly equivalent for the wood or cellulose content, while no terpenes were encountered during processing of pure PLA. The TVOC ERs ranged between 2.6 and 3.6×10^2 $\mu g/min$ during filament extrusion, and between 2.9 and 3.4×10^2 $\mu g/min$ during 3D printing, and no consistent emission differences were found between the pure PLA and BC feedstocks.

The concentrations of carbonyl compounds were notably affected by the higher extrusion temperature of the 3D printer in comparison to the lower processing temperature used during filament production. The measured carbonyl concentrations are presented in Table 3. 2-Butanone, acetaldehyde, acetone, and formaldehyde were the most abundantly encountered carbonyls which together contributed for 84–98% of the cumulative carbonyl concentrations which ranged between 60–91 $\mu g/m^3$ during filament extrusion and 190–253 $\mu g/m^3$ during 3D printing. Acetone was detected in the highest concentration, at 83 $\mu g/m^3$ level during 3D printing of pure PLA. Peak concentrations for 2-butanone, acetaldehyde and formaldehyde were 73, 32, and 41 $\mu g/m^3$, respectively, measured

while printing different BC feedstocks. Several other carbonyls (acrolein, methacrolein and benzaldehyde) were detected at low (below 5 $\mu g/m^3$) concentrations as well. The following carbonyls were detected at below 5 $\mu g/m^3$ levels in the background: 2-butanone, acetaldehyde, acetone, acrolein, formaldehyde, hexaldehyde, and propionaldehyde. The used analysis method was selective and only the compounds in the reference material were able to be identified, and other carbonyls evaded the method. However, no distinct phantom peaks representing unidentified compounds were found in the chromatograms.

Particulate matter

The obtained particulate matter concentrations and ERs for UFPs are presented in Table 4, and background particle concentrations are listed in Supplementary Table 5. Filament extrusion and 3D printing processes produced rather constant amounts of particles as no major concentration peaks were recorded and the concentrations fluctuated only mildly. Time series data illustrating the evolution of particle (UFP, PM$_{2.5}$, and PM$_{10}$) concentrations during thermal processing of pure PLA, Formi 20, and BC 30% are presented in Supplementary Figures 1–3. The top UFP concentrations were 2.30×10^2 and 1.41×10^3 #/cm^3 for pure PLA during filament extrusion and 3D printing, respectively, while the

corresponding peak values were 1.25×10^3 and 3.42×10^3 #/cm³ for BC feedstocks. Pure PLA was documented to produce slightly lower amounts of UFPs than BCs during filament extrusion but not during 3D printing; the respective average concentrations for PLA were 0.85×10^2 and 6.25×10^2 #/cm³ (which represent ERs of 5.3×10^8 and 3.9×10^9 #/min). The corresponding C_n ranges were 1.30×10^2–1.05×10^3 and 6.05×10^2–2.09×10^3 #/cm³ for BC materials, which represent ER ranges of 8.1×10^8–6.6×10^9 during filament extrusion and 3.8×10^9–1.3×10^{10} during 3D printing. Overall, only moderate UFP concentration or ER differences are observable between the commercial and custom feedstocks, and the 3D printer produced principally more UFPs than the filament extruder.

$PM_{2.5}$ and PM_{10} particles were also produced during the extrusion processes. $PM_{2.5}$ particles were documented at the average C_m range of 0.2–0.6 µg/m³ during filament extrusion, and between 1.2–2.2 µg/m³ during 3D printing. C_m peaks for the respective processes were 2.8 and 3.1 µg/m³ and no coherent differences were identified between the feedstocks. The highest C_m of PM_{10} particles (85 µg/m³) was detected during pure PLA filament extrusion, while the top C_m measured during the production of BC filaments was 75 µg/m³ (Formi 20). Mild concentration fluctuations were observed, but not in a consistent manner. The highest average filament extrusion PM_{10} C_m was 20 µg/m³, measured during BC 15% processing. 3D printing produced lower amounts of PM_{10} particles, and the highest peak value was only 20 µg/m³ recorded using Formi 40 feedstock. Otherwise, the average PM_{10} concentrations ranged between 5–10 µg/m³ during both filament extrusion and 3D printing processes.

Discussion

The production of functional custom 3D printable filaments using only raw materials and commercial level machines was achieved in this study. An open 3D printer and a filament extruder produced particulate matter and chemical compounds at fair concentration levels when the machines were operated at reasonable temperatures in a medium-sized and adequately ventilated office space. The measured contaminant concentrations and calculated ERs were generally at anticipated levels based on the existing literature.

The measured CO_2 values were far from air quality compromising levels despite the occasional exceeding of the background concentrations by a few hundred ppm (FMSAH 2015, 2020). The elevated concentrations can be explained with the presence of the 3D printer and measurement personnel. The feedstocks were not noticed to burn in the extruder nozzles during the experiment, which is a relatively common malfunction in ME 3D printing. This is supported by the measured moderate UFP levels which are known to increase drastically in such situations and thus, the extrusion processes as the sources for CO_2 are unlikely. The other air quality parameters remained constant and therefore the operated machines had a negligible influence on them. The recorded low RH levels may have diminished the total production of VOCs. Regardless, internal VOC results comparison is unperturbed by the RH levels owing to their consistency.

VOCs and carbonyls

The VOC concentrations measured during the filament extruder and 3D printer operations were very analogous. Lactide was the most abundant compound detected throughout the experiment and a common thermal degradation product of PLA. It does not have an official occupational exposure limit (OEL) value. Evidence for its toxicity was found only after 2 weeks of daily high ($\geq$1,000 mg/kg body weight) oral dosing in an animal study (Hébert et al. 1999), while no human toxicity data was found by the authors. Thus, the measured exposure levels are not expected to be hazardous for humans, despite the concentration being calculated as a toluene equivalent. Majority of the other VOCs found at the highest concentrations (acetic acid and various aldehydes or alcohols) corresponded with existing literature as well (Kim et al. 2015a, Azimi et al. 2016; Steinle 2016; Stefaniak et al. 2017; Davis et al. 2019; Pohleven et al. 2019; Väisänen et al. 2019, 2021a). These compounds are not particularly harmful for human health at the measured concentration levels either, as they do not possess eminent hazardous properties which is reflected by their high OELs (FMSAH 2020), or maximum acceptable workplace concentrations (MAKs, DFG 2021). A limitation of this study is that the presented compound concentrations are calculated as toluene equivalents and the administrative guideline values are derived using the response curves of the individual compounds. Therefore, the concentrations acquired in this study do not perfectly match the true concentrations of the compounds in the air. Examples of these values are 500 mg/m³ for 8-hr exposure to 1-propanol, and 42 mg/m³ for acute exposure to hexanal (FMSAH

2020). Like lactide, 1-nonanol has no established OEL, but exposure to the recorded levels ($2–8\,\mu g/m^3$) are unlikely to produce adverse health impacts based on the available toxicity data (PubChem 2022). Furfural, a compound originating from heat-treating of wood (Pohleven et al. 2019) was inconsistently detected during BC extrusion processes at up to $6\,\mu g/m^3$ level. It has a lowest health-based concentration of interest (LCI) value of $10\,\mu g/m^3$ in the air because of its hepatotoxic properties (WHO 1995; EC 2020), thus making it the only compound which approached its available official limit value in the current study. Acetic acid is another wood-originated compound, but its measured concentration is likely underestimated because the used VOC sampling method is most accurate for the collection of compounds in 6–16 carbon atom range. Its OEL of $13\,mg/m^3$ for 8-hr exposure is, however, far higher than the recorded concentration magnitude (FMSAH 2020). The measured TVOC levels correspond rather well with the previously documented concentrations obtained using PLA and BC feedstocks in 3D printers (Kim et al. 2015a; Azimi et al. 2016; Floyd et al. 2017, Mendes et al. 2017, Stefaniak et al. 2017, Du Preez et al. 2018; Väisänen et al. 2019, 2021a). The TVOC levels were also low in comparison to the proposed occupational indoor air guidelines in Finland; 3000 or $250\,\mu g/m^3$ for industrial workplaces, or office and analogous environments, respectively (Tuomi and Vainiotalo 2016). Similarly, TVOC values fell below the Finnish residential space threshold TVOC value of $400\,\mu g/m^3$ and the individual non-health-based compound limit of $50\,\mu g/m^3$ was not exceeded, either (FMSAH 2015). While TVOC is not a health-based parameter, it is an applicable indicator of indoor air quality (Tuomi and Vainiotalo 2016). The indoor air quality of an adequately ventilated medium sized office space is not jeopardized by operation of a single 3D printer or filament extruder using PLA or PLA-based BC feedstocks on this basis. TVOC ERs calculated for PLA and BC feedstocks in previous studies (Azimi et al. 2016; Steinle 2016; Floyd et al. 2017; Stefaniak et al. 2017, 2019; Davis et al. 2019) express remarkable differences. Stefaniak et al. (2017) calculated a TVOC ER of ca. $2\,\mu g/min$ for a closed printer in a chamber, but in a later study Stefaniak et al. (2019) documented up to $4.4 \times 10^4\,\mu g/min$ ER using an open printer in a laboratory with a ventilation rate of 2 ACH. The documented TVOC ERs have been more modest, around $10–50\,\mu g/min$ in chamber studies (Azimi et al. 2016; Steinle 2016; Floyd et al. 2017). The ERs calculated in the current study represent the chamber studies more accurately than those obtained in the laboratory study, suggesting moderate TVOC emissions. The different research methods and environments contribute to the diversity of the results, as for example, a real-time TVOC sensor has been used in multiple studies as opposed to adsorption tube sampling made use of in others, like the current one.

Terpene compounds were found on all occasions when wood or cellulose was present in the feedstock material, even though pure cellulose should not contain terpenes. In contrast, no terpenes were present during processing of pure PLA. Drying sawdust for 3 months likely contributed to the fair obtained terpene levels as a portion of the compounds had time to spontaneously depart the wood matter (Roffael 2006; Höllbacher et al. 2015). Nonetheless, terpenes contributed to ca. 20–40% of the TVOC levels. While not particularly toxic, they may impair indoor air quality as they are precursors for air quality deteriorating secondary chemical reactions and UFP formation in the presence of ozone (Sarwar et al. 2004; Weschler 2011; Rohr 2013; Kim et al. 2015b; Wolkoff 2020). Secondary compounds produced in the chemical interactions in air include reactive species and carbonyls of low molecular weight, e.g., carcinogenic formaldehyde (Weschler 2011; Rohr 2013; Kim et al. 2015b; Wolkoff 2020). However, many terpenes are purposefully used in significant quantities in various consumer products, such as fragrances, and some of their benefits have also been recognized (Kim et al. 2020). The measured air concentrations were low in comparison to their LCI or MAK values ($2.5\,mg/m^3$ for α-pinene, $1.5\,mg/m^3$ for 3-carene, 28 or $5\,mg/m^3$ for d-limonene, $1\,mg/m^3$ for cymene, and $8.5\,mg/m^3$ for isoprene) and, thus, they are expected to have a minute impact on indoor air quality or little contribution to the induction of adverse health impacts in 3D printer operators (EC 2020; DFG 2021).

3D printing with PLA and PLA-based composite filaments have previously been documented to emit various carbonyls, e.g., acetaldehyde, acetone, and formaldehyde in moderate concentrations (Kim et al. 2015a; Mendes et al. 2017; Stefaniak et al. 2017; Du Preez et al. 2018; Davis et al. 2019; Väisänen et al. 2019). Unexpectedly, the filament extruder and 3D printer produced similar levels of VOCs, but the carbonyl concentrations were substantially higher, ca. two- to four-fold from the 3D printer in comparison to the filament extruder. The obtained levels were not affected by the feedstock material. It should be noted that the filament extruder operates at the lowest

temperature settings that makes feedstock extrusion and spooling plausible, which is lower than the temperatures used in 3D printers. The applied temperature is one factor which contributes to the higher carbonyl levels from the 3D printer in comparison to the filament extruder. Despite existing at moderate levels at highest, all carbonyls fell below their OELs (FMSAH 2020), MAK values (DFG 2021), LCIs (EC 2020), and residential space threshold values given by WHO (2018) and FMSAH (2015). The lowest official (long-term) limit value of $50\,\mu g/m^3$ given for formaldehyde in residential spaces in Finland was almost exceeded during 3D printing (FMSAH 2015). The lowest corresponding reference values given for acetaldehyde ($300\,\mu g/m^3$, EC 2020), acetone (120 or mg/m^3, EC 2020), and 2-butanone ($20\,mg/m^3$, EC 2020) are notably higher than the concentrations obtained in this study. Long-term exposure to formaldehyde and acetaldehyde still cannot be deemed completely innocuous due to their toxic properties (WHO 2006; Sarigiannis et al. 2011; Klaasen et al. 2013). Otherwise, the compounds are not expected to be hazardous for 3D printer personnel at the recorded levels. In addition to being more readily volatilized than VOCs, carbonyls are formed in secondary chemical interactions in the air as described above. It is plausible that these factors contributed to the unexpectedly high carbonyl levels.

Particulate matter

3D printers are identified as significant UFP emitters, but the obtained concentration levels were far below a proposed lightweight UFP exposure reference value of 4×10^4 #/cm^3 given for manufactured nanomaterials (Van Broekhuizen et al. 2012), the only available reference as no authoritative OELs exist. PLA and BC feedstocks have been recorded to emit UFPs with an aerodynamic diameter of 20 nm and above mainly in 5×10^2–5×10^4 #/cm^3 concentration levels when 200–220 °C temperatures are used (Kim et al. 2015a; Yi et al. 2016; Azimi et al. 2016; Floyd et al. 2017; Kwon et al. 2017; Mendes et al. 2017; Vance et al. 2017; Du Preez et al. 2018; Väisänen et al. 2019, 2021a; Byrley et al. 2019; Jeon et al. 2020). These concentration ranges represent calculated ERs of ca. 10^8–10^{11} #/min (Kwon et al. 2017; Vance et al. 2017; Byrley et al. 2019; Jeon et al. 2020). The concentrations documented in the current study are equivalent to the lower end of the documented concentration spectrum, while the calculated UFP ERs also fall within the previously reported ER ranges. The ERs

calculated in the current study are, however, very likely underestimated because of the used calculation method. The studied BC feedstocks are, nevertheless, very similar UFP emitters as pure PLA feedstocks based on the results and previous literature. The filament extruder produced slightly lesser amounts of UFPs in comparison to the 3D printer, which is a consistent finding with the carbonyl levels. A filament extruder can be identified as an equivalent or a slightly lesser UFP emitter as a desktop ME 3D printer. In addition to VOCs, a higher 3D printer nozzle temperature is documented to increase UFP emissions by several studies (Yi et al. 2016; Byrley et al. 2019; Jeon et al. 2020; Stefaniak et al. 2021), and the findings of the current study reflect that (except the case of BC 30% which produced the most particles during filament extrusion). The obtained UFP levels were stable, and the absence of concentrations peaks indicates that the extrusion processes were principally undisturbed by the wood or cellulose particles.

To the best knowledge of the authors, PM$_{2.5}$ levels from the operation of ME 3D printers have been only studied once in a chamber, and only using ABS as the feedstock. PM$_{2.5}$ levels were documented to gradually increase from zero to as high as $900\,\mu g/m^3$ level in the study by Rao et al. (2017). Higher RH was associated with higher particle levels; the highest concentration was achieved at 80% RH. A concentration level of $600\,\mu g/m^3$ was reached at 40% RH. These values are far higher than those found in the current study, but neither the study designs nor used feedstocks are comparable. WHO (2021) has introduced a 24-hr average PM$_{2.5}$ guideline value of $15\,\mu g/m^3$ for ambient air, which is a suitable reference for comparison. This limit value was not reached during the current study using the CPC instrument, as the highest observed peak value was only $3.1\,\mu g/m^3$, and only up to $2.2\,\mu g/m^3$ average PM$_{2.5}$ levels were recorded over full thermal processes. It must be emphasized that the CPC instrument could not detect particles smaller than $0.3\,\mu m$ in diameter and thus the true PM$_{2.5}$ (and PM$_{10}$) concentrations in the air are greater than what was detected in the current study, as the UFPs were not included in the recorded mass concentrations. Larger particles are occasionally documented to be emitted by 3D printers at fair to moderate, up to $100\,\mu g/m^3$ concentrations, if at all (Kim et al. 2015a; Yi et al. 2016; Väisänen et al. 2019; Mendes et al. 2017; Kwon et al. 2017; Byrley et al. 2019). The PM$_{10}$ concentrations measured in this study correspond with the previously documented levels. No official OELs are established for PM$_{10}$ particles, either, but

they can be substituted by guideline values for ambient air and residential indoor environments. These established health-based values are almost universally set at 50 µg/m^3, while WHO suggests a stricter long-term value of 20 µg/m^3 for residential spaces (EU 2008; FMSAH 2015; WHO 2018, 2021). The PM$_{10}$ guideline of 50 µg/m^3 was temporarily exceeded during filament extrusion processes, but all average concentrations were below it. The closest comparable Finnish OEL is the one for total inhalable organic dust set at 5 mg/m^3 (FMSAH 2021), which is far higher than the measured PM$_{10}$ concentrations. The exposure levels to PM$_{2.5}$ and PM$_{10}$ particles are therefore not a significant concern for a process operator, albeit the machines temporarily produced particles at concentrations that exceeded the established PM$_{10}$ guideline values.

The filament extruder

Similar UFP ERs, but far higher particle concentration levels for PLA feedstocks were documented in a study by Byrley et al. (2020) in comparison to this experiment. The extruder was in a chamber unlike in the current study, which naturally resulted in different particle concentration readings. A pulverized PLA feedstock produced as high UFP concentration peak as 3.5×10^5 #/cm^3, while a granulated PLA feedstock peaked at 2.5×10^4 #/cm^3. No as radical concentration differences and peaks were found in the current study. The ERs reported by Byrley et al. (2020) were 1.7×10^9 and 5.6×10^{10} #/min for the granulated and shredded feedstocks, respectively. In comparison, the calculated ER for PLA was 5.3×10^8 #/min in the current study, while the commercial BC granules produced fairly higher emissions, and the custom BC shreds emitted the most particles (up to 6.6×10^9 #/min), which is a consistent finding with the previous study. Additionally, Byrley et al. (2020) calculated C$_m$ for PM$_{2.5}$ using resolved UFP size distributions and feedstock densities. In this study, C$_m$ of PM$_{2.5}$ was sampled directly with the OPS instrument. The results are not comparable though, as the minimum detection limit of the OPS instrument is 0.3 µm, and thus, the majority of particles went undetected by the device in this experiment. The previously reported PM$_{2.5}$ concentrations were ca. 35 µg/m^3 for granulated PLA, and ca. 125 µg/m^3 for shredded PLA. The highest C$_m$ peak of PM$_{2.5}$ particles during filament extrusion processes was a mere 2.8 µg/m^3 in the current study, while the average concentrations were below 1 µg/m^3 throughout the experiment. Also, no

PM$_{2.5}$ C$_m$ differences existed between the studied feedstocks. Similarly, the obtained PM$_{10}$ C$_m$ values were indifferent between the used feedstocks in the current study, with the highest peak value reaching 85 µg/m^3 and the highest average concentration being 20 µg/m^3. The VOCs detected by Byrley et al. (2020) included lactide, benzene derivates, and various acids and alcohols among others. These compounds correspond well with previous 3D printer emission literature and the findings of the current study, which supports the emission similarity assumption between filament extruders and 3D printers using similar feedstocks. Byrley et al. (2020) ultimately identified filament extruders and desktop 3D printers as very similar emission sources, and the findings of the current study support the claim.

Conclusions

It was demonstrated in this study that functional and 3D printable BC feedstocks can be produced from commercially available plastic granules and raw wood fibers without expensive and technically advanced machines. The airborne contaminant compositions, levels, and ERs produced by a filament extruder resemble those from an open ME 3D printer when equivalent feedstocks are used in both. This was the first time this was confirmed. Emission products originated from PLA-based BC feedstocks could not be identified as severely more hazardous than those from a pure PLA feedstock, albeit some differences in chemical compositions existed. Certain compounds that originate from thermal treatment of wood, including terpenes and furfural were the most obvious differences. Terpenes can impair indoor air quality through secondary chemical reactions and UFP formation, but their impact on air quality is not expected to be significant based on the concentration levels obtained in the current study. Furfural may produce toxic effects in prolonged exposure, but it was found inconsistently and only at low concentration levels. PLA-based BC materials can be identified as environmentally friendly feedstocks which express similar hazardous properties in comparison to traditional petroleum-derived polymers based our findings as the addition of bio-content both reduced the portion of plastic-originated emission products and introduced new chemical emission products, while no major impact was observed on the produced particle levels. Nonetheless, emission control measures should be always applied when thermal extruders are operated.

Findings by Byrley et al. (2020) were mostly confirmed in this study. The emissions from a filament extruder resemble those from a 3D printer accurately, for both the composition and magnitude. Filament extruders are often operated at lower temperature settings than 3D printers which contributes to slightly reduced emissions. This was observable in this study on behalf of carbonyls and UFPs. On the other hand, PM_{10} particles were observed at slightly greater concentrations when a filament extruder was operated, while the recorded VOC and $PM_{2.5}$ particle levels were identical between the machines. The contaminant concentration levels were mostly low or moderate based on the previous literature and administrative guidelines, indicating that emissions produced by a single 3D printer or filament extruder are not excessive in a moderately sized, well-ventilated office space. Further suggested research topics include the expansion of the studied feedstocks in a filament extruder, and the examination of the mechanical properties of (customized) BCs feedstocks which could further support the transition toward sustainable 3D printer materials.

Recommendations

Similar emission and exposure control measures can and should be applied on filament extruders as on 3D printers. These measures include the use of machine enclosures, local exhaust systems and lowest functional temperature settings, and spending the least possible time in the same premises with the operated machines to prevent exposure to their emissions. The use of wood-containing BC materials does not require further protective measures than generic feedstocks.

Conflicts of interest

The authors declare no conflict of competing interest.

Data availability statement

The authors confirm that the data supporting the findings of this study are available within the article and its supplementary materials and are shared upon request.

References

Azimi P, Zhao D, Pouzet C, Crain NE, Stephens B. 2016. Emissions of ultrafine particles and volatile organic compounds from commercially available desktop three-dimensional printers with multiple filaments. Environ Sci Technol. 50(3):1260–1268. doi:10.1021/acs.est.5b04983

Byrley P, Geer Wallace MA, Boyes W, Rogers K. 2020. Particle and volatile organic compound emissions from a 3D printer filament extruder. Sci Total Environ. 736: 139604. doi:10.1016/j.scitotenv.2020.139604

Byrley P, George B, Boyes W, Rogers K. 2019. Particle emissions from fused deposition modeling 3D printers: evaluation and meta-analysis. Sci Total Environ. 655:395–407. doi:10.1016/j.scitotenv.2018.11.070

Calí M, Pascoletti G, Gaeta M, Milazzo G, Ambu R. 2020. A new generation of bio-composite thermoplastic filaments for a more sustainable design of parts manufactured by FDM. Appl Sci. 10(17):5852. doi:10.3390/app10175852

Calvino C, Macke N, Kato R, Rowan SJ. 2020. Development, processing and applications of bio-sourced cellulose nanocrystal composites. Prog Polym Sci. 103: 101221. doi:10.1016/j.progpolymsci.2020.101221

Chan FL, House R, Kudla I, Lipszyc JC, Rajaram N, Tarlo SM. 2018. Health survey of employees regularly using 3D printers. Occup Med. 68(3):211–214. doi:10.1093/occmed/kqy042

Davis AY, Zhang Q, Wong JPS, Weber RJ, Black MS. 2019. Characterization of volatile organic compound emissions from consumer level material extrusion 3D printers. Build Environ. 160:106209. doi:10.1016/j.buildenv.2019.106209

[DFG] Deutsche Forschungsgemeinschaft. 2021. Permanent Senate Commission for the investigation of health hazards of chemical compounds in the work area. Report 57. List of MAK and BAT Values 2021; [accessed Dec 8]. mbwl_2021_eng.pdf (publisso.de)

Du Preez S, Johnson AR, LeBouf RF, Linde SJL, Stefaniak AB, Du Plessis J. 2018. Exposures during industrial 3-D printing and post-processing tasks. RPJ. 24(5):865–871. doi:10.1108/RPJ-03-2017-0050

European Commission (EC). 2020. EU-LCI values; [accessed 2021 Nov 22]. https://ec.europa.eu/growth/sectors/construction/eu-lci-subgroup/eu-lci-values_en.

European Union (EU). 2008. Directive 2008/50/EC of the European Parliament and of the Council on ambient air quality and cleaner air for Europe. Off J Eur Union L 152:1–44. https://eur-lex.europa.eu/eli/dir/2008/50/oj.

Floyd EL, Wang J, Regens JL. 2017. Fume emissions from a low-cost 3-D printer with various filaments. J Occup Environ Hyg. 14(7):523–533. doi:10.1080/15459624.2017.1302587

Finnish Ministry of Social Affairs and Health (FMSAH). 2015. Decree 545/2015 of the Ministry of Social Affairs and Health on health-related conditions of housing and

other residential buildings and qualification requirements for third-party experts; [accessed 2021 Nov 25]. https://www.finlex.fi/en/.

Finnish Ministry of Social Affairs and Health (FMSAH). 2020. Concentrations known to be harmful; [accessed 2021 Nov 22]. https://julkaisut.valtioneuvosto.fi/handle/10024/162457.

Ford S, Despeisse M. 2016. Additive manufacturing and sustainability: an exploratory study of the advantages and challenges. J. Clean Prod. 137:1573–1587. doi:10.1016/j.jclepro.2016.04.150

Hébert CD, Giles HD, Heath JE, Hogan DB, Modderman JP, Conn RE. 1999. Toxicity of lactide in dogs after 2 and 13 weeks of daily oral dosing. Food Chem Toxicol. 37(4):335–342. doi:10.1016/S0278-6915(99)00014-9

Höllbacher E, Rieder-Gradinger C, Strateva D, Srebotnik E. 2015. A large-scale test set-up for measuring VOC emissions from wood products under laboratory conditions in simulated real rooms. Holzforschung. 69(4):457–462. doi:10.1515/hf-2014-0129

House R, Rajaram N, Tarlo SM. 2017. Case report of asthma associated with 3D printing. Occup Med. 67(8):652–654. doi:10.1093/occmed/kqx129

Jeon H, Park J, Kim S, Park K, Yoon C. 2020. Effect of nozzle temperature on the emission rate of ultrafine particles during 3D printing. Indoor Air. 30(2):306–314. doi:10.1111/ina.12624

Kasanen J-P, Pasanen A-L, Pasanen P, Liesivuori J, Kosma V-M, Alarie Y. 1999. Evaluation of sensory irritation of 3-carene and turpentine, and acceptable levels of monoterpenes in occupational and indoor environment. J Toxicol Environ Health A. 57(2):89–114. doi: 10.1080/009841099157809.

Klaasen CD, Casarett LJ, Doull J. 2013. Casarett & Doull's toxicology: the basic science of poisons. 8th ed. Manhattan (NY): McGraw Hill Education.

Kim S, Kim J-A, Kim H-J, Kim SD. 2006. Determination of formaldehyde and TVOC emission factor from wood-based composites by small chamber method. Polymer Testing. 25(5):605–614. doi:10.1016/j.polymertesting.2006.04.008

Kim S, Hong S-H, Bong C-K, Cho M-H. 2015b. Characterization of air freshener emission: the potential health effects. J Toxicol Sci. 40(5):535–550. doi:10.2131/jts.40.535

Kim T, Song B, Cho KS, Lee I-S. 2020. Therapeutic potential of volatile terpenes and terpenoids from forests for inflammatory diseases. Int J Mol Sci. 21(6):2187. doi:10.3390/ijms21062187

Kim Y, Yoon C, Ham S, Park J, Kim S, Kwon O, Tsai P-J. 2015a. Emissions of nanoparticles and gaseous material from 3D printer operation. Environ Sci Technol. 49(20):12044–12053. doi:10.1021/acs.est.5b02805

Kim YW, Kim MJ, Chung BY, Bang DY, Lim SK, Choi SM, Lim DS, Cho MC, Yoon K, Kim HS, et al. 2013. Safety evaluation and risk assessment of d-limonene. J Toxicol Environ Health B Crit Rev. 16(1):17–38. doi:10.1080/10937404.2013.769418

Kwon O, Yoon C, Ham S, Park J, Lee J, Yoo D, Kim Y. 2017. Characterization and control of nanoparticle emissions during 3D printing. Environ Sci Technol. 51(18):10357–10368. doi:10.1021/acs.est.7b01454

Manoukian A, Buiron D, Temime-Roussel B, Wortham H, Quivet E. 2016. Measurements of VOC/SVOC emission factors from burning incenses in an environmental test chamber: influence of temperature, relative humidity, and air exchange rate. Environ Sci Pollut Res Int. 23(7):6300–6311. doi:10.1007/s11356-015-5819-2

Mazzanti V, Malagutti L, Mollica F. 2019. FDM 3D printing of polymers containing natural fillers: a review of their mechanical properties. Polymers. 11(7):1094. doi:10.3390/polym11071094

Mendes L, Kangas A, Kukko K. 2017. Characterization of emissions from a desktop 3D printer. J. Ind. Ecol. 14:94–106. doi:10.1111/jiec.12569

Mossman BT, Borm PJ, Castranova V, Costa DL, Donaldson K, Kleeberger SR. 2007. Mechanisms of action of inhaled fibers, particles and nanoparticles in lung and cardiovascular diseases. Part Fibre Toxicol. 4:4. doi:10.1186/1743-8977-4-4

Peng T, Kellens K, Tang R, Chen C, Chen G. 2018. Sustainability of additive manufacturing: an overview on its energy demand and environmental impact. Addit Manuf. 21:694–704. doi:10.1016/j.addma.2018.04.022

Pohleven J, Burnard MD, Kutnar A. 2019. Volatile organic compounds emitted from untreated and thermally modified wood—a review. WFS. 51(3):231–224. doi:10.22382/wfs-2019-023

Pope CA, Dockery DW. 2006. Health effects of fine particulate air pollution: lines that connect. J Air Waste Manag Assoc. 56(6):709–742. doi:10.1080/10473289.2006.10464485

PubChem. 2022. Compound summary. Nonan-1-ol; [accessed 2022 Feb 15]. https://pubchem.ncbi.nlm.nih.gov/compound/1-Nonanol.

Rao C, Gu F, Zhao P, Sharmin N, Gu H, Fu J. 2017. Capturing $PM_{2.5}$ emissions from 3D printing via nanofiber-based air filter. Sci Rep. 7(1):10366. doi: 10.1038/s41598-017-10995-7.

Roffael E. 2006. Volatile organic compounds and formaldehyde in nature, wood and wood based panels. Holz Roh Werkst. 64(2):144–149. doi:10.1007/s00107-005-0061-0

Rohr AC. 2013. The health significance of gas- and particle-phase terpene oxidation products: a review. Environ Int. 60:145–162. doi:10.1016/j.envint.2013.08.002

Sarigiannis DA, Karakitsios SP, Gotti A, Liakos IL, Katsoyiannis A. 2011. Exposure to major volatile organic compounds and carbonyls in European indoor environments and associated health risk. Environ Int. 37(4):743–765. doi:10.1016/j.envint.2011.01.005

Sarwar G, Olson DA, Corsi RL, Weschler CJ. 2004. Indoor fine particles: the role of terpene emissions from consumer products. J Air Waste Manag Assoc. 54(3):367–377. doi:10.1080/10473289.2004.10470910

Shahnaz B, Hayes A, Dechsakulthorn F. 2012. Nanoparticles: a review of particle toxicology following inhalation exposure. Inhal Toxicol. 24(2):125–135. doi:10.3109/08958378.2010.642021

Stabile L, Scungio M, Buonanno G, Arpino F, Ficco G. 2017. Airborne particle emission of a commercial 3D printer: the effect of filament material and printing temperature. Indoor Air. 27(2):398–408. doi:10.1111/ina.12310

Stefaniak AB, Du Preez S, Du Plessis JL. 2021. Additive manufacturing for occupational hygiene: a comprehensive

review of processes, emissions & exposures. J. Toxicol. Environ. Health B. 24(5):173–222. doi:10.1080/10937404.2021.1936319

Stefaniak AB, Johnson AR, du Preez S, Hammond DR, Wells JR, Ham JE, LeBouf RF, Menchaca KW, Martin SB, Duling MG, et al. 2019. Evaluation of emissions and exposures at workplaces using desktop 3-dimensional printer. J Chem Health Saf. 26(2):19–30. doi:10.1016/j.jchas.2018.11.001

Stefaniak AB, LeBouf RF, Yi J, Ham J, Nurkewicz T, Schwegler-Berry DE, Chen BT, Wells JR, Duling MG, Lawrence RB, et al. 2017. Characterization of chemical contaminants generated by a desktop fused deposition modeling 3-dimensional printer. J Occup Environ Hyg. 14(7):540–550. doi:10.1080/15459624.2017.1302589

Steinle P. 2016. Characterization of emissions from a desktop 3D printer and indoor air measurements in office settings. J Occup Environ Hyg. 13(2):121–132. doi:10.1080/15459624.2015.1091957

Tuomi T, Vainiotalo S. 2016. The guideline and target values for total volatile organic compound concentrations in industrial indoor environments in Finland. Indoor Built Environ. 25(2):424–434. doi:10.1177/1420326X14554270

Vaidya AA, Collet C, Gaugler M, Lloyd-Jones G. 2019. Integrating softwood biorefinery lignin into polyhydroxybutyrate composites and application in 3D printing. Mater Today Commun. 19:286–196. doi:10.1016/j.mtcomm.2019.02.008

Van Broekhuizen P, Van Veelen W, Streekstra W-H, Schulte P, Reijnders L. 2012. Exposure limits for nanoparticles: report of an international workshop on nano reference values. Ann Occup Hyg. 56(5):515–524. doi:10.1093/annhyg/mes043

Van Kampen V, Merget R, Baur X. 2000. Occupational airway sensitizers: an overview on the respective literature. Am J Ind Med. 38(2):164–218. doi:10.1002/1097-0274(200008)38:2 < 164::AID-AJIM7 > 3.0.CO;2-2

Vance ME, Pegues V, Van Montfrans S, Leng W, Marr LC. 2017. Aerosol emissions from fuse-deposition modeling 3D printers in a chamber and in real indoor environments. Environ Sci Technol. 51(17):9516–9523. doi:10.1021/acs.est.7b01546

Weschler CJ. 2011. Chemistry in indoor environments: 20 years of research. Indoor Air. 21(3):205–218. doi:10.1111/j.1600-0668.2011.00713.x

World Health Organization (WHO). 1995. Dry cleaning, some chlorinated solvents and other industrial chemicals.

IARC monographs on the evaluation of carcinogenic risk to humans. Vol. 63. Geneve (Switzerland): World Health Organization.

World Health Organization (WHO). 2006. Formaldehyde, 2-butoxyethanol and 1-tert-butoxypropan-2-ol. IARC monographs on the evaluation of carcinogenic risks to humans. Vol. 88. Geneve (Switzerland): World Health Organization.

World Health Organization (WHO). 2018. WHO housing and health guidelines. Geneva (Switzerland): World Health Organization.

World Health Organization (WHO). 2021. WHO global air quality guidelines. Particulate matter ($PM_{2.5}$ and PM_{10}), ozone, nitrogen dioxide, sulfur dioxide and carbon monoxide. Geneva (Switzerland): World Health Organization.

Wolkoff P. 2020. Indoor air chemistry: terpene reaction products and airway effects. Int J Hyg Environ Health. 225:113439. doi:10.1016/j.ijheh.2019.113439

Wolkoff P, Wilkins CK, Clausen PA, Nielsen GD. 2006. Organic compounds in office environments—sensory irritation, odor, measurements and the role of reactive chemistry. Indoor Air. 16(1):7–19. doi:10.1111/j.1600-0668.2005.00393.x

Väisänen AJK, Alonen L, Ylönen S, Hyttinen M. 2021a. The impact of thermal reprocessing of 3D printable polymers on their mechanical performance and airborne pollutant profiles. J Polym Res. 28:436. doi:10.1007/s10965-021-02723-7.

Väisänen A, Alonen L, Ylönen S, Hyttinen M. 2022. Organic compound and particle emissions of additive manufacturing with photopolymer resins and chemical outgassing of manufactured resin products. J Toxicol Environ Health A. 85(5):198–216. doi:10.1080/15287394.2021.1998814.

Väisänen AJK, Hyttinen M, Ylönen S, Alonen L. 2019. Occupational exposure to gaseous and particulate contaminants originating from additive manufacturing of liquid, powdered, and filament plastic materials and related post-processes. J Occup Environ Hyg. 16(3):258–271. doi:10.1080/15459624.2018.1557784

Yi J, LeBouf RF, Duling MG, Nurkiewicz T, Chen BT, Schwegler-Berry D, Virji MA, Stefaniak AB. 2016. Emission of particulate matter from a desktop three-dimensional (3D) printer. J Toxicol Environ Health A. 79(11):453–465. doi:10.1080/15287394.2016.1166467

ARTICLE IV

Väisänen A., Alonen L., Ylönen S. & Hyttinen M. 2022. Organic compound and particle emissions of additive manufacturing with photopolymer resins and chemical outgassing of manufactured resin products. *Journal of Toxicology and Environmental Health, Part A 85(5):198–216.*

ANTTI VÄISÄNEN

The use of additive manufacturing technologies has increased drastically over the past decades. Investigation of the exposure agents encountered in additive manufacturing processes contribute to safer adoption of the technologies in the various environments they are used in. Chemical and particulate hazards related to multiple technologies were studied in this work, and the results indicate that the encountered exposures are advisable to be controlled in additive manufacturing works.

UNIVERSITY OF
EASTERN FINLAND

uef.fi